





**LIBRARY**  
**Michigan State**  
**University**

This is to certify that the  
dissertation entitled

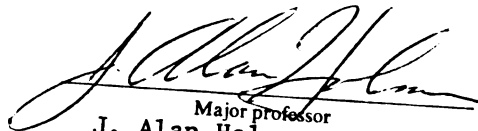
**Skeletal Tissue as Physiological Agents in Turtles**  
**(Reptilia: Testudines)**

presented by

**Kenneth Dale Andrews**

has been accepted towards fulfillment  
of the requirements for

Ph.D. degree in Zoology

  
Major professor  
**J. Alan Holman**

Date 8/10/2000

**PLACE IN RETURN BOX** to remove this checkout from your record.  
**TO AVOID FINES** return on or before date due.  
**MAY BE RECALLED** with earlier due date if requested.

DATE DUE	DATE DUE	DATE DUE

Skeletal Tissue as Physiological Agents in Turtles  
(Reptilia: Testudines)

By

Kenneth Dale Andrews

A DISSERTATION

Submitted to

Michigan State University

in partial fulfillment of the requirements

for the degree of

DOCTOR OF PHILOSOPHY

Department of Zoology

2000



## **ABSTRACT**

### **Skeletal Tissue as Physiological Agents in Turtles (Reptilia: Testudines)**

**By**

**Kenneth Dale Andrews**

Neural bones from extant chelonians and fifteen bones from fossil chelonians were observed in the Scanning Electron Microscope. The surface of the bones were examined to determine possible taxonomic differences and physiological uses of the vascular canals that interact with the surface of the shell. Different carapacial and plastral bones of one individual were examined for individual variation. Neural sections were extracted from extant turtles to make histological specimens. They were viewed to assess the compatibility of the structure of the carapace with previous explanations and to determine the shell's use as a metabolic unit for chelonians. Femora from extant chelonians were measured for total length and bisected at the narrowest margin. Measurements of the inside and outside diameters of the bones at both the narrow and wide sections of the bone were recorded. Calculations from these measurements were made for  $K$  (internal diameter/external diameter),  $KR$  (radius of marrow cavity),  $R$  (radius of outside measurement),  $t$  (thickness of bone), and  $R/t$  values.

The outer surface of the carapace was found to be similar in appearance. The other parts of the carapace varied greatly in appearance and numbers of canals. Type A canals (perpendicular to surface) were found to be the most common type of vascular canal interacting with the outer surface of the carapace. Type B canals could be used as

indicators for the total area of the surface occupied by vascular canals. Small vascular canals were found in the acellular outer layer of the carapace that was termed the subscute blood layer. This subscute blood layer allowed the blood to be affected quickly by the temperature of the outer surface (scutes) of the carapace. Cardiac shunting along with the blood flowing through the subscute blood layer was determined to be an active component of the thermoregulatory physiology of chelonians. Osteoclasts were observed in the histology sections of the carapace giving evidence for the carapace as an active storage area for Calcium.

The K value derived from the femora showed a much smaller K value than any others reported in the literature. The lower K value indicated that the long bones had a very thick bone wall to support the weight of the shell. The thickened bone wall of the femur reflected the small amount of marrow that the long bone had and this lack of marrow was compensated for in the shell bones. The shell was found to be an active part of the metabolism of the chelonian as a thermoregulatory structure and a mineral storage area for the animal.

## ACKNOWLEDGMENTS

I would like to thank my committee (Dr. J. Alan Homan, Dr. Thomas Burton, Dr. Karen Klomparens, and Dr. Donald Straney) for their support and guidance.

There are many graduate and undergraduate students who have helped me in some way. Among them are Kenneth Ford, John Paul Zonneveld, Andrew Scwda, Maria Moscmovitz, as well as numerous other graduate students that discussed various topics with me.

I would like to thank the histology department of the Michigan State University Medical School for their aid in determining the procedures needed for the decalcification process and use of their histology equipment.

Finally, I would like to thank my wife, Susan, for her support in so many different ways. Without her support, I would have not been able to complete this work.

## TABLE OF CONTENTS

	PAGE
Acknowledgments.....	i
Table of Contents.....	ii
List of Tables.....	iii
List of Figures.....	v
Introduction.....	1
Materials and Methods.....	17
Results.....	30
Discussion.....	72
Literature Cited.....	108
Appendix 1.....	112
Appendix 2.....	115
Appendix 3.....	121

# LIST OF TABLES

TABLE	PAGE
1. Z distribution analysis data on significant differences in number of canal types for all chelonians examined. Sample variances were not significantly different.....	25
2. T distribution analysis data on significant differences in number of canal types for the family Emydidae. Sample variances were not significantly different.....	25
3. T distribution analysis data on significant differences in number of canal types for the family Testudinidae. Sample variances were not significantly different.....	25
4. Percentage area of the scanning electron microscope (SEM) images occupied by canals at both a standard threshold and a variable threshold for different surfaces of varied bony elements of a single <u>Chrysemys picta</u> specimen (MSU-H 2025).....	45
5. Percentage area of the scanning electron microscope (SEM) images occupied by canals at both a standard threshold and a variable threshold for fossil specimens.....	45
6. Linear regressions of neural (N2) Scanning Electron Microscope (SEM) photograph area analysis compared to the different canal types for all Testudines.....	59
7. Linear regressions of neural (N2) Scanning Electron Microscope (SEM) photograph area analysis compared to the different canal types for members of the family Emydidae.....	59
8. Linear regressions of neural (N2) Scanning Electron Microscope (SEM) photograph area analysis compared to the different canal types for members of the family Testudinidae.....	59
9. Linear regressions of neural (N2) Scanning Electron Microscope (SEM) photograph area analysis compared to the different canal types for members of <u>Chrysemys picta</u> .....	59

10. Percentage area of the scanning electron microscope (SEM) images occupied by canals at both a standard threshold and a variable threshold for fossil specimens.....	61
11. Linear regressions of femur measurements and calculations for all Testudines.....	71
12. Linear regressions of femur measurements and calculations for members of the family Emydidae.....	71
13. Linear regressions of femur measurements and calculations for members of the family Testudinidae...	71

## LIST OF FIGURES

FIGURE	PAGE
1. Side view of a turtle showing the arrangement of the carapace and plastron.....	6
2. Diagram of the bony elements of the carapace including the nuchal (Nu), neurals (Ne), costals (C), peripherals (Pe), suprapygals (S), and pygal (Py).....	9
3. Diagram of the bony elements of the plastron including the epiplastron (Epi), hyoplastron (Hyo), hypoplastron (Hypo), and xiphiplastron (X).....	10
4. Conventions for the calculations of the bisected long bone measurements.....	14
5. Diagrammatic presentation of the three different canals and their arrangement with the surface of the carapace.....	20
6. Scanning Electron Microscope (SEM) micrograph of the outer surface of a neural bone of <u>Chrysemys picta</u> (MSU-H 14309) showing an example of a Type A canal. 60X magnification.....	21
7. Photograph of a hematoxylin and Eosin (H+E) prepared histological slide from <u>Chrysemys picta</u> (MSU-H 14309) showing an example of a Type A canal. 40X magnification.....	21
8. Scanning Electron Microscope (SEM) micrograph of the outer surface of a neural bone of <u>Chrysemys picta</u> (MSU-H 14309) showing an example of a Type B canal. 60X magnification.....	22
9. Photograph of a hematoxylin and Eosin (H+E) prepared histological slide from <u>Chrysemys picta</u> (MSU-H 14309) showing an example of a Type B canal. 40X magnification.....	22
10. Scanning Electron Microscope (SEM) micrograph of the outer surface of a neural bone of <u>Chrysemys picta</u> (MSU-H 14309) showing an example of a Type C canal. 60X magnification.....	23

11. Photograph of a hematoxylin and Eosin (H+E) prepared histological slide from Chrysemys picta (MSU-H 14309) showing an example of a Type C canal. 40X magnification.....23
12. Scanning Electron Microscope (SEM) photograph of the bisected femur of Chrysemys picta (MSU-H 2025). 30X magnification.....28
13. Scanning Electron Microscope (SEM) photograph of the outer surface of a neural bone of Trachemys scripta elegans (MSU-H 2716). 3000X magnification.....28
14. Scanning Electron Microscope (SEM) photograph of the outer surface of a neural bone of Kinosternon flavescens (MSU-H 2920). 320X magnification.....31
15. Scanning Electron Microscope (SEM) photograph of the outer surface of a neural bone of Clemmys insculpta (MSU-H 4336). 2000X magnification.....31
16. Scanning Electron Microscope (SEM) photograph of the outer surface of a neural bone showing the lining of one of the vascular canals of Trachemys scripta elegans (MSU-H 2716). 1000X magnification.....32
17. Scanning Electron Microscope (SEM) photograph of the outer surface of a neural bone showing the lining of one of the vascular canals of Chrysemys picta (MSU-H 2025). 600X magnification.....32
18. Scanning Electron Microscope (SEM) photograph of the outer surface of a neural bone showing the lining of one of the vascular canals of Chelydra serpentina (MSU-H 3436). 360X magnification.....33
19. Scanning Electron Microscope (SEM) photograph of the outer surface of a neural bone of Chelydra serpentina (MSU-H 3436). 60X magnification.....33
20. Scanning Electron Microscope (SEM) photograph of the outer surface of a neural bone of Chrysemys picta (MSU-H 14309). 60X magnification.....35
21. Scanning Electron Microscope (SEM) photograph of the outer surface of a neural bone of Chrysemys picta (MSU-H 14310). 60X magnification.....35
22. Scanning Electron Microscope (SEM) photograph of the outer surface of a neural bone of Chrysemys picta



	(MSU-H 14312). 60X magnification.....	36
23.	Scanning Electron Microscope (SEM) photograph of the outer surface of a neural bone of <u>Kinosternon flavescens</u> (MSU-H 2920). 60X magnification.....	36
24.	Scanning Electron Microscope (SEM) photograph of the outer surface of a neural bone of <u>Kinosternon leucostomum</u> (MSU-H 1414). 60X magnification.....	37
25.	Scanning Electron Microscope (SEM) photograph of the outer surface of a neural bone of <u>Kinosternon subrubrum</u> (MSU-H 2477). 60X magnification.....	37
26.	Photograph of a Hematoxylin and Eosin (H+E) prepared histological slide showing the bisected carapace with the thin outer layer of compact bone shown between the non-staining scute and the deep spongy bone.....	38
27.	Photograph of a Hematoxylin and Eosin (H+E) prepared histological slide showing the spongy middle layer of a carapace with the marrow evident in the central areas.....	38
28.	Photograph of a Hematoxylin and Eosin (H+E) prepared histological slide showing a close view of the interconnection of the scute, compact bone layer, and vascular canal.....	39
29.	Photograph of a Hematoxylin and Eosin (H+E) prepared histological slide showing the different paths for blood through the subscute layer.....	39
30.	Photograph of a Hematoxylin and Eosin (H+E) prepared histological slide showing the subscute blood layer.....	41
31.	Photograph of a Hematoxylin and Eosin (H+E) prepared histological slide showing the osteocytes in their lacunae.....	41
32.	Photograph of a Hematoxylin and Eosin (H+E) prepared histological slide showing an osteoclast dissolving bone.....	43
33.	photograph of a Hematoxylin and Eosin (H+E) prepared histological slide showing osteoblasts lining the trabeculae of spongy bone.....	43

34. Scanning Electron Microscope (SEM) photograph of the edge surface of a peripheral bone of Chrysemys picta (MSU-H 2025). 60X magnification.....44
35. Scanning Electron Microscope (SEM) photograph of the inner surface of a peripheral bone of Chrysemys picta (MSU-H 2025). 60X magnification.....44
36. Scanning Electron Microscope (SEM) photograph of the outer surface of a costal bone of Chrysemys picta (MSU-H 2025). 60X magnification.....46
37. Scanning Electron Microscope (SEM) photograph of the outer surface of a peripheral bone of Chrysemys picta (MSU-H 2025). 60X magnification.....46
38. Scanning Electron Microscope (SEM) photograph of the outer surface of a neural bone of Chrysemys picta (MSU-H 2025). 60X magnification.....47
39. Scanning Electron Microscope (SEM) photograph of the outer surface of a plastral bone of Chrysemys picta (MSU-H 2025). 60X magnification.....47
40. Scanning Electron Microscope (SEM) photograph of the edge surface of a costal bone of Chrysemys picta (MSU-H 2025). 60X magnification.....49
41. Scanning Electron Microscope (SEM) photograph of the edge surface of a neural bone of Chrysemys picta (MSU-H 2025). 60X magnification.....49
42. Scanning Electron Microscope (SEM) photograph of the edge surface of a plastral bone of Chrysemys picta (MSU-H 2025). 60X magnification.....50
43. Scanning Electron Microscope (SEM) photograph of the inner surface of a neural bone of Chrysemys picta (MSU-H 2025). 60X magnification.....50
44. Scanning Electron Microscope (SEM) photograph of the inner surface of a costal bone of Chrysemys picta (MSU-H 2025). 60X magnification.....51
45. Scanning Electron Microscope (SEM) photograph of the inner surface of a plastral bone of Chrysemys picta (MSU-H 2025). 60X magnification.....51
46. Scanning Electron Microscope (SEM) photograph of the outer surface of a neural bone of Trionyx ferox

(MSU-H 478). 60X magnification.....	53
47. Frequency distribution of average number of the three different canal types in the family Emydidae...	54
48. Frequency distribution of average number of the three different canal types in the family Testudinidae.....	55
49. Frequency distribution of average number of the three different canal types in <u>Chrysemys picta</u> .....	57
50. Frequency distribution of average percentage area occupied by canals in the families of Testudines.....	58
51. Scanning Electron Microscope (SEM) photograph of the outer surface of a neural bone of <u>Chelus</u> <u>fimbriatus</u> (MSU-H 2613). 60X magnification.....	53
52. Scanning Electron Microscope (SEM) photograph of a "scrap" fossil of an unknown chelonian bone. 60X magnification.....	62
53. Scanning Electron Microscope (SEM) photograph of a "scrap" fossil of an unknown chelonian bone. 60X magnification.....	62
54. Scanning Electron Microscope (SEM) photograph of a "scrap" fossil of an unknown chelonian bone. 60X magnification.....	63
55. Scanning Electron Microscope (SEM) photograph of a "scrap" fossil of an unknown chelonian bone. 60X magnification.....	63
56. Scanning Electron Microscope (SEM) photograph of a "scrap" fossil of an unknown chelonian bone. 60X magnification.....	64
57. Scanning Electron Microscope (SEM) photograph of a "scrap" fossil of an unknown chelonian bone showing large foreign material on the surface of the fossil. 60X magnification.....	64
58. Scanning Electron Microscope (SEM) photograph of a "scrap" fossil of an unknown chelonian bone showing foreign material on the surface of the fossil. 60X magnification.....	65
59. Scanning Electron Microscope (SEM) photograph of	

a "scrap" fossil of an unknown chelonian bone showing erosion of the fossil material. 60X magnification.....	65
60. Frequency distribution of average K (small) values for the families of Testudines.....	67
61. Frequency distribution of average K (large) values for the families of Testudines.....	68
62. Frequency distribution of average R/t (small) values for the families of Testudines.....	69
63. Frequency distribution of average R/t (large) values for the families of Testudines.....	70
64. Scanning Electron Microscope (SEM) photograph of the outer surface of a neural bone of <u>Chrysemys picta</u> (MSU-H 2025). 60X magnification.....	73
65. Scanning Electron Microscope (SEM) photograph of the outer surface of a neural bone of <u>Chrysemys picta</u> (MSU-H 2025). 60X magnification.....	73
66. Number of Type A canals versus the number of Type B canals in all Testudines examined.....	77
67. Percent Area occupied by all canals versus number of Type A canals in all Testudines examined.....	78
68. Percent Area occupied by all canals versus number of Type A canals in the family Testudinidae.....	79
69. Percent Area occupied by all canals versus number of Type A canals in <u>Chrysemys picta</u> .....	80
70. Percent Area occupied by all canals versus number of Type A canals in the family Emydidae.....	81
71. Percent Area occupied by all canals versus number of Type C canals in the family Testudinidae.....	82
72. Percent Area occupied by all canals versus number of Type C canals in the family Emydidae.....	83
73. Percent Area occupied by all canals versus number of Type C canals in <u>Chrysemys picta</u> .....	84
74. Percent Area occupied by all canals versus number of Type C canals in the family Testudinidae.....	85

75. Photograph of a Hematoxylin and Eosin (H+E) prepared histological slide showing the subscute blood flow.....	87
76. Photograph of a Hematoxylin and Eosin (H+E) prepared histological slide showing an osteoclast dissolving bone.....	87
77. Total length of the femur versus the KR (small) value for all Testudines examined.....	94
78. Total length of the femur versus the KR (large) value for all Testudines examined.....	95
79. Total length of the femur versus the KR (small) value for the family Emydidae.....	96
80. Total length of the femur versus the KR (large) value for the family Emydidae.....	97
81. Total length of the femur versus the KR (small) value for the family Testudinidae.....	98
82. Total length of the femur versus the KR (large) value for the family Testudinidae.....	99
83. K (large) value versus the KR (large) value for all Testudines examined.....	100
84. K (small) value versus the KR (small) value for all Terstudines examined.....	101
85. K (large) value versus the R/t (large) value for all Testudines examined.....	102
86. K (small) value versus the R/t (small) value for all Testudines examined.....	103
87. Hematoxylin and Eosin (H+E) photograph of a carapace showing the single cell layer that produces the scute of the shell.....	106

## **INTRODUCTION**

The morphology of shell and long bones in turtles has been studied in some detail, but little work has been conducted to determine if and how these elements are involved in the physiology of this animal, encumbered as it is by a massive shell. This study will examine the long bones and shells of testudines to look for mechanisms of physiological control exerted by these structures. The surface of the carapace will be examined for morphological structures used to regulate or control blood flow. Physiological areas of study included will be temperature control by blood flow throughout the carapace, the carapace and long bones as an agent for calcium and phosphate reserves, and weight constraints of the shell on both the morphology of the limbs as well as a factor in the size of the marrow cavity. As a prefix to the text that is to follow, a general introduction to types of bone and a review of previous turtle shell and long bone work is given as follows.

### **Types of Bone**

The skeleton of vertebrate animals is composed of mineralized connective tissue commonly called bone. The primary step in the formation of skeletal tissue is the

synthesis of collagen by fibroblasts. Collagen is a proteinaceous fibril that aggregates to form bundles. These bundles are woven into compact networks. It is on this network that the Calcium Phosphate and collagen fibers are deposited to form bone. The bony tissue of vertebrate animals has been classified into six main groups (Kent, 1987). These groups are categorized as compact, spongy, dentin, acellular, membrane, and replacement bone.

Compact bone (also called Haversian bone) is characterized by lamellae of mineralized collagenous bundles arranged concentrically around a Haversian canal. These Haversian canals are the channels where the vascular tissue brings blood to the bone cells.

Spongy bone (also called Cancellous bone) is characterized by bony trabeculae and marrow. Trabeculae are an assemblage of beams, bars, and rods that, like architectural trusses, form a rigid framework that provides maximum strength at areas of stress. These trabeculae are irregularly arranged lamellae without Haversian canals.

Dentin is the material that covers teeth of vertebrates and scales of ganoid and elasmobranch fishes. It has the same constituents as compact and spongy bone except that the odontoblasts (dentin forming cells) are not trapped during osteogenesis. Thus, the odontoblasts are always at the inner border of the bone. These odontoblasts leave behind

canaliculi which are the protoplasmic processes for the dentin.

Acellular bone (also called Aspidin) is characterized by the osteoblasts (bone forming cells) that retreat as they deposit bone (as in dentin) and in addition leave no canaliculi behind (Bloom and Fawcett, 1962).

Membrane and Replacement bone are characterized by their different depositional patterns. Before bone can be deposited, a preskeletal blastema must develop. A blastema is an aggregation of mesenchyme that differentiates into varied tissues. Once the preskeletal blastema is formed, some mesenchyme cells become fibroblasts and secrete collagen while others become either osteoblasts or chondroblasts (cartilage forming cells) and secrete enzymes essential for the formation of bone or cartilage. The collagenous matrix is then impregnated with hydroxyapatite crystals.

Membrane bone is deposited directly within a membranous blastema without having been preceded by a cartilaginous model. Membrane bone may be compact or spongy, and lamellar or non-lamellar. Because of the arrangement of the blood vessels that participate in the deposition of the bone, membrane bone lacks Haversian canals. Dermal bone is derived either ontogenetically or phylogenetically from the dermis of the skin . The term Dermal bone denotes its



history, not its histologic features. Dermal bone is a form of membrane bone.

Replacement bone is deposited where hyaline cartilage already exists. In this process, the cartilage degenerates and eventually disappears. In replacement ossification, the cartilage must be removed before the hydroxyapatite crystals (bone) may be deposited. The cartilage is replaced by spongy bone which may later be eroded and replaced by compact bone, spongy bone, or a marrow cavity, depending on its location.

### **Bones of Testudines**

Suzuki (1963) grouped the bones of chelonians into three major classifications. These classifications are Primary Vascular bone, Endosteal Haversian bone, and Avascular bone.

Primary vascular bone was subdivided into three categories. These subdivisions were longitudinal, reticular, and prothaversian. Longitudinal primary vascular bone has vascular canals that are parallel to the long axis of the osseous tissue. Reticular primary vascular tissue has vascular canals that are patterned in a network. Prothaversian primary vascular tissue has osseous lamellae arranged concentrically around large irregularly shaped primary vascular channels or marrow cavities simulating Haversian canals.

Endosteal Haversian bone has concentric lamellae of bone deposited around a rounded vascular channel and is confined to the endosteal margin of the bone.

Avascular bone has no vascular canals and the osteocytes are arranged concentrically around the marrow cavity.

### **Carapace and Plastron**

The turtle shell (carapace and plastron) is morphologically arranged as a domed carapace and a flat plastron (Fig. 1). The outermost covering of shell structures is a horny covering primarily composed of Keratin called scutes. These scutes are periodically replaced as the turtle grows (Cagle, 1950). Underlying the scutes are the bony elements. The bony elements are comprised of two layers, the superficial epithecal layer and the central thecal layer. The epithecal layer is only present in marine and some freshwater turtles (Suzuki, 1963). Adult chelonians have appositional growth of the bony elements on the inner and outer surface forming layers of compact bone on both surfaces. These are called the inner and outer tables while the thecal layer has been called the intermediate diploe (Wallis, 1927). The outer table consists of a primary longitudinal vascular pattern and the inner table is a primary reticular vascular pattern. The vascular channels near the sutures of the bones are arranged

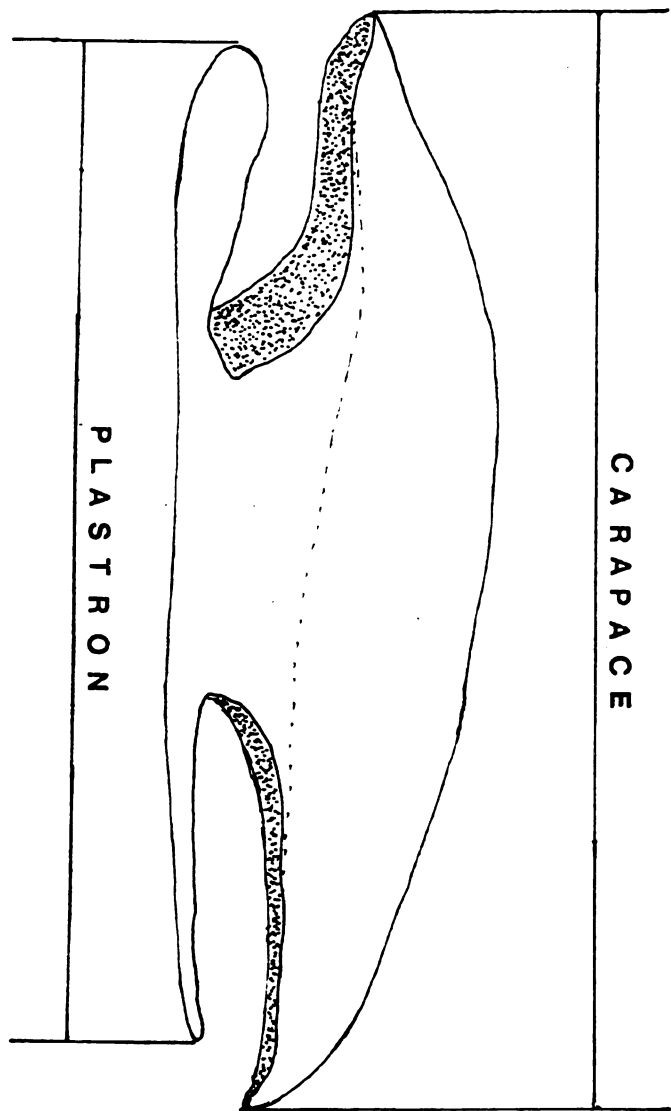


Figure 1. Side view of a turtle shell showing the arrangement of the carapace and plastron.

transversely to the plane of the sutures and gradually modified as they anastomose with the more mature parts of the carapace (Suzuki, 1963). Enlow and Brown (1957) noted differences between the vascular patterns in the outer and inner table of a dermal bone from a Cretaceous turtle, Glyptops. No mention was made if such variation existed in modern turtles.

The shell is composed of modified vertebral column elements, ribs, and dermal bones except for Dermochelys (Zangerl, 1939). The turtle body plan represents a major exception of the structural "bauplan" (body plan) of the vertebrates. This exception is that the girdle elements of the chelonian skeleton are inside the ribs instead of outside the ribs as in all other vertebrates (Burke, 1989).

The carapace of most turtles is composed of six different bony elements arranged in an ovoid shape. A central row of bones (nuchal, neurals, suprapygal, and pygal) are surrounded by rectangular bones (costals). Finally, arranged around the outer rim of the costals are the peripherals (Ernst and Barbour, 1989) (Fig. 2).

The plastron of most chelonians is composed of four paired bony plates (epiplastron, hyoplastron, hypoplastron, and xiphiplastron) and a single entoplastron between the epiplastra and hyoplastra (Fig. 3).

The number and arrangement of these bones has some

familial and species specific variations (Hay, 1908; McDowell, 1964). There are also extra bones that are present in some groups. Examples of this is the presence of a mesoplastron between the hyoplastra and hypoplastra in some taxa of the Family Pelomedusidae and in Claudius of the Kinosternidae.

### **Previous Shell Work**

The testudine carapace has been widely used in taxonomic studies. The main characters that have been used are scute pattern, bone suture pattern, and relationship of scutes to the underlying bone (Pritchard, 1979; Ernst and Barbour, 1989).

There are occasional reports of bone abnormalities in the shell. These anomalous bones are almost always reported the abnormalities with no explanation as to cause or effect of the abnormalities (Newman, 1906; Procter, 1922).

Turtles have one of the largest body mass to body volume ratios of the vertebrates (Hall, 1924). This is caused mainly by the bony shell. The extra weight that chelonians carry causes major changes in the animals habits and mode of locomotion. The testudinal gait reflects the need to exert enough force to move a body along with the burden of a heavy shell (Jayes and Alexander, 1980). The shell restricts the range of motion in many turtles and forces the animals to move in short strides. This gait

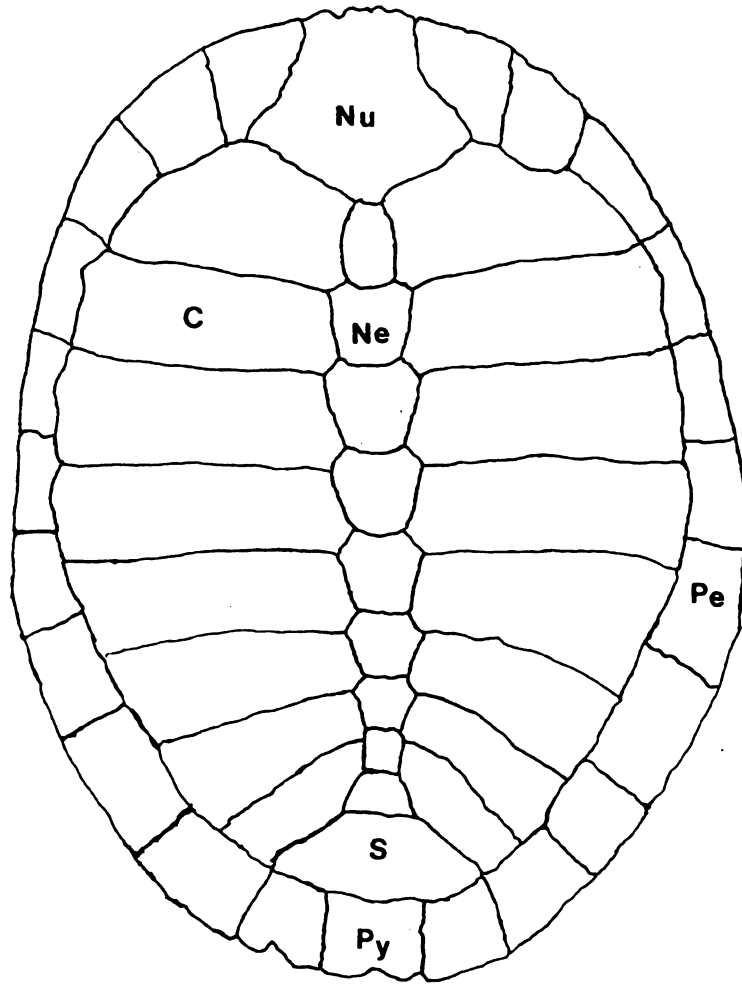


Figure 2. Diagram of the bony elements of the carapace including the nuchal (Nu), neurals (Ne), costals (C), peripherals (Pe), suprapygals (S), and pygal (Py).

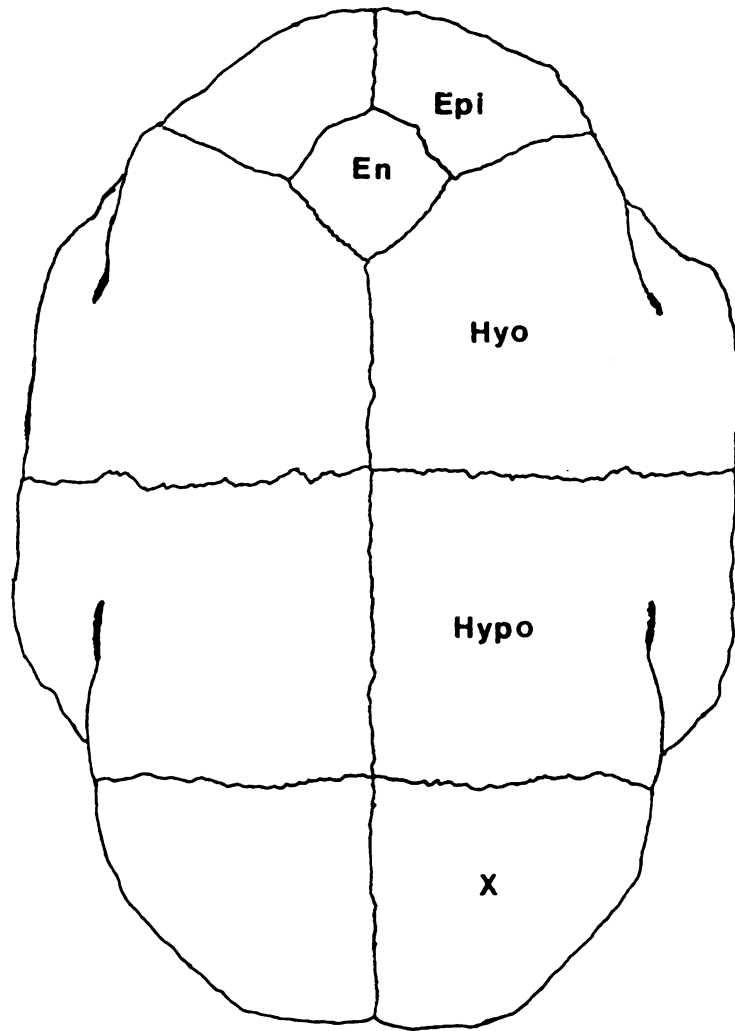


Figure 3. Diagram of the bony elements of the plastron including the epiplastron (Epi), entoplastron (En), hyoplastron (Hyo), hypoplastron (Hypo), and xiphiplastron (X).

allows the weight of the shell to reside almost entirely on one leg at a time (Alexander, 1982). Marvin and Lutterschmidt (1997) determined that the stride length of Terrapene carolina was affected by their body mass. The more weight that the chelonian carried, the shorter the length of the stride.

The shell has generally been assumed to be metabolically inert (Hall, 1924; Benedict, 1932; Hutton, et al., 1960; Hughes, et al., 1971; Dunson, 1986). However, using regression equations, Bennett and Dawson (1976) failed to detect any significant differences in body weight versus metabolic rate in lizards, snakes, and turtles. This indicates either (1) that the shell is metabolically active or (2) that the metabolic rate of other tissues in turtles is enough higher (20-40%) than other reptiles to compensate exactly for the inert character of the shell in the total metabolism (Bennett and Dawson, 1976). The carapace has been reported to have no seasonal change in density, (Suzuki, 1963), thus supporting the hypothesis that the carapace is metabolically inert.

In a study of Pseudemys and Chelydra shells, application of radiant heat to the carapace increased local blood flow; whereas cooling of the carapace decreased it, implying that local blood flow can be controlled by the animal (Avery, 1982). Changes in heart rate also aid in



rapid absorption or radiation of heat (Zug, 1993). Zug (1993) also stated that to retard cooling, reptiles reduce heart rate and peripheral circulation. The reduction of the heart rate and reduction of the peripheral circulation or the pulmonary circulation is commonly called cardiac shunting (Hicks and Wang, 1996).

### **Long Bones**

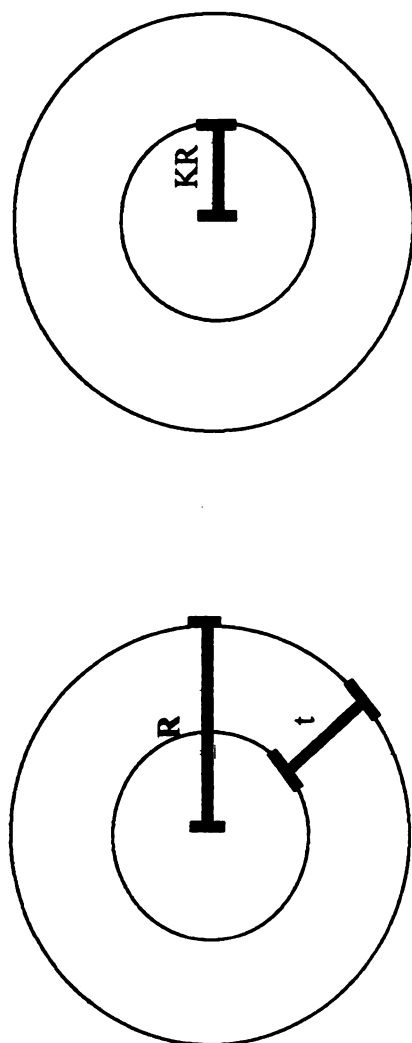
The limb bones of chelonians allow growth only on the inner surface of the marrow filled cavity. This leads to reduction in the size of the marrow cavity over time. Reabsorption of bone tissue acting as a calcium reserve in the long bones occurs for metabolic purposes (Suzuki, 1963). It is known that the endosteal long bones have lamellar layers of growth (Enlow, 1969). This allows the assumption that the marrow cavity of the long bones of turtles is reduced over time.

Long bones are much stronger or resistant to bending if the center section (marrow cavity) is hollow or filled with a material less dense than the bone (Alexander, 1982). The strength of these long bones can be calculated if the material in the cavity is known (Currey and Alexander, 1985). Turtle long bone cavities are filled with marrow which is about 0.44% as dense as bone.

The direction from which pressure is exerted on a long bone also determines its strength or resistance to bending.

These "stresses" can also alter the shape of the long bone during growth (Currey, 1984). Additional pressure on chelonian limb bones is caused by the excess weight of the shell.

Comparison of the size of the marrow cavity to the thickness of the bone wall (Currey and Alexander, 1985) is labeled as K (Fig. 4). K may range from 0.0 (where the bone is solid) to near 1.0 (where the bone is very thin with a large marrow cavity). This value depends on whether it is selected for yield strength, fatigue strength, ultimate strength, impact strength, or stiffness. Yield strength is described as the tissue being strong enough not to yield under the greatest bending moments likely to act on it. Fatigue strength is described as the tissue being strong enough not to fail by fatigue under the bending moments expected to act repeatedly on it. Ultimate strength is described as the tissue being strong enough not to fracture under the greatest bending moments likely to act on it. Impact strength is described as the tissue being strong enough in bending under impact loading. Stiffness is described as the tissue being stiff enough in bending. The optimum values for these were computed so that the K values would reflect the limiting factor on the limb being examined. These optimum values are 0.67 (Yield or Fatigue Strength); 0.56 (Ultimate Strength); 0.75 (Stiffness); and



- R** = Radius of the Outside Measurement  
**KR** = Radius of the Marrow Cavity  
**t** = Thickness of the Bone  
**K** = Ratio of the Internal Diameter to the External Diameter  
**R/t** = Ratio of the Radius of the Outside Measurement (R) to the Thickness of the Bone (t)

Figure 4. Conventions for the calculations of the bisected femur measurements.

0.55 (Impact Strength).

Currey and Alexander (1985) also compared the K values in limb bones of mammals, birds, and reptiles. They concluded that air filled bones of birds have very high K values due to the fact that bird bones require much bending strength and require a minimized mass for flight. Mammals have lower values of K as they increase in size. Aquatic animals like the alligator and marine mammals have low values of K, as this loss of marrow size is thought to aid the animal in attaining neutral buoyancy.

Currey and Alexander (1985) examined the ratio of the ratio of the radius of the complete bone (R) to the thickness of the bone wall (t), which yields the value  $R/t$ . This value is used to emphasize how greatly the shape changes as K approaches one. The value  $(R/t)$  is often used as well as or instead of K.  $R/t$  equals  $1/(1-K)$ .

If the marrow cavities of the long bones of testudines were the only place for the reabsorption of calcium, one would assume that the long bones would be reduced over time (ontogeny) and the strength of the bone would be greatly affected by the current calcium status of the turtle in question.

#### **Previous Long Bone Work**

The long bones of the unique pelagic turtle Dermochelys coreacea (Rhodin, et al., 1981) were studied relative to the

quantity of vascular canals in their cartilaginous plates. It was found that the chondro-osseous plates of Dermochelys has many vascular canals, a characteristic that is shared among many different marine vertebrates, but that is unique among the reptiles.

The osseous growth marks of long bones have been studied to indicate the age of turtles (Castanet and Cheylan, 1979) and it has been shown that the growth marks are useful in determining the age of turtles up to about twenty years.

## MATERIALS AND METHODS

Turtle shell bones were studied under the SEM to reveal the minute canalicular vascular system within them and histological slides were made to detect cells, such as osteoclasts, that would reflect metabolic activity in the shell. Long bones (femora) were sectioned and analyzed to reflect mechanical and physiological factors related to the restraints imposed by the shell.

### SEM Methods

The neural plates of 44 specimens from 9 families of Testudines were viewed in the Scanning Electron Microscope (SEM) in order to view their minute canalicular vascular system within them. Carapacial bones from 15 fossil turtles were also viewed in the SEM. Varied skeletal elements (neural, peripheral, costal, and plastral) from one Chrysemys picta specimen (MSU-H 2025) were viewed. Moreover, several different areas of the outer surface of the above neural were examined to evaluate variability within it.

The neural plates of the extant species were either taken as a complete neural bone from disarticulated specimens or a section of the neural bone was cut from whole specimens by using a dremel tool.

The fossil turtle specimens were taken as whole fragments of "scrap" fossil chelonian specimens from the MSU Museum collection. Scrap fossils are pieces that are usually identifiable only to the generic level.

The neural plates were cut to sizes compatible with mounting on stubs. After cutting, the bones were mounted on the stubs with an adhesive. The mounted bones were critical point dried (Balzers Critical Point Dryer). After critical point drying, the mounted bones were sputter-coated with gold (Emscope Sputter Coater).

Each mounted bone was then viewed in a Scanning Electron Microscope (SEM) (model JEOL JSM-35C). Micrographs were taken with the SEM at sixty times normal size to allow for maximal viewing of the neural with the best clarity. These micrographs also could be enlarged to many times the current magnification with little or no reduction in the clarity of the micrographs.

Some neurals were examined under high magnification to assess the type of bone growth on the surface of the shell as well as the lining of the vascular canal.

The different shell elements from one specimen of Chrysemys picta (MSU-H 2025) were observed to determine if variation occurred in the different surfaces of each bone. SEM micrographs were taken from each elements outer, edge and inner surfaces to assess the variation of these

elements.

The SEM micrographs were digitized by scanning into computer formats (TIFS). The computer files were then used in area analysis using Bioscan Optimas. The area analysis was collected using two different light intensity thresholds. The first threshold was set at a standard of one hundred (100) for all specimens for control purposes. The accurate method used a variable light intensity threshold that filled all of the holes allowing no bleeding of light into the bony tissue. The resulting numbers yielded percentages of the area of the micrograph that was occupied by canals.

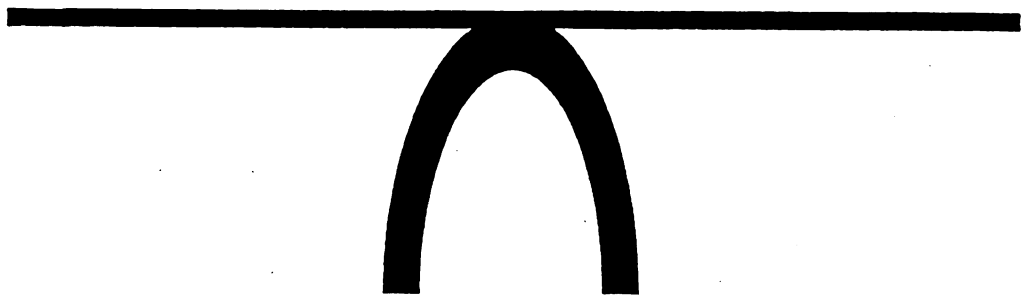
The vascular canals of the bones were divided into three categories. These were Types A, B, and C (Fig. 5). Type A vascular canals have a perpendicular arrangement with the outer surface of the carapace with no retreating vascular canal from the surface (Figs. 6 and 7). Type B vascular canals have a nearly perpendicular arrangement with the outer surface and an immediately adjacent retreating vascular canal (Figs. 8 and 9). Type C vascular canals have a tangential arrangement with the outer shell with a long parallel junction with the outer surface before the retreating tangential vascular canal (Figs. 10 and 11).

A Z-distribution analysis of canal types compared with each other was conducted for all testudines (Table 1). T-





TYPE A CANAL



TYPE B CANAL



TYPE C CANAL

Figure 5. Diagrammatic representation of the three different canals and their arrangement with the surface of the carapace.

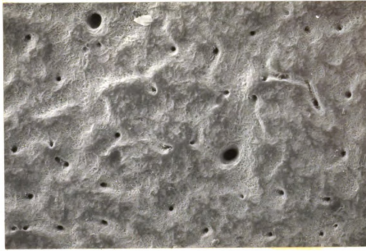


Figure 6. Scanning Electron Microscope (SEM) micrograph of the outer surface of a neural bone of Chrysemys picta (MSU-H 14309) showing an example of a Type A canal. 60X magnification.

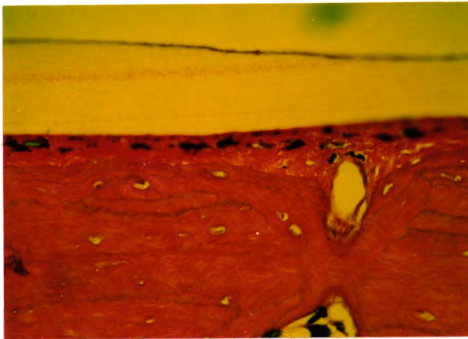


Figure 7. Photograph of a Hematoxylin and Eosin (H+E) prepared histological slide from Chrysemys picta (MSU-H 14309) showing an example of a Type A canal. 40X magnification.

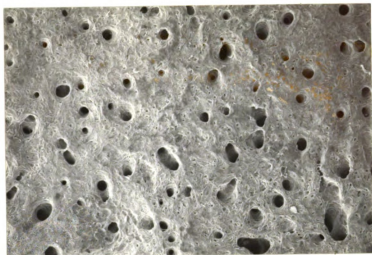


Figure 8. Scanning Electron Microscope (SEM) photograph of the outer surface of a neural bone of Chrysemys picta (MSU-H ) showing an example of a Type B canal. 60X magnification.

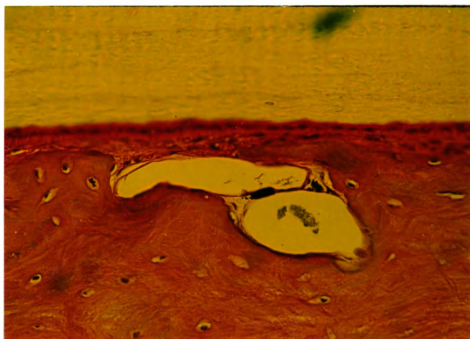


Figure 9. Photograph of a Hematoxylin and Eosin (H+E) prepared histological slide from Chrysemys picta (MSU-H ) showing an example of a Type B canal. 40X magnification.

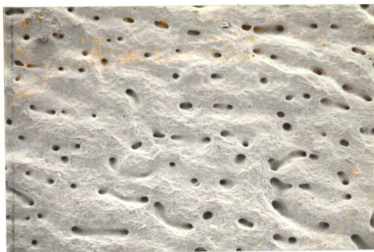


Figure 10. Scanning Electron Microscope (SEM) photograph of the outer surface of a neural bone of Chrysemys picta (MSU-H ) showing an example of a Type C canal. 60X magnification.

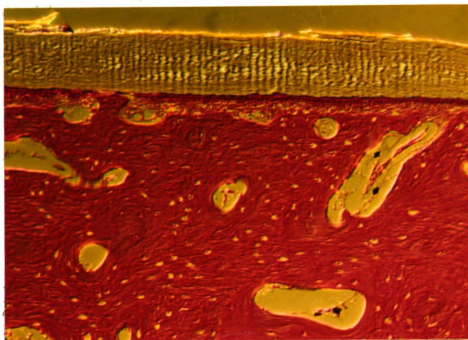


Figure 11. Photograph of a Hematoxylin and Eosin (H+E) prepared histological slide from Chrysemys picta (MSU-H ) showing an example of a Type C canal. 40X magnification.

distribution analyses of the canal types compared to each other were conducted for the families Emydidae (Table 2) and Testudinidae (Table 3).

Linear regressions were performed for each type of canal (A, B, and C) compared to the percent area of the canals. The tests were performed for all turtles examined, the members of the family Emydidae, the members of Chrysemys picta, and the members of the family Testudinidae. These data were derived from the SEM photographs previously scanned into the TIF files. The level of significance was placed at .05. All statistical analyses were conducted using the Softstat program (Softstat, 1996).

### **Histological Specimens**

Histological slides of turtle bones were made in order to identify cells capable of physiological activity. Neural bones (N2) of a formalin preserved specimen of Trachemys scripta elegans, Chelydra serpentina, and Terrapene carolina carolina were cut from the complete individual using a dremel tool. The pieces were then decalcified using the formic acid method (Sheehan and Hrapchak, 1980). The specimens were placed in a formic acid solution to allow for the tissues decalcification. The formic acid solution contained 500 ml of 88% formic acid and 500 ml of 10% neutral buffered formalin. The bones were washed in the solution for 24-48 hours. The bones were then washed with

**Table 1. Z distribution analysis data on significant differences in number of canal types for all testudines examined. Sample variances were not significantly different.**

Taxa	Average	Variance	Z-value	Prob>T
Type A Canals vs. Type B Canals	44.02 3.64	29.57 10.01	14.26	0.00
Type A Canals vs. Type C Canals	44.02 9.69	350.89 72.49	11.19	0.00
Type B Canals vs. Type C Canals	3.64 9.69	10.01 72.49	-4.46	0.00

**Table 2. T distribution analysis data on significant differences in number of canal types for the family Emydidae. Sample variances were not significantly different.**

Taxa	N	Mean	T	DF	Prob>T
Type A Canals vs. Type B Canals	28 28	51.36 3.21	18.24	27	0.00
Type A Canals vs. Type C Canals	28 28	51.36 10.28	12.80	27	0.00
Type B Canals vs. Type C Canals	28 28	3.21 10.28	4.79	27	0.00

**Table 3. T distribution analysis data on significant differences in number of canal types for the family Testudinidae. Sample variances were not significantly different.**

Taxa	N	Mean	T	DF	Prob>T
Type A Canals vs. Type B Canals	7 7	29.57 4.00	4.39	6	0.00
Type A Canals vs. Type C Canals	7 7	29.57 7.43	3.09	6	0.02
Type B Canals vs. Type C Canals	7 7	4.00 7.43	1.29	6	0.23



running water for 3 to 8 hours. After washing, the bones were mounted in paraffin and then sectioned to 4 micrometers. The sections were mounted and stained with Hematoxylin and Eosin using Sheehan and Hrapchak's method (1980).

These histological slides were compared with descriptions of the histological arrangement of carapacial bones in Suzuki (1963). The slides were viewed for the presence of cells that indicate metabolic activity in the shell such as osteoclasts and were viewed for the presence of other structures associated with physiological activities.

### **Long Bone Specimens**

Long bones were sectioned and analyzed to reflect mechanical and physiological factors related to the burden of the shell. Femora from 49 specimens from 6 families were obtained from skeletal collection specimens of the Michigan State University Museum (MSU-H). The femora were cut at the narrowest point of diaphyses using a dremel tool.

The greatest total length of the femur was measured before the specimens were cut with the dremel tool. The femora were measured using vernier calipers to the nearest hundredth of a millimeter. The femora of chelonians are not round as the cross section of the bone has a roughly triangular shape (Fig. 12). This triangular shape gives the



bone both a narrowest and widest point. This allowed for two complete sets of measurements. Sets of measurements were made of the bisected femora at the inside diameter of the marrow cavities and the outside diameter of the femora. Inside measurements were made by inserting the vernier calipers into the outermost section of marrow cavity in the long bone.

The measured values of the bisected femora allowed for many other values to be calculated (Appendix 3). Both sets of data were used for each set of calculations. These calculations start with the value  $K$ , which is defined as the ratio of the outer bone diameter to the inner bone diameter. The bone has a radius  $R$  (half the measured diameter) and a marrow cavity of radius  $KR$  (half the measured inside diameter). The thickness of the bone wall ( $t$ ) results from subtracting the inside diameter from the outside diameter. Finally, the ratio of the radius of the complete femur ( $R$ ) to the thickness of the bone wall ( $t$ ), will yield  $R/t$ .

Linear regressions were performed of the different measurements and calculations from the long bones to determine which of the measurements or calculations would be most useful in determining relationships of turtles on the basis of their long bones. The measurements and calculations used in the linear regressions were total length of the bone,  $K$  (large),  $K$  (small),  $KR$  (large),  $KR$

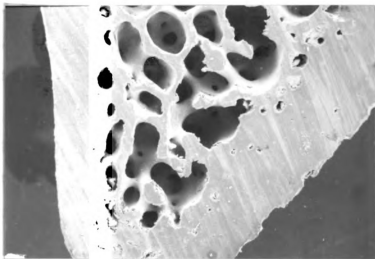


Figure 12. Scanning Electron Microscope (SEM) photograph of the bisected femur of Chrysemys picta (MSU-H 2025). 30X magnification.

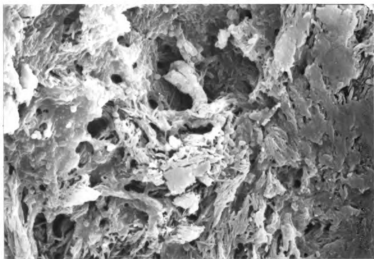


Figure 13. Scanning Electron Microscope (SEM) photograph of the outer surface of a neural bone of Trachemys scripta elegans (MSU-H 2716). 3000X magnification.

(small), R/T (large), R/T (small). These regressions were performed for all turtles examined, members of the family Emydidae, and members of the family Testudinidae. The level of significance for these regressions was placed at the .05 level.

Images in this dissertation are presented in color. All Hematoxylin and Eosin (H+E) prepared photographs are color photographs.

## RESULTS

This section presents the results of the SEM studies, the histology work and the analyses of the long bone data.

### **Types of bone throughout the shell**

Neurals that were examined under high magnification (up to 6600X) showed that the outer layer of the shell was composed of acellular bone composed of a fibrous matrix in which the orientation of collagenous fibers are in a random arrangement (Enlow, 1969) (Figs. 13, 14, and 15). The lining of the vascular canals were also composed of acellular bone (those areas that could be seen with the SEM) (Figs. 16, 17, and 18).

The surfaces of the different chelonian neurals were structurally diverse. They all had the same type of bone (acellular) on their surface although the appearance of the matrix was diverse. Acellular bone is characterized by a unorganized aggregation of collagen fibril bundles (Bloom and Fawcett, 1962). The collagen fibers in some photographs were very large and gave the matrix a rugose appearance. The Chelydra serpentina specimen is a good example of this rugose matrix (Fig. 19). The collagen fibers in other photographs were small and gave the matrix a smooth

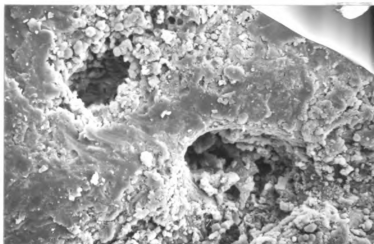


Figure 14. Scanning Electron Microscope (SEM) photograph of the outer surface of a neural bone of Kinosternon flavescens (MSU-H 2920). 320X magnification.

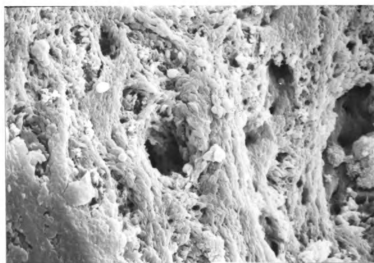


Figure 15. Scanning Electron Microscope (SEM) photograph of the outer surface of a neural bone of Clemmys insculpta (MSU-H 4336). 2000X magnification.

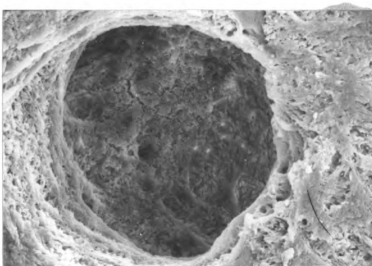


Figure 16. Scanning Electron Microscope (SEM) photograph of the outer surface of a neural bone showing the lining of one of the vascular canals of Trachemys scripta elegans (MSU-H 2716). 1000X magnification.

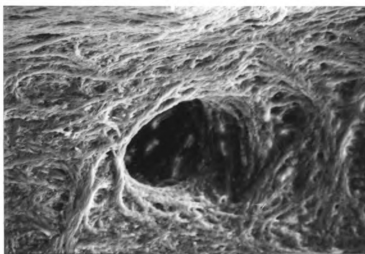


Figure 17. Scanning Electron Microscope (SEM) photograph of the outer surface of a neural bone showing the lining of one of the vascular canals of Chrysemys picta (MSU-H 2025). 600X magnification.

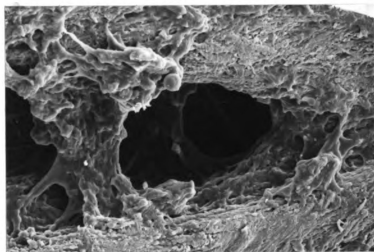


Figure 18. Scanning Electron Microscope (SEM) photograph of the outer surface of a neural bone showing the lining of one of the vascular canals of Chelydra serpentina (MSU-H 3436). 360X magnification.

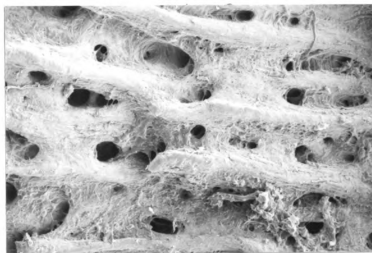


Figure 19. Scanning Electron Microscope (SEM) photograph of the outer surface of a neural bone of Chelydra serpentina (MSU-H 3436). 60X magnification.

appearance. The Chrysemys picta specimens have a smooth appearing matrix (Figs. 20, 21, and 22). A few neurals had matrix that appeared granular. This appearance comes from the lack of collagen fibers with the primary amount of matrix being the calcium phosphate. The members of the Family Kinosternidae are good examples of this type of matrix (Figs. 23, 24, and 25).

The cross sectional slides of the shell in Trachemys scripta elegans, Chelydra serpentina, and Terrapene carolina carolina were similar in that they all had an outer table and an inner table (diploe) of compact bone (Fig. 26) and a middle section of spongy bone (Fig. 27). The outer and inner tables were proportionally thin as the middle spongy layer comprised most of the shell. This spongy layer was the location of the majority of the canals that carry blood to the surface of the shell as seen in the SEM photos. The canals are lined with acellular bone unlike the trabeculae found in the spongy middle layer composed of trabecular bone and marrow. The canals do not form a direct route to the surface of the shell, but follow a tortuous winding path to the surface and back down again to the marrow. In fact, it is the type of connection of these canals to the surface that defines the structural makeup of the different canal types (see fig. 28).

A feature observed here that has not been previously



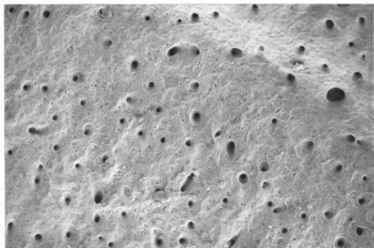


Figure 20. Scanning Electron Microscope (SEM) photograph of the outer surface of a neural bone of Chrysemys picta (MSU-H 14309). 60X magnification.

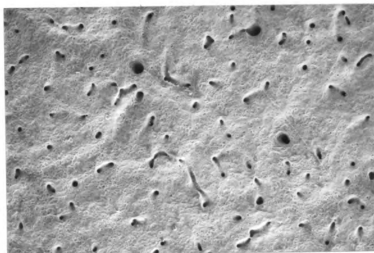


Figure 21. Scanning Electron Microscope (SEM) photograph of the outer surface of a neural bone of Chrysemys picta (MSU-H 14310). 60X magnification.



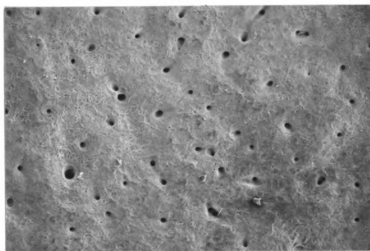


Figure 22. Scanning Electron Microscope (SEM) photograph of the outer surface of a neural bone of Chrysemys picta (MSU-H 14312). 60X magnification.

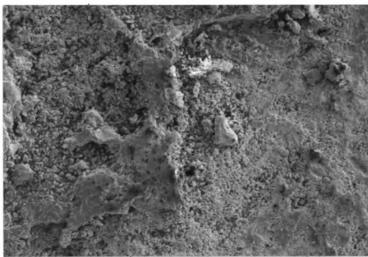


Figure 23. Scanning Electron Microscope (SEM) photograph of the outer surface of a neural bone of Kinosternon flavescens (MSU-H 2920). 60X magnification.

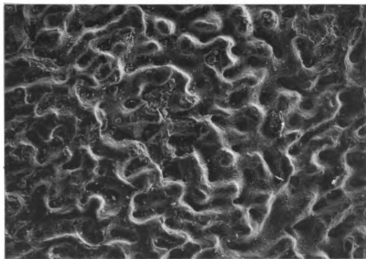


Figure 24. Scanning Electron Microscope (SEM) photograph of the outer surface of a neural bone of Kinosternon leucostomum (MSU-H 1414). 60X magnification.

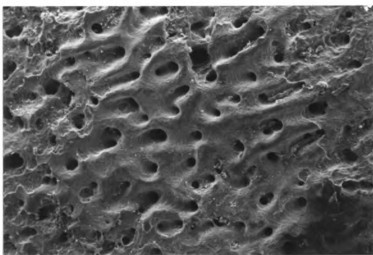


Figure 25. Scanning Electron Microscope (SEM) photograph of the outer surface of a neural bone of Kinosternon subrubrum (MSU-H 2477). 60X magnification.

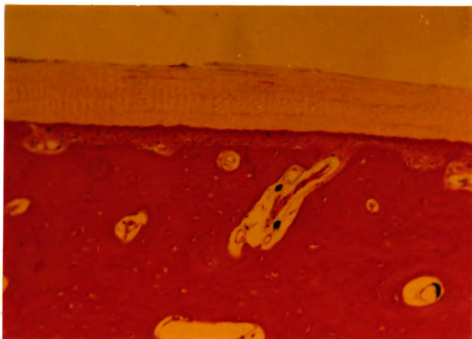


Figure 26. Photograph of a Hematoxylin and Eosin (H+E) prepared histological slide showing the bisected carapace with the thin outer layer of compact bone shown between the non-staining scute and the deep spongy bone.

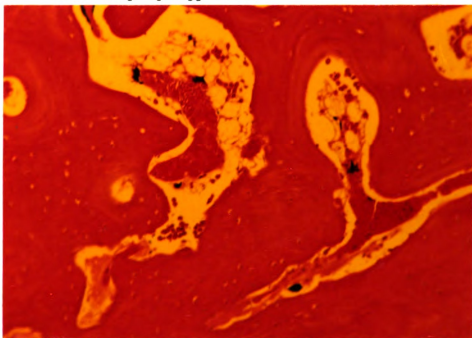


Figure 27. Photograph of a Hematoxylin and Eosin (H+E) prepared histological slide showing the spongy middle layer of a carapace with the marrow evident in the central areas.

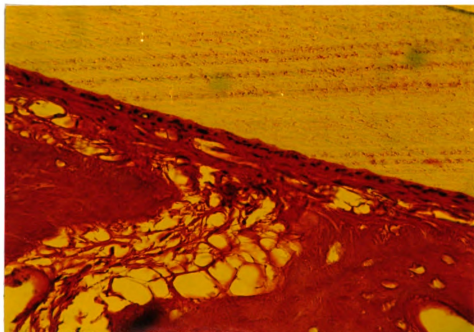


Figure 28. Photograph of a Hematoxylin and Eosin (H+E) prepared histological slide showing a close view of the interconnection of the scute, compact bone layer, and vascular canal

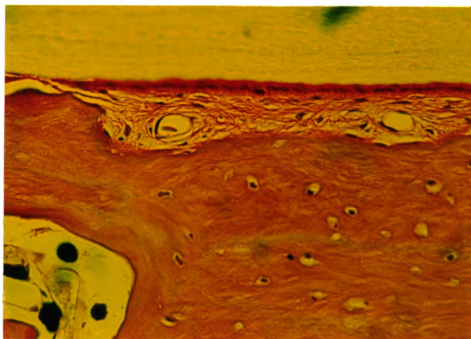


Figure 29. Photograph of a Hematoxylin and Eosin (H+E) prepared histological slide showing the different paths for blood through the subscute layer.



discussed in the literature occurs between the outer table of bone and the scutes of the shell as a thin layer of blood. This blood moves from relatively large canals to canals of (as small as) a single blood cell in thickness. These subscute blood flow is immediately beneath the scutes with no bone between the capillary and the scute. This arrangement would allow the blood in the capillary to absorb or radiate heat with no interference from the thick acellular bone. The scute would be the only interference with the ambient temperature of the external environment. Bone is much less dense than Scutes. This allows the keratin of the scutes to change temperature in relationship to its surroundings much faster than bone (Monteith, 1973). The blood flowing through the capillaries was contiguous with other blood in the system except that it was not determined how its flow was directed through the subscute layer of the shell (Figs. 29 and 30).

#### **Metabolic materials observed in the shell**

There were no living cells detected in the thin inner and outer tables. The middle layer of spongy bone was very similar in appearance to the marrow cavity of a long bone as trabeculae were present in large quantities. Osteocytes were also observed in the trabeculae of the spongy middle layer (Fig. 31). These "mature bone cells" maintain normal bone structure by recycling the calcium salts in the bony



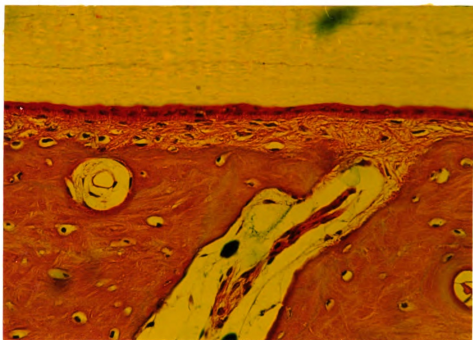


Figure 30. Photograph of a Hematoxylin and Eosin (H+E) prepared histological slide showing the subscute blood layer.

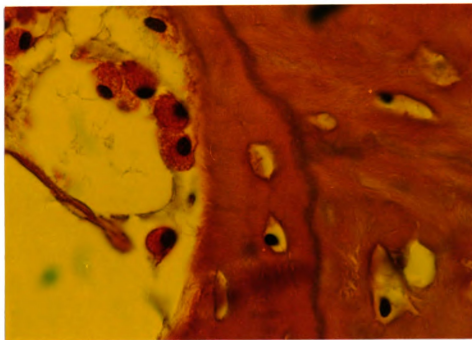


Figure 31. Photograph of a Hematoxylin and Eosin (H+E) prepared histological slide showing the osteocytes in the lacunae.

matrix around themselves and assisting in repairs (Martini and Bartholomew, 2000). Osteoclasts are large multinucleated cells that secrete acids to break down bone and release the calcium and phosphate that is bound in the tissue (Martini and Bartholomew, 2000). Osteoclasts were observed in the process of osteolysis (Fig. 32). Osteoblasts are cells that produce the fibers and matrix of bone or the production of new bone (Martini and Bartholomew, 2000). Osteoblasts were observed lining the marrow cavities of the spongy bone (Fig. 33).

#### **Variation of the shell of an individual Organism**

The elements from a single specimen of Chrysemys picta (MSU-H 2025) showed large variations in the number and types of canals. The percentage of canals compared to the bony tissue ranged from 5.34% to 42.35%. The only two measurements that exceeded 15% occurred in the edge of the peripheral bone (Fig. 34) and the inner surface of the peripheral bone (Fig. 35) (Table 4). The photomicrographs of the outer surfaces of the costal, peripheral, and neural were all similar in appearance with large numbers of Type A canals and moderate numbers of Types B and C canals (Figs. 30, 31, and 32). The outer surface of the plastron had differences in types of canals present. Only Type C canals occurred in the outer surface photograph of the plastron (Fig. 39). Cross cut edge photographs of all specimens were

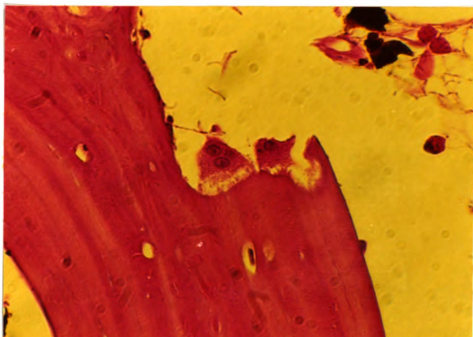


Figure 32. Photograph of a Hematoxylin and Eosin (H+E) prepared histological slide showing an osteoclast in the process of dissolving bone.

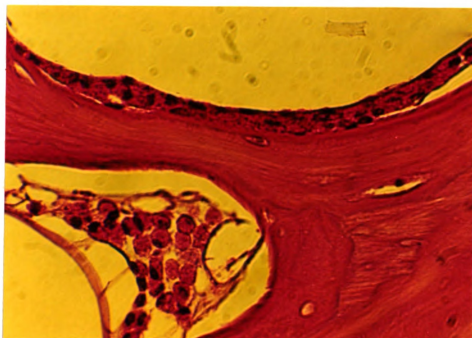


Figure 33. Photograph of a Hematoxylin and Eosin (H+E) prepared histological slide showing osteoblasts lining the trabeculae of spongy bone.

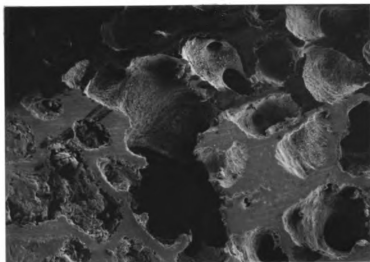


Figure 34. Scanning Electron Microscope (SEM) photograph of the edge surface of a peripheral bone of Chrysemys picta (MSU-H 2025). 60X magnification

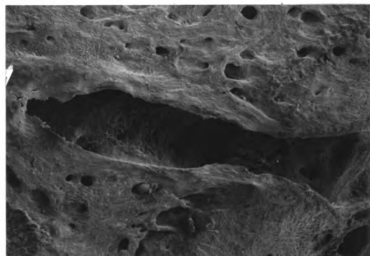


Figure 35. Scanning Electron Microscope (SEM) photograph of the inner surface of a peripheral bone of Chrysemys picta (MSU-H 2025). 60X magnification.

Table 4. Percentage area of the scanning electron microscope (SEM) images occupied by canals at both a standard threshold and a variable threshold for different surfaces of varied bony elements of a single *Chrysemys picta* specimen (MSU-H 2025).

Shell Element	Surface	% Area (100)	% Area (Var.)	Var.
Neural	Outer	09.71	10.09	110
Neural	Inner	16.86	06.83	40
Neural	Edge	14.60	08.78	50
Peripheral	Outer	20.71	12.34	57
Peripheral	Inner	48.13	26.26	45
Peripheral	Edge	66.22	42.35	45
Costal	Outer	15.00	08.99	57
Costal	Inner	26.55	12.83	46
Costal	Edge	60.19	12.88	23
Plastral	Outer	23.18	10.69	42
Plastral	Inner	28.68	07.84	48
Plastral	Edge	76.31	05.34	30

Table 5. Percentage area of the scanning electron microscope (SEM) images occupied by canals at both a standard threshold and a variable threshold for fossil specimens.

MSU-VP #	% Area (100)	% Area (Var.)	(Var.)
847	08.36	09.04	135
849	09.04	07.91	91
Williston, FL	10.06	06.13	70
Williston, FL	09.40	07.79	80
Keya Paha Co., NE	12.82	10.27	75
Keya Paha Co., NE	09.02	11.76	130
Keya Paha Co., NE	11.47	09.53	85
Keya Paha Co., NE	09.51	09.58	105
Keya Paha Co., NE	09.18	08.92	90
Keya Paha Co., NE	08.93	08.55	95
Keya Paha Co., NE	12.52	11.40	85
Keya Paha Co., NE	09.06	08.46	90
Keya Paha Co., NE	07.50	08.25	110
Keya Paha Co., NE	50.88	09.82	40
Keya Paha Co., NE	20.40	07.25	50
Keya Paha Co., NE	09.40	07.79	80

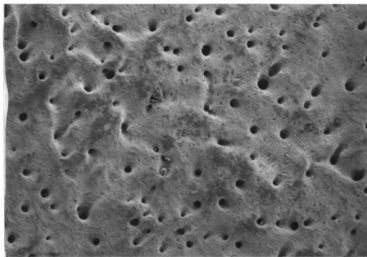


Figure 36. Scanning Electron Microscope (SEM) photograph of the outer surface of a costal bone of Chrysemys picta (MSU-H 2025). 60X magnification.

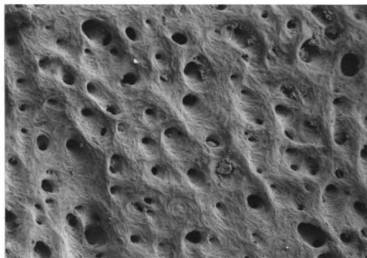
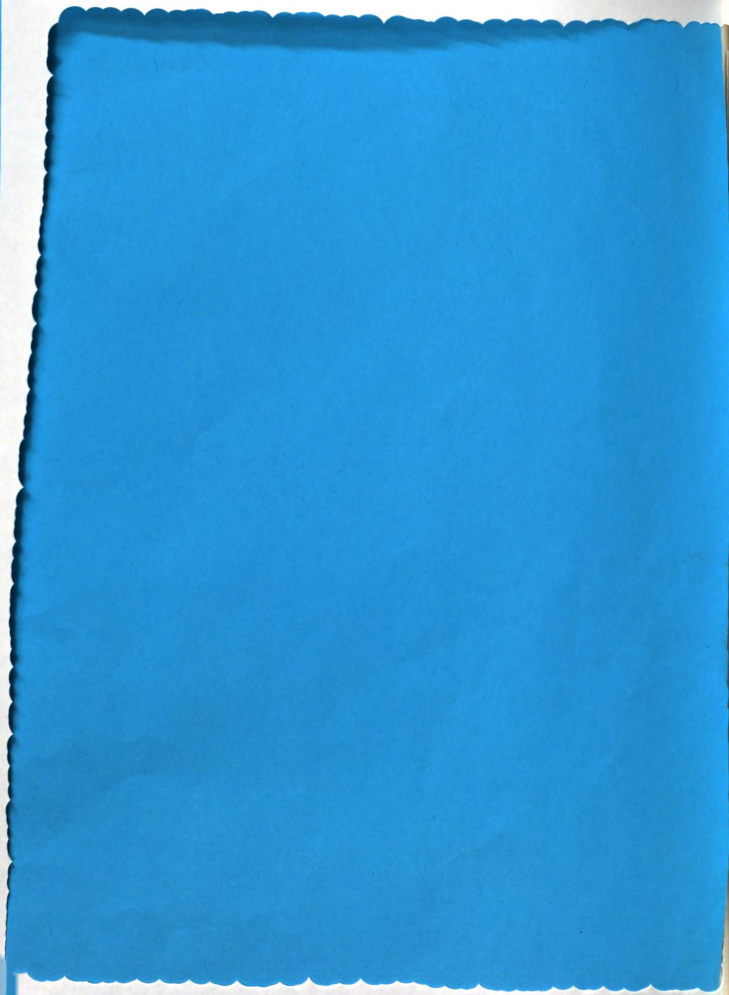


Figure 37. Scanning Electron Microscope (SEM) photograph of the outer surface of a peripheral bone of Chrysemys picta (MSU-H 2025). 60X magnification.







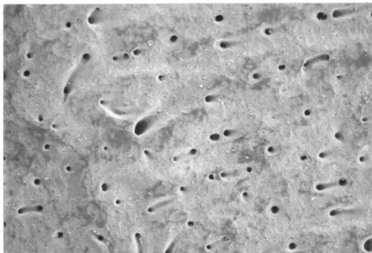


Figure 38. Scanning Electron Microscope (SEM) photograph of the outer surface of a neural bone of Chrysemys picta (MSU-H 2025). 60X magnification.

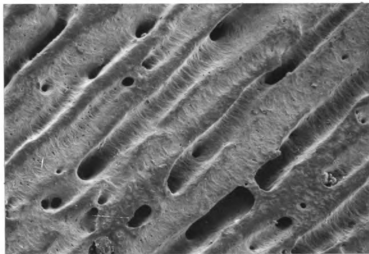


Figure 39. Scanning Electron Microscope (SEM) photograph of the outer surface of a plastral bone of Chrysemys picta (MSU-H 2025). 60X magnification.

similar in appearance with low amounts of vascularization near the outer and inner tables and high amounts in the middle table. (Figs. 34, 40, 41, and 42).

Inner surface photographs were the most diverse in appearance, as well as the size and type of canals. The inner surface of the neural (Fig. 43) had 3 Type A canals and 2 Type B canals (all small in size) within a very smooth matrix. The inner surface of the peripheral (Fig. 23) had one large Type B canal with several other smaller canals of Type A and B. The matrix was rugose with the collagen fibers easily seen in this view. The inner surface of the costal (Fig. 44) had a large number of all types of canals along with the presence of a rugose matrix. The inner surface of the plastral (Fig. 45) had 5 moderately sized Type B canals and one Type C canal. The matrix appeared intermediate between the matrix of the neural and the matrices of the peripheral and costal.

#### **Variation of shells of different groups examined**

Several families of turtles were so structurally distinct that they could be identified from the photographs without the use of statistics. These families include the Trionychidae, Chelydridae, and Kinosternidae. The modern Trionychid specimen (Fig. 46) had very few large canals within a smooth matrix. The Chelydrid specimen (Fig. 19) had a large number of large Type C canals (the only specimen

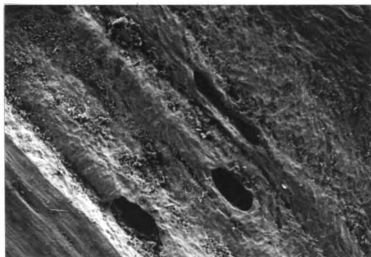


Figure 40. Scanning Electron Microscope (SEM) photograph of the edge surface of a costal bone of Chrysemys picta (MSU-H 2025). 60X magnification.

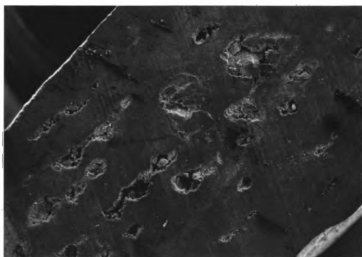


Figure 41. Scanning Electron Microscope (SEM) photograph of the edge surface of a neural bone of Chrysemys picta (MSU-H 2025). 60X magnification.

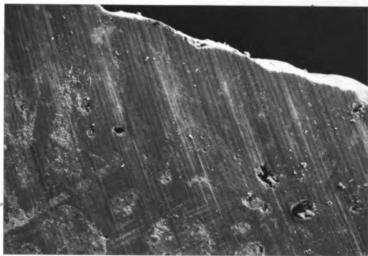


Figure 42. Scanning Electron Microscope (SEM) photograph of the edge surface of a plastral bone of Chrysemys picta (MSU-H 2025). 60X magnification.

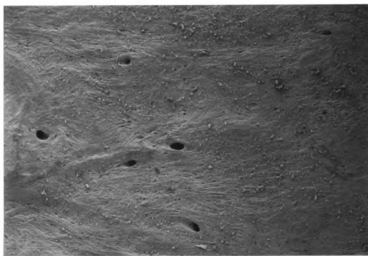


Figure 43. Scanning Electron Microscope (SEM) photograph of the inner surface of a neural bone of Chrysemys picta (MSU-H 2025). 60X magnification.

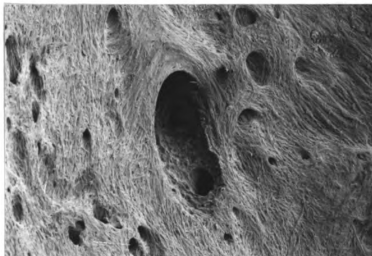


Figure 44. Scanning Electron Microscope (SEM) photograph of the inner surface of a costal bone of Chrysemys picta (MSU-H 2025). 60X magnification.

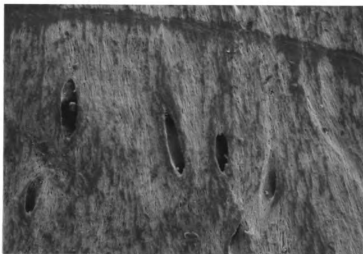


Figure 45. Scanning Electron Microscope (SEM) photograph of the inner surface of a plastral bone of Chrysemys picta (MSU-H 2025). 60X magnification.

with Type C canals equaling the number of Type A canals) within a rugose matrix. The Kinosternid specimens (Figs. 23, 24, and 25) had generally small canals within a primarily calcium phosphate matrix. One of the Kinosternid specimens had a large number of Type C canals (the only specimen with Type C canals exceeding the number of Type A canals).

The types of surface-reaching canals markedly differed between taxonomic groups (Appendix 2), although all turtles, both at the ordinal and familial level, had significantly more Type A canals than either of the other types of canals (Tables 1, 2, and 3). The average number of each canal type was compared between the families Emydidae (Figure 47) and Testudinidae (Fig. 48). Although the number of canals in each family was different, the variance between the numbers of each type of canal was similar. The Type A canals were significantly larger than the other two types in both families, but Type C canals were significantly larger than the Type B canals in the family Emydidae but not in the Testudinidae. All specimens of Chrysemys picta were examined for comparisons of averages of canal types (T-tests) (Table 5) with each type of canal significantly different than the other (Fig. 49).

The area analysis of the SEM photographs was averaged with the percentage of area occupied by canals in the

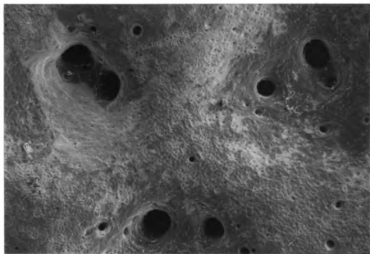


Figure 46. Scanning Electron Microscope (SEM) photograph of the outer surface of a neural bone of Trionyx ferox (MSU-H 478). 60X magnification.

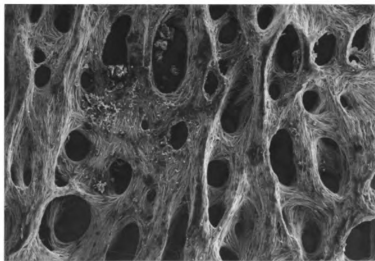


Figure 51. Scanning Electron Microscope (SEM) photograph of the outer surface of a neural bone of Chelus fimbriatus (MSU-H 2613). 60X magnification.

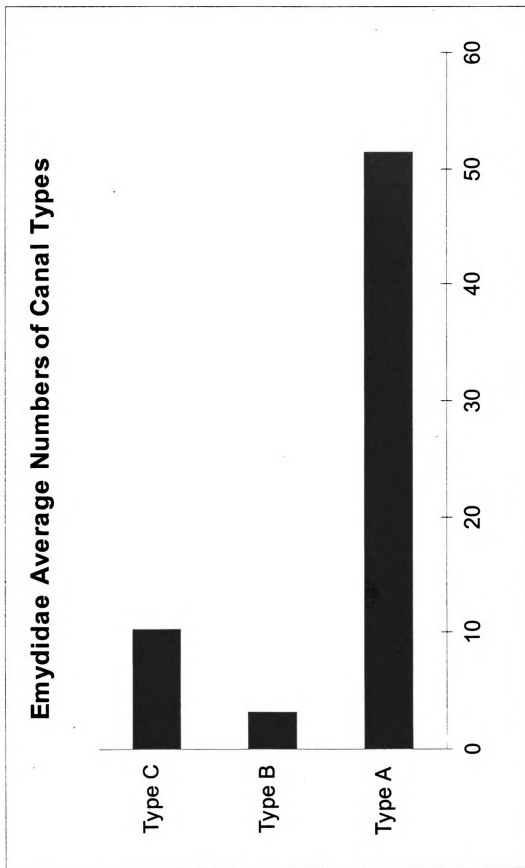


Figure 47. Frequency distribution of average numbers of the three different canal types in the family Emydidae.



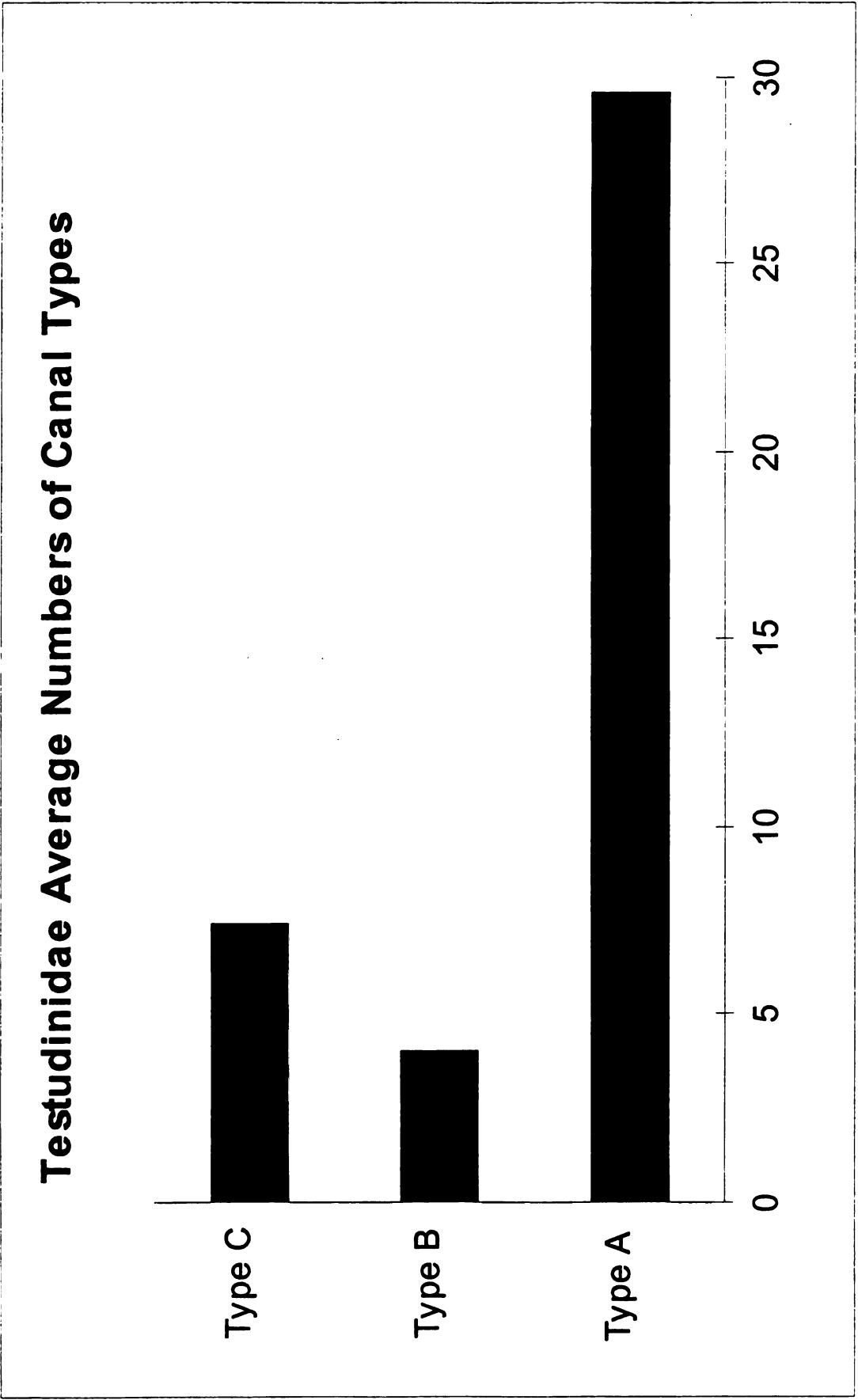


Figure 48. Frequency distribution of average numbers of the three different canal types in the family Testudinidae.

photographs. This data enabled the comparison of the different families of chelonians by their percentage of area occupied by canals (Fig. 50). Figure 50 is misleading because the other category contains many of the testudines that live in unique or unusual habitats. In fact, the largest area occupied by canals was in a single individual of the cheliid genus, Chelus fimbriatus (Fig. 51).

The linear regressions of the types of canals compared to the area occupied by canals for all chelonia was significant for type B canals but not for type A or C canals (Table 6). The linear regressions of the types of canals compared to the area occupied by canals for the family Emydidae was significant for types A and B canals but not for type C canals (Table 7). The linear regressions of the types of canals compared to the area occupied by canals for the family Testudinidae (Table 8) and for specimens of *Chrysemys picta* (Table 9) were not significant for any of the three canal types.

#### **Fossil specimens examined and techniques applied to them**

The fossil specimens photographed were examined for the percentage area that the canals occupied compared to the matrix of the bone (Table 10). Variable percentage area occupied by the canals ranged from 6.13 percent to 11.76 percent.

The fossil specimens examined had the same general

### C. picta Average Numbers of Canal Types

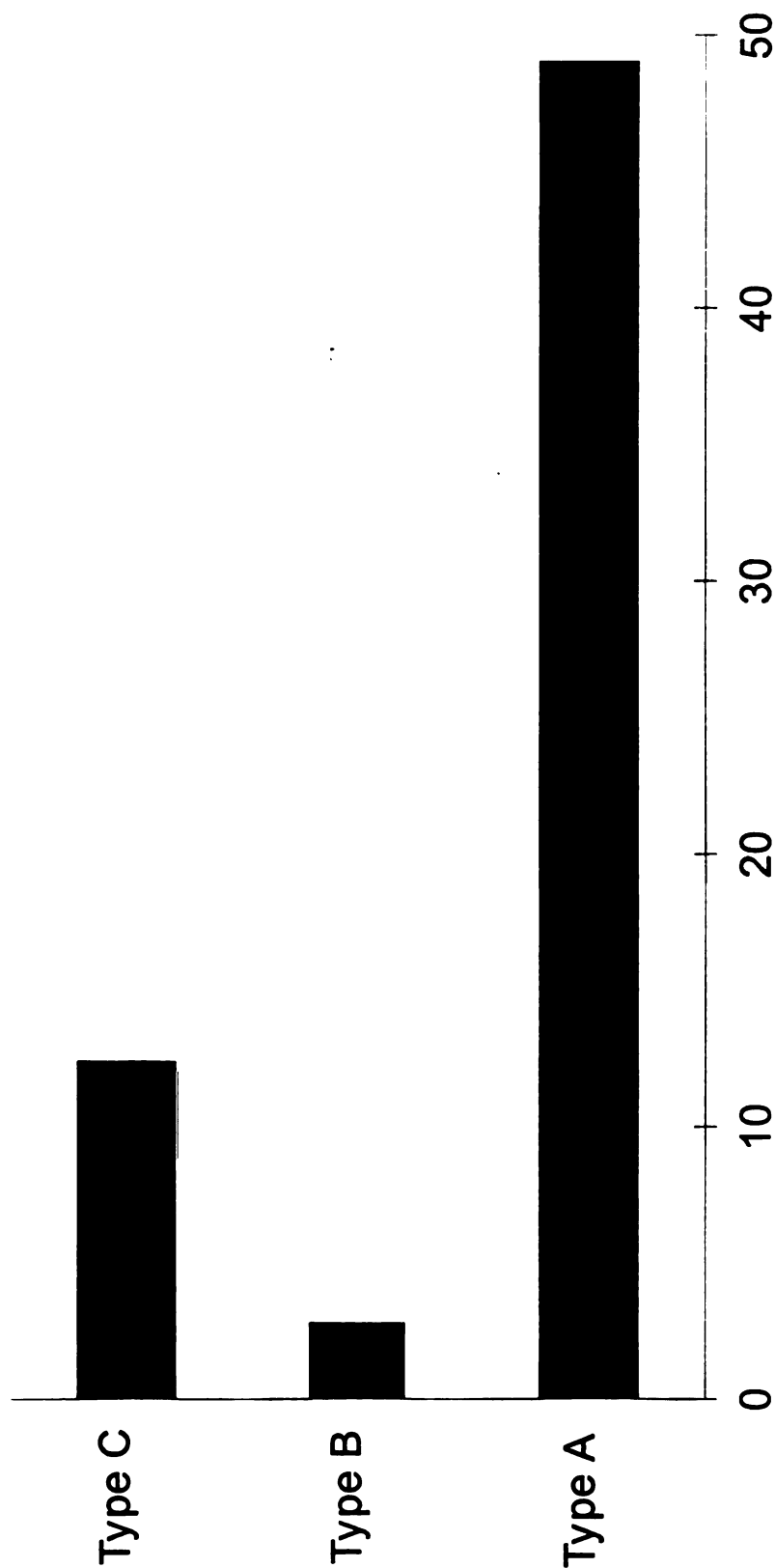


Figure 49. Frequency distribution of average numbers of the three different canal types in Chrysemys picta.

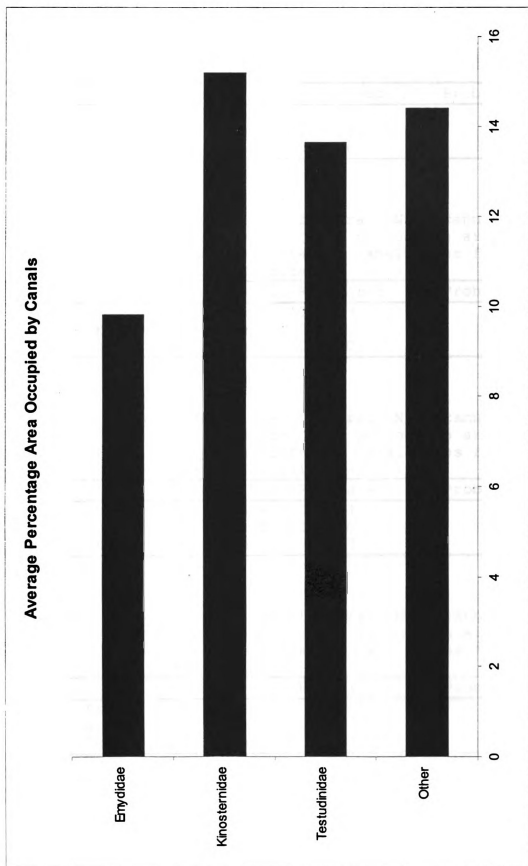


Figure 50. Frequency distribution of average percentage area occupied by canals in the families of Testudines.

Table 6. Linear regressions of neural (N2) Scanning Electron Microscope (SEM) photograph area analysis compared to the different canal types for all Testudines.

Independ. Var.	Dependent Var.	R-squared	Prob. Value
Percent Area	Canal Type A	0.0073	0.5649
Percent Area	Canal Type B	0.3027	0.0001
Percent Area	Canal Type C	0.0166	0.3827

Table 7. Linear regressions of neural (N2) Scanning Electron Microscope (SEM) photograph area analysis compared to the different canal types for members of the family Emydidae.

Independ. Var.	Dependent Var.	R-squared	Prob. Value
Percent Area	Canal Type A	0.2269	0.0106
Percent Area	Canal Type B	0.3821	0.0005
Percent Area	Canal Type C	0.0000	0.9928

Table 8. Linear regressions of neural (N2) Scanning Electron Microscope (SEM) photograph area analysis compared to the different canal types for members of the family Testudinidae.

Independ. Var.	Dependent Var.	R-squared	Prob. Value
Percent Area	Canal Type A	0.0004	0.9643
Percent Area	Canal Type B	0.1040	0.4718
Percent Area	Canal Type C	0.0627	0.5811

Table 9. Linear regressions of neural (N2) Scanning Electron Microscope (SEM) photograph area analysis compared to the different canal types for members of Chrysemys picta.

Independ. Var.	Dependent Var.	R-squared	Prob. Value
Percent Area	Canal Type A	0.0266	0.4947
Percent Area	Canal Type B	0.1227	0.1247
Percent Area	Canal Type C	0.1597	0.0918

structure of ground substance relative to the canal types present as did the extant specimens (Fig. 52). Many different problems were detected in viewing the fossil specimens. All problems arose from foreign materials associated with the fossil or from erosion of the specimen at the microscopic level. In many specimens the canals were covered or filled in with foreign material (Figs. 53, 54, 55, and 56). Foreign material occurred on the surface of five different fossils (Figs. 57 and 58). Erosion of the carapace occurred in one fossil specimen (Fig. 59) which affected the canal area data for that specimen.

#### **Long Bone Data**

The long bones of the chelonian samples provided data on total length, inside diameter (small), inside diameter (large), outside diameter (small), and outside diameter (large). These data were used to make multiple calculations which include  $K$  (small),  $K$  (large),  $R$  (small),  $R$  (large),  $KR$  (small),  $KR$  (large),  $t$  (small),  $t$  (large),  $R/t$  (small), and  $R/t$  (large) [see Appendix 3].

Averages for  $K$  (small) and  $K$  (large) were compared between the different families of turtles (Figs. 60 and 61) and were larger for the families Trionychidae, Kinosternidae, and Chelydridae. The averages of  $R/t$  (small) and  $R/t$  (large) were compared between the different families of turtles (Figs. 62 and 63) and were also larger for the

Table 10. Percentage area of the scanning electron microscope(SEM) images occupied by canals at both a standard threshold and a variable threshold for fossil specimens.

MSU-VP #	% Area (100)	% Area (Var.)	(Var.)
847	08.36	09.04	135
849	09.04	07.90	91
Williston, FL	10.06	06.12	70
Williston, FL	09.39	07.78	80
Keya Paha Co., NE	12.82	10.27	75
Keya Paha Co., NE	09.02	11.76	130
Keya Paha Co., NE	11.47	09.53	85
Keya Paha Co., NE	09.51	09.57	105
Keya Paha Co., NE	09.18	08.92	90
Keya Paha Co., NE	08.93	08.55	95
Keya Paha Co., NE	12.52	11.39	85
Keya Paha Co., NE	09.06	08.46	90
Keya Paha Co., NE	07.49	08.24	110
Keya Paha Co., NE	50.88	09.81	40
Keya Paha Co., NE	20.40	07.25	50
Keya Paha Co., NE	09.39	07.78	80

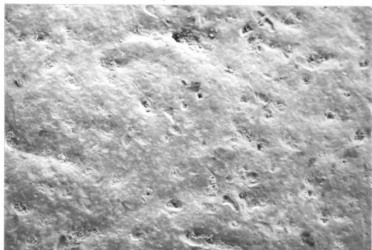


Figure 52. Scanning Electron Microscope (SEM) photograph of a "scrap" fossil of an unknown chelonian bone. 60X magnification.

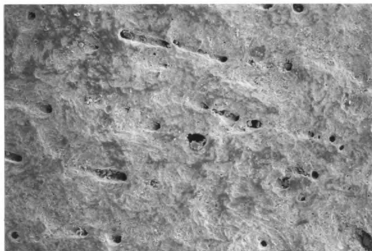


Figure 53. Scanning Electron Microscope (SEM) photograph of a "scrap" fossil of an unknown chelonian bone. 60X magnification.



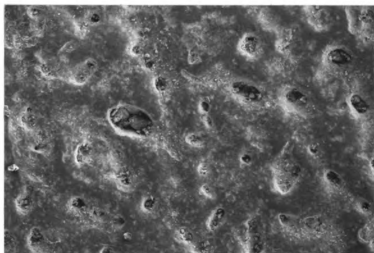


Figure 54. Scanning Electron Microscope (SEM) photograph of a "scrap" fossil of an unknown chelonian bone. 60X magnification.

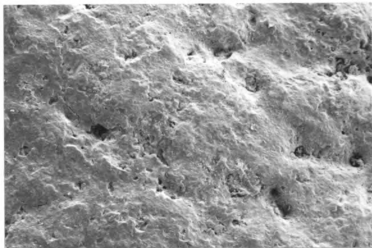


Figure 55. Scanning Electron Microscope (SEM) photograph of a "scrap" fossil of an unknown chelonian bone. 60X magnification.

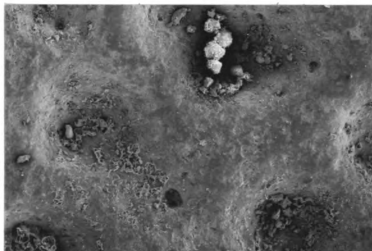


Figure 56. Scanning Electron Microscope (SEM) photograph of a "scrap" fossil of an unknown chelonian bone. 60X magnification.

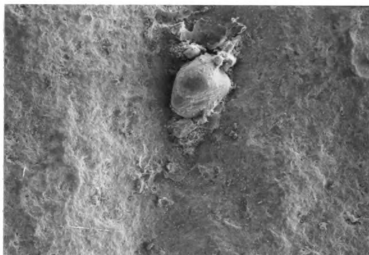


Figure 57. Scanning Electron Microscope (SEM) photograph of a "scrap" fossil of an unknown chelonian bone showing large foreign material on the surface of the fossil. 60X magnification.

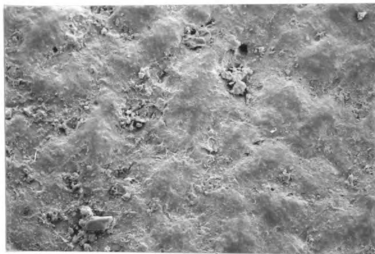


Figure 58. Scanning Electron Microscope (SEM) photograph of a "scrap" fossil of an unknown testudine bone showing foreign material on the surface of the fossil. 60X magnification.

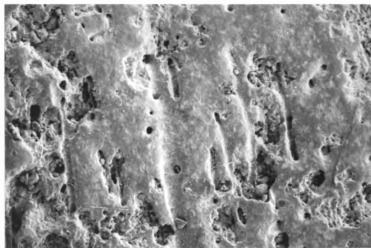


Figure 59. Scanning Electron Microscope (SEM) photograph of a "scrap" fossil of an unknown testudine bone showing erosion of the fossil material. 60X magnification.

families Trionychidae, Kinosternidae, and Chelydridae.

The linear regressions of total length of the femur compared to the K values (small and large) for all chelonians (Table 11), the family Emydidae (Table 12) and the family Testudinidae (Table 13) were not significant at the .05 level. The linear regressions for total length of the femur compared to the KR values (small and large) for all chelonians were significant (Table 11), the family Emydidae (Table 12), and the family Testudinidae (Table 13) were significant at the .05 level. The linear regressions for total length of the femur compared to the R/t (small and large) for all chelonians (Table 11), the family Emydidae (Table 12), and the family Testudinidae (Table 13) were not significant at the .05 level. The linear regressions for the K values (small and large) compared to the KR values (small and large) for all chelonians (Table 11), the family Emydidae (Table 12), and the family Testudinidae (Table 13) were significant at the .05 level. The linear regressions for the K values (small and large) compared to the R/t values (small and large) for all chelonians (Table 11), the family Emydidae (Table 12), and the family Testudinidae (Table 13) were significant at the .05 level.

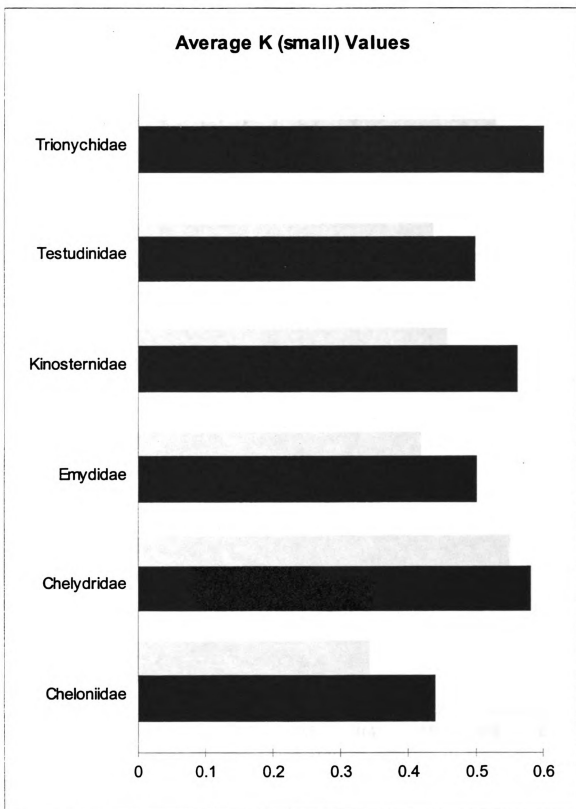


Figure 60. Frequency distribution of average K (small) values for the families of Testudines.

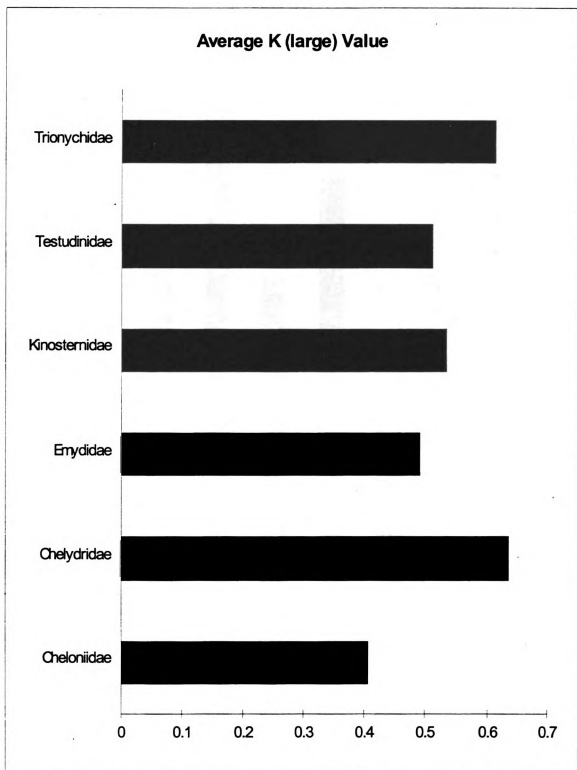


Figure 61. Frequency distribution of average K (large) values for the families of Testudines.

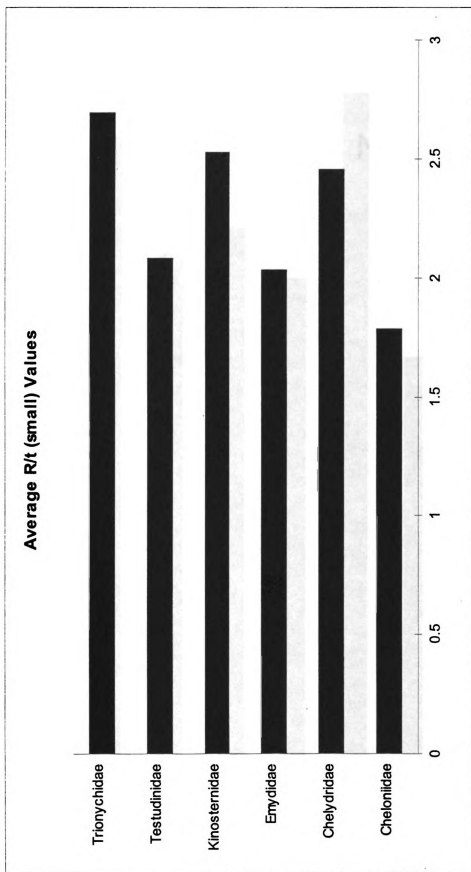


Figure 62. Frequency distribution of average R/t (small) values for the families of Testudines.

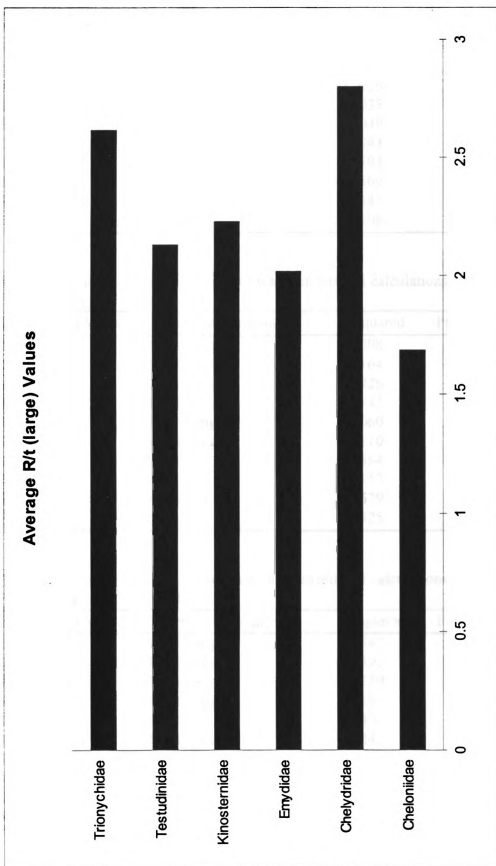


Figure 63. Frequency distribution of average R/t (large) values for the families of Testudines.



Table 11. Linear regressions of femur measurements and calculations for all testudines.

Independent Variable	Dependent Variable	R-squared	Probability value
K (small)	Total Length	0.0022	0.7438
K (large)	Total Length	0.0006	0.8660
KR (small)	Total Length	0.7626	0.0000
KR (large)	Total Length	0.7035	0.0000
R/t (small)	Total Length	0.0049	0.6222
R/t (large)	Total Length	0.0043	0.6430
KR (small)	K (small)	0.1594	0.0046
KR (large)	K (large)	0.1860	0.0020
R/t (small)	K (small)	0.8847	0.0000
R/t (large)	K (large)	0.9508	0.0000

Table 12. Linear regressions of femur measurements and calculations for members of the family Emydidae.

Independent Variable	Dependent Variable	R-squared	Probability value
K (small)	Total Length	0.0008	0.8976
K (large)	Total Length	0.0164	0.5504
KR (small)	Total Length	0.6926	0.0000
KR (large)	Total Length	0.4743	0.0003
R/t (small)	Total Length	0.0060	0.7206
R/t (large)	Total Length	0.0110	0.6264
KR (small)	K (small)	0.1884	0.0393
KR (large)	K (large)	0.2417	0.0176
R/t (small)	K (small)	0.8679	0.0000
R/t (large)	K (large)	0.9425	0.0000

Table 13. Linear regressions of femur measurements and calculations for members of the family Testudinidae.

Independent Variable	Dependent Variable	R-squared	Probability value
K (small)	Total Length	0.1547	0.1697
K (large)	Total Length	0.1592	0.1627
KR (small)	Total Length	0.8230	0.0000
KR (large)	Total Length	0.7684	0.0001
R/t (small)	Total Length	0.1400	0.1943
R/t (large)	Total Length	0.1242	0.2246
KR (small)	K (small)	0.4877	0.0081
KR (large)	K (large)	0.4697	0.0099
R/t (small)	K (small)	0.9737	0.0000
R/t (large)	K (large)	0.9610	0.0000

## DISCUSSION

A discussion of the results of the analysis if the SEM data, histological slides, and long bone studies of turtle skeletal tissues as physiological agents follows as well as added comments on metabolic uses of the shell and its part in thermoregulation.

### **Role of the Three Canal Types in Thermoregulation**

The large differences between surfaces of the varied elements of a single shell of Chrysemys picta (MSU-H 2025) show that only certain surfaces are similar enough to use for a comparative analysis; these being the outer surfaces of the neural, costal, and peripheral bones (see Figs. 36, 37, and 64). In fact, five photographs from the same neural of this specimen (see Figs. 38, 64, and 65) were so similar that without codes on the SEM negatives the specimens could easily have been confused. Therefore, it was determined that any outer surface of the carapace could have been used for this study.

The three types of canals in the shell represent a unique method of determining the amount of blood that is exposed to the outside environment by controlling not only the amount of blood that is exposed at one time to the surface but how much change in temperature occurs over that

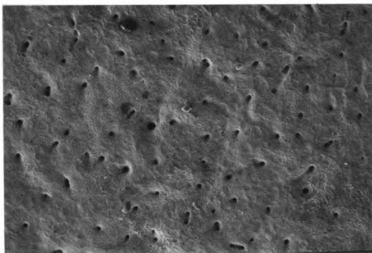


Figure 64. Scanning Electron Microscope (SEM) photograph of the outer surface of a neural bone of Chrysemys picta (MSU-H 2025). 60X magnification.

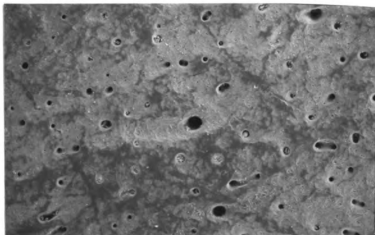


Figure 65. Scanning Electron Microscope (SEM) photograph of the outer surface of a neural bone of Chrysemys picta (MSU-H 2025). 60X magnification.

time.

Type A canals (Figs. 6 and 7) form a T with the surface of the bone. These canals force blood into the subscute blood capillary layers. The blood would have to flow across the surface to another canal. This small amount of blood flowing just under the surface of the scute would have a high surface area to volume ratio that would allow all of the blood to be affected by the temperature of the scute at the same rate. This would make an excellent fine adjustment to the temperature of the blood and thereby, the temperature of the ectothermic turtle.

Type B canals (Figs. 8 and 9) form an inverted V with the surface of the bone. This type of canal would not provide much interaction of the blood with the temperature of the scute and would have little or no effect on the temperature of the chelonian.

Type C canals (Figs. 10 and 11) come to the surface of the bone and follow along the surface for some time before plunging back deep into the bone. This type of canal would allow large amounts of blood to come into contact with the scute at one time and keep that contact for a moderate amount of time. This type of canal would allow for large amounts of temperature change in a relatively short amount of time but with little fine control of the temperature.

### **Actions of Temperature Control in the Carapace**

All chelonians have significantly more type A canals than any other type of canal (see Figs. 47, 48, and 49) (Tables 1, 2, 3, and 5). This fact combined with the proposed function of type A canals would allow chelonians to maintain excellent fine control of their temperature by determining the flow of blood to the carapace. The regulatory mechanism for this was not discovered in this study.

All chelonians except members of the family Testudinidae (see Table 3) have significantly fewer type B canals than any other type of canal (Tables 1, 2, and 5). This fact when compared with the proposed lack of thermal control for this type of canal would support the supposition that this type of canal lacks a thermodynamic function.

The linear regression of the type B canals compared to the total area occupied by canals of the neural was significant for all chelonians (0.0001) (Table 6) and the family Emydidae (0.0005) (Table 7). This suggests that this low number of type B canals can be used to predict the total area of canals in the bone (Figs. 63, 64, and 65). But, the fact that type B canals are not significant predictors of percent area occupied by all canals for members of the family Testudinidae (Table 8) and members of Chrysemys picta (Table 9) would argue against that prediction.

A possible explanation for Type B significance when used to predict percent area occupied by all canals could be that the type A canals are extensions or processes of the type B canal. This hypothesis is not supported by further testing. A linear regression of type A canals compared to type B canals resulted in a rejection of the hypothesis (0.0838) at the 0.05 level (Fig. 66).

The most numerous type of canal in all chelonians examined were the type A canals. It would be logical to assume that this type of canal would be a good predictor of the total area occupied by canals. This assumption is incorrect in all groups (Figs. 67, 68, and 69) (Tables 6, 8, and 9) except the Family Emydidae (Figs. 70) (Tables 7). The fact that the linear regressions of the type A canals compared to the total area of canals is significant only for the family Emydidae (0.0106) does not support the hypothesis that type B canals are primary sources of type A canals. The area of anastomosis between different canal types would be an area that would benefit from further research.

Linear regressions of type C canals compared to total area were not significant for any group examined (Figs. 71, 72, 73, and 74). As type C canals are the largest type of canal, it lends evidence to the proposed function of type C canals. If a single type C canal has the ability to greatly modify the temperature of the organism, there would

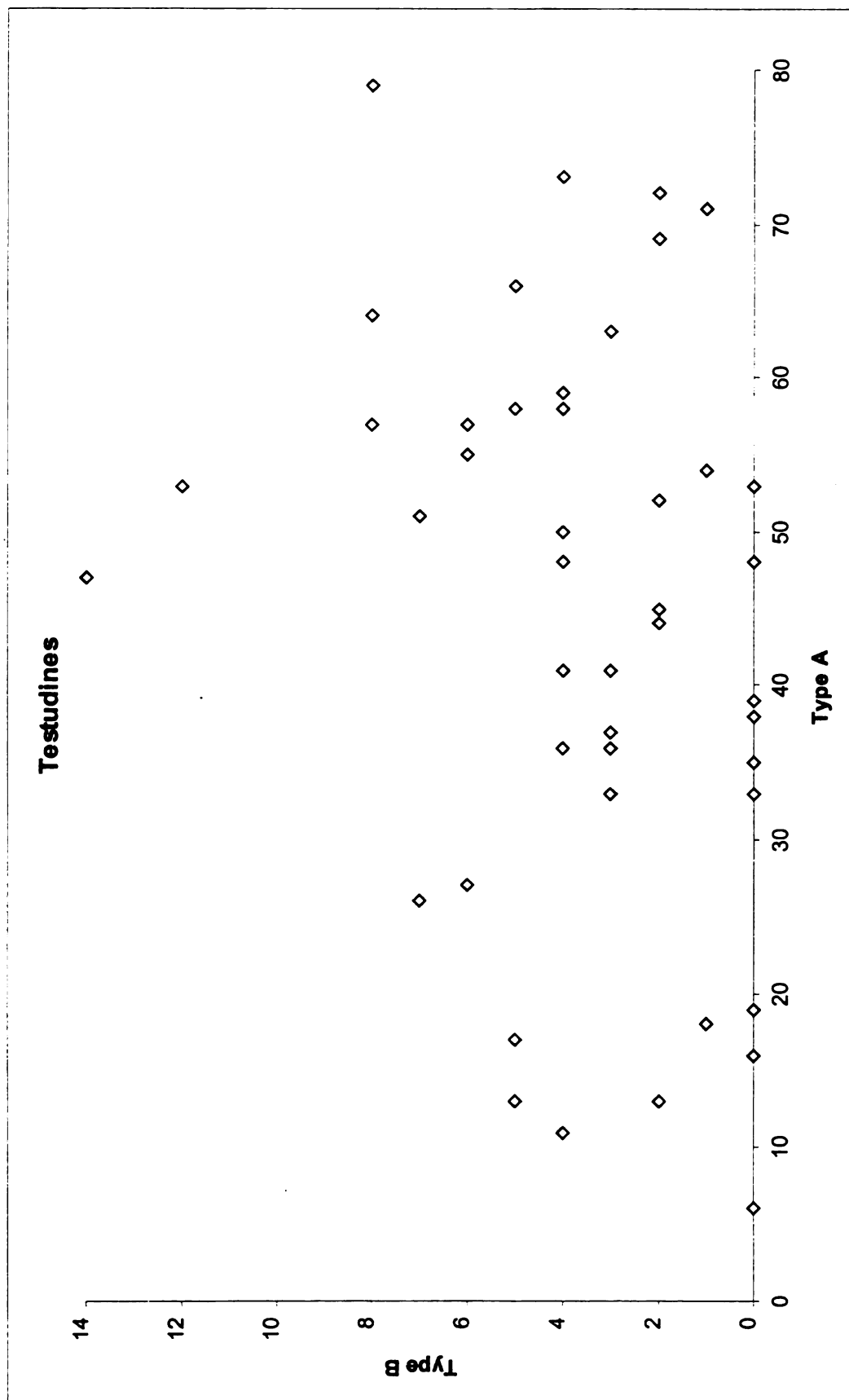


Figure 66. Number of Type A canals versus the number of Type B canals in all testudines examined.

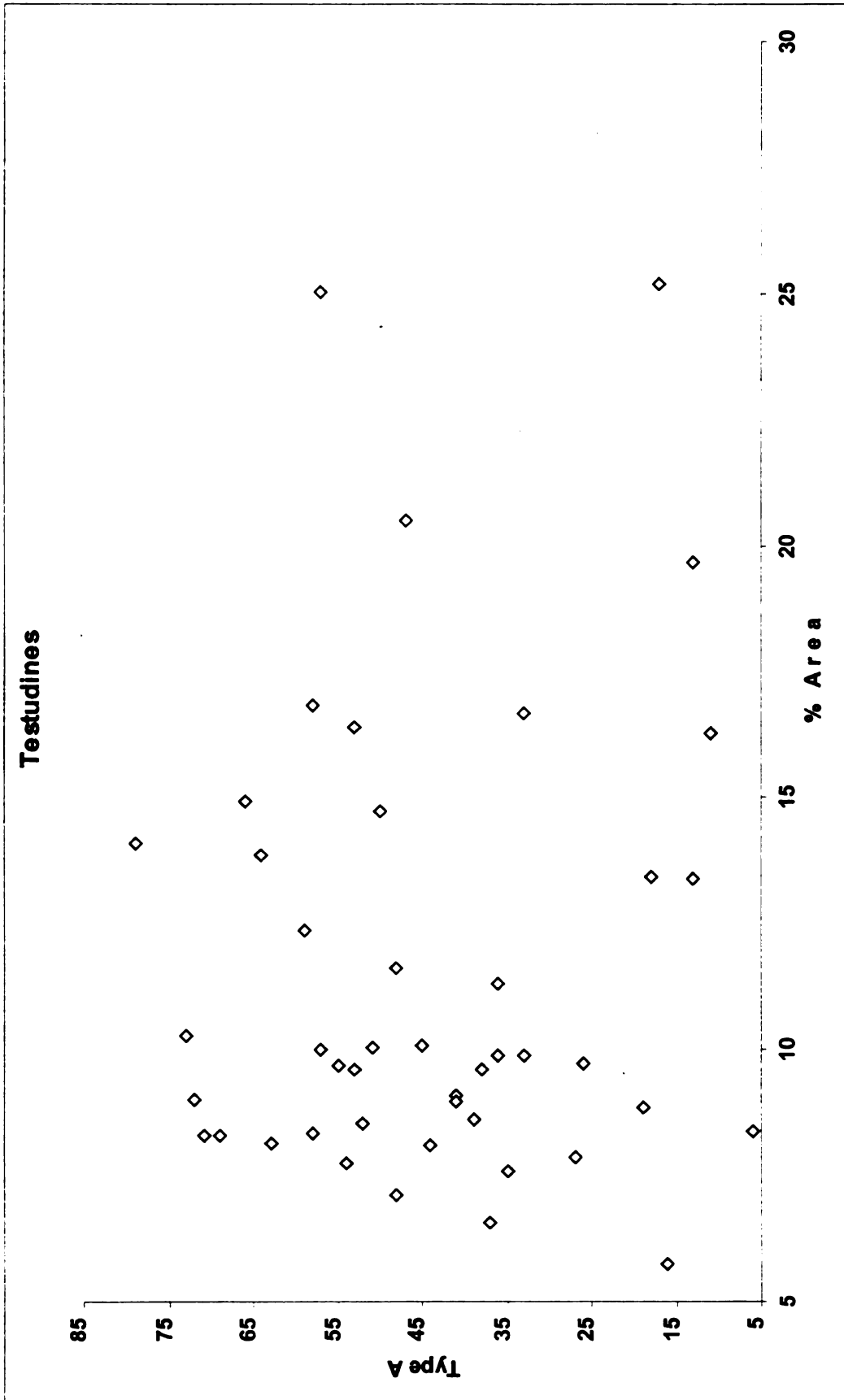


Figure 67. Percent area occupied by all canals versus number of Type A canals in all testudines examined.



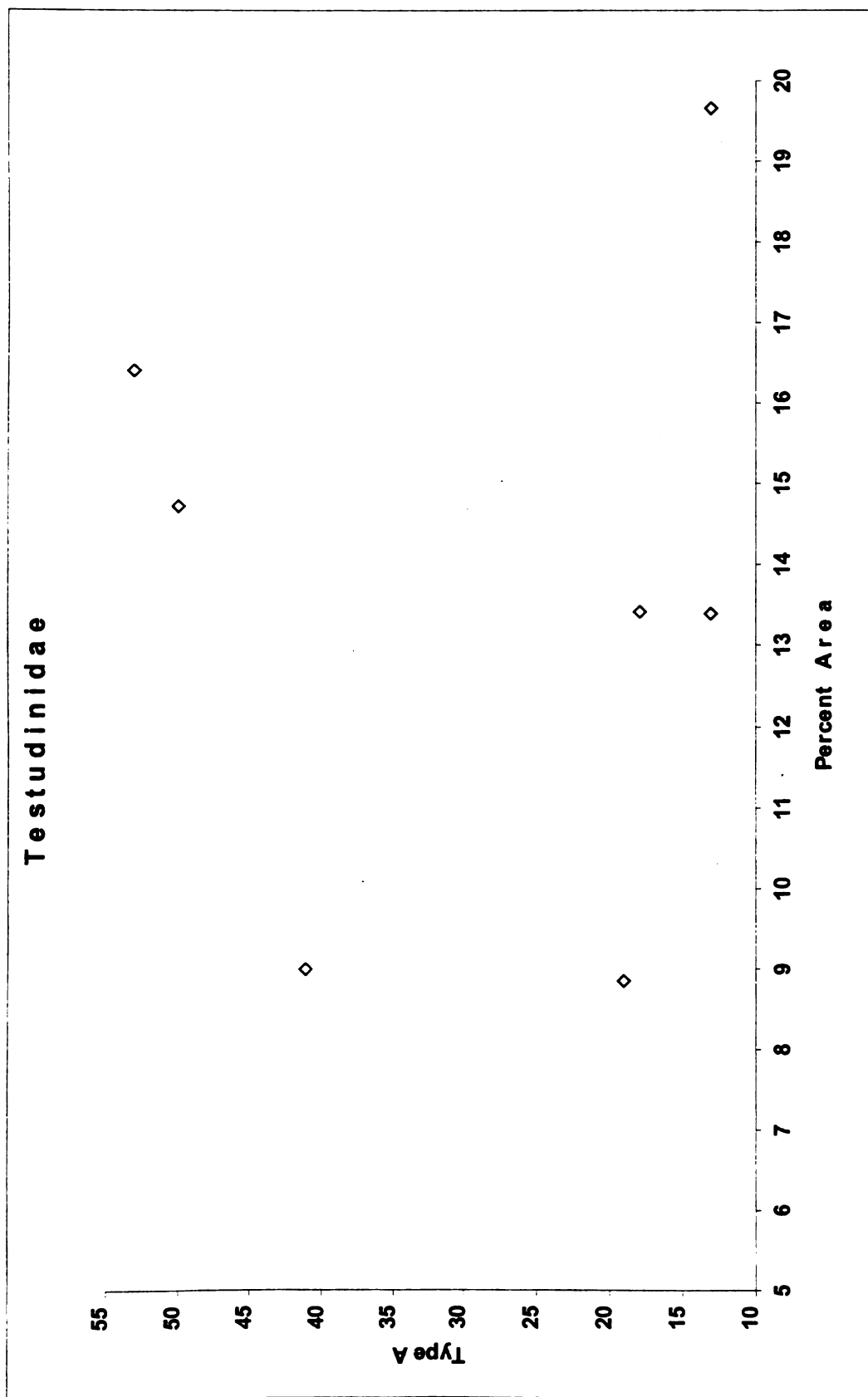


Figure 68. Percent area occupied by all canals versus number of Type A canals in the family Testudinidae.

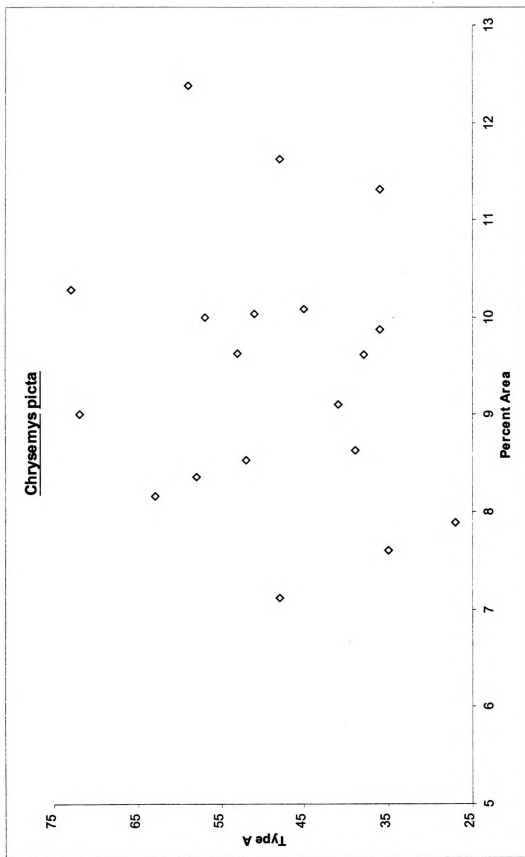


Figure 69. Percent area occupied by all canals versus number of Type A canals in Chrysemys picta.

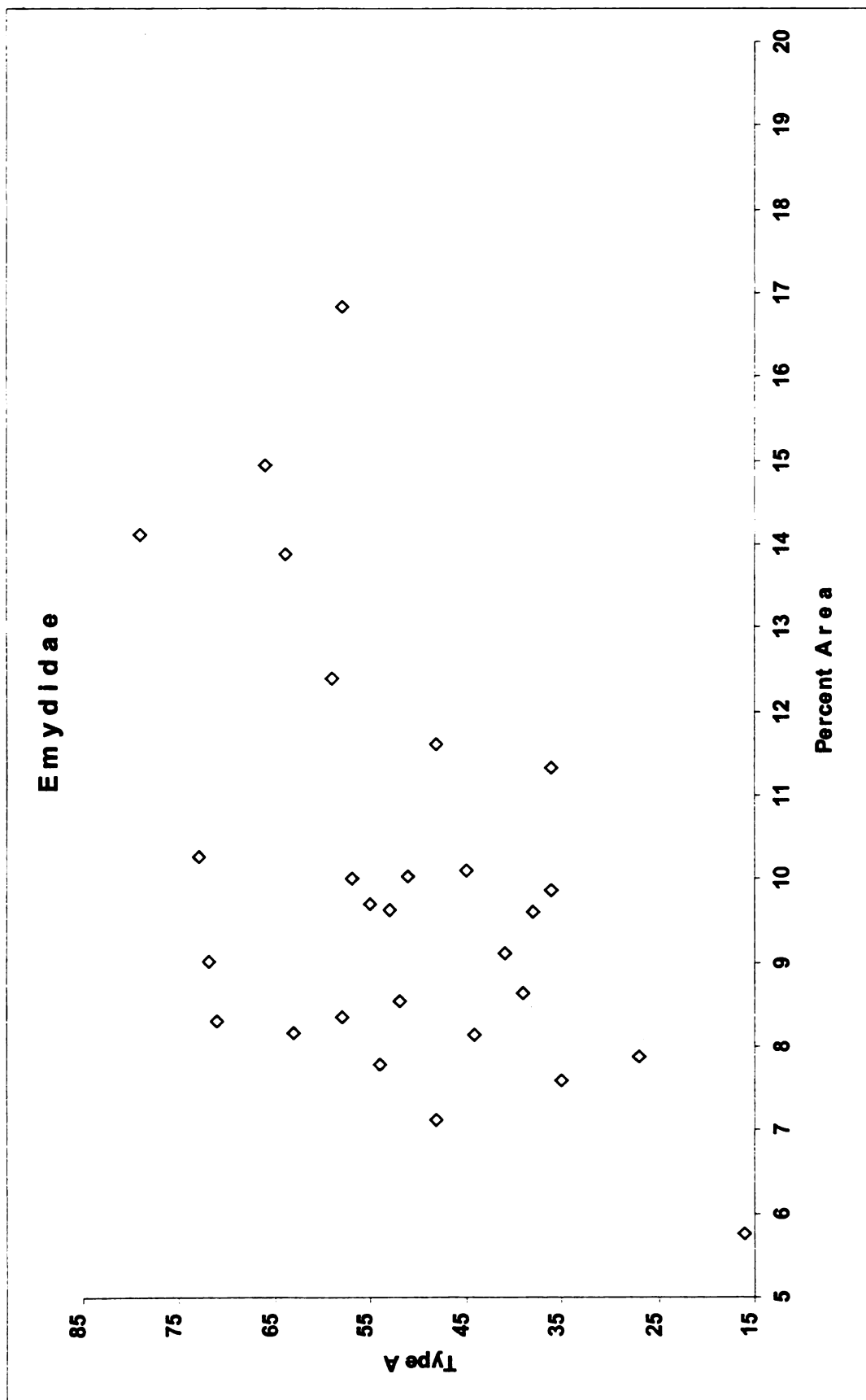


Figure 70. Percent area occupied by all canals versus number of Type A canals in the family Emydidae.

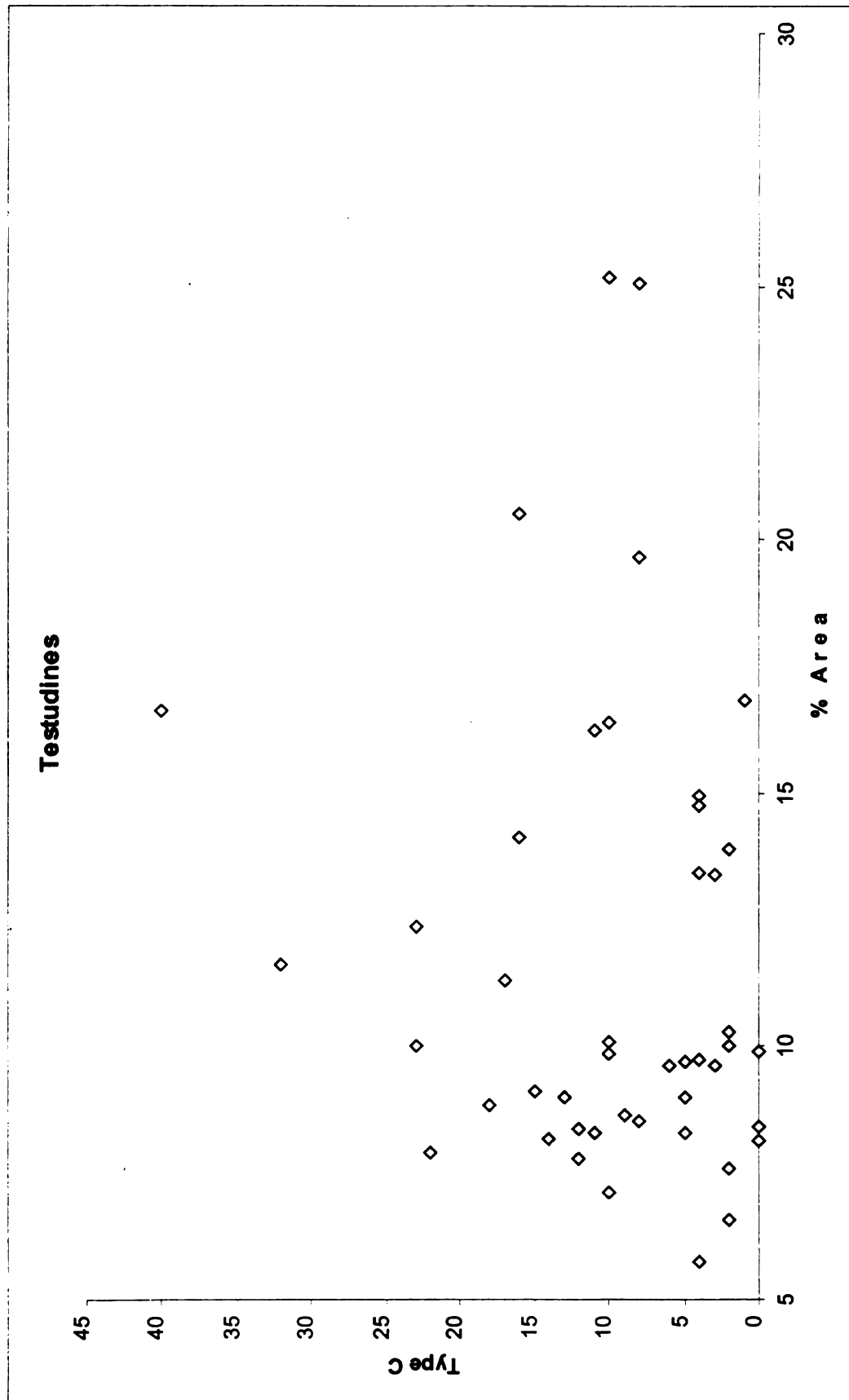


Figure 71. Percent area occupied by all canals versus number of Type C canals in the family Testudinidae.

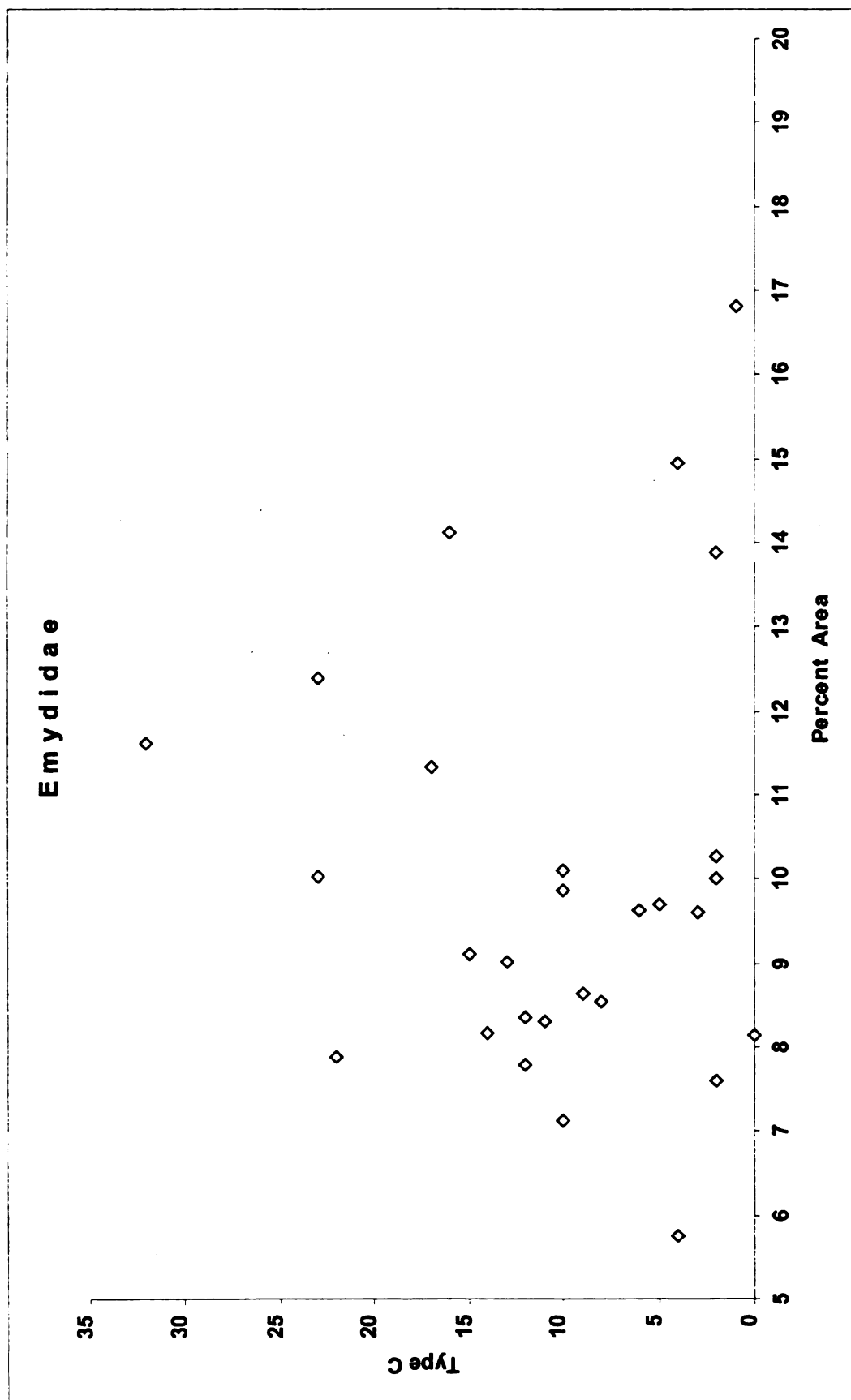


Figure 72. Percent area occupied by all canals versus number of Type C canals in the family Emydidae.

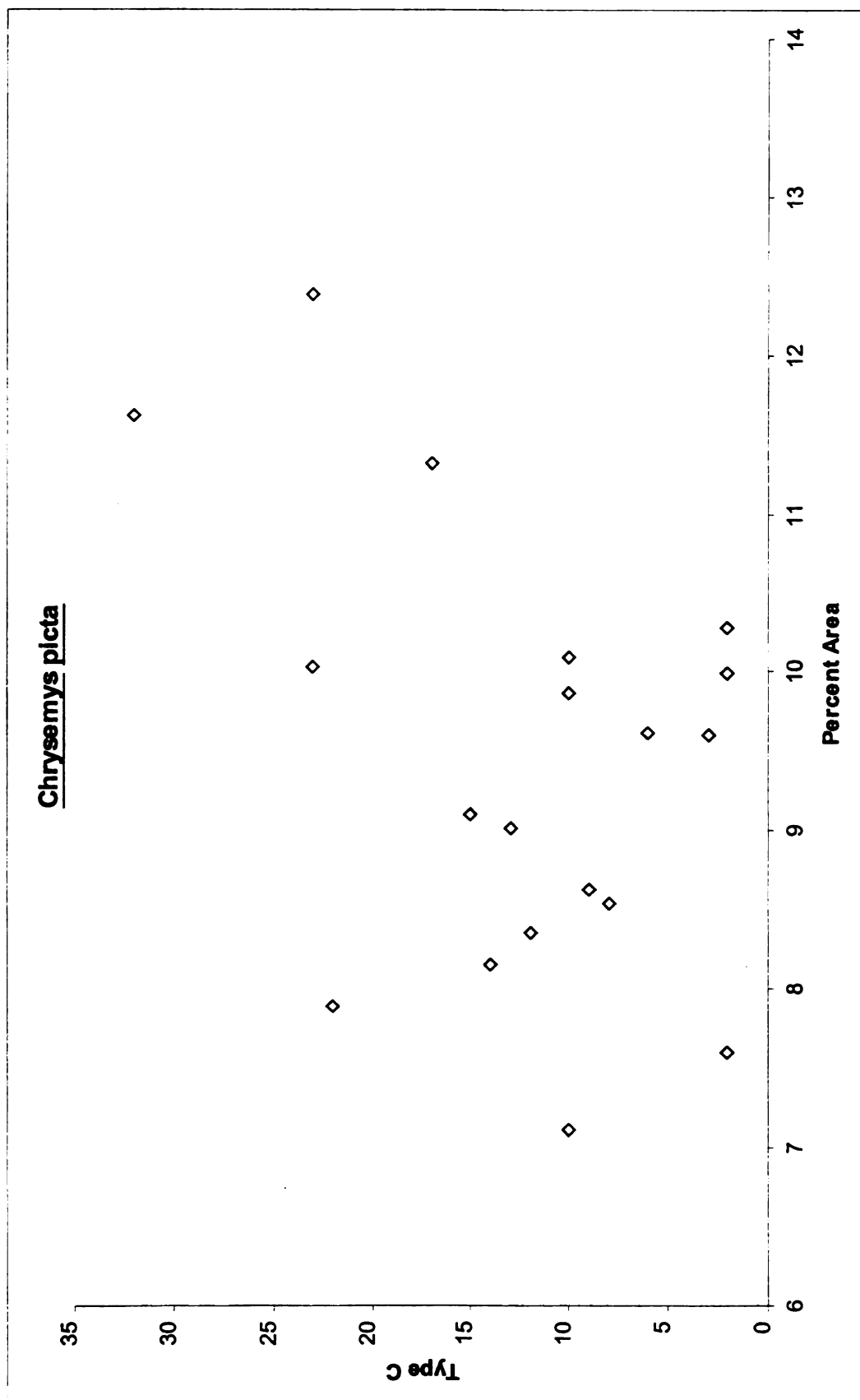


Figure 73. Percent area occupied by all canals versus number of Type C canals in Chrysemys picta.

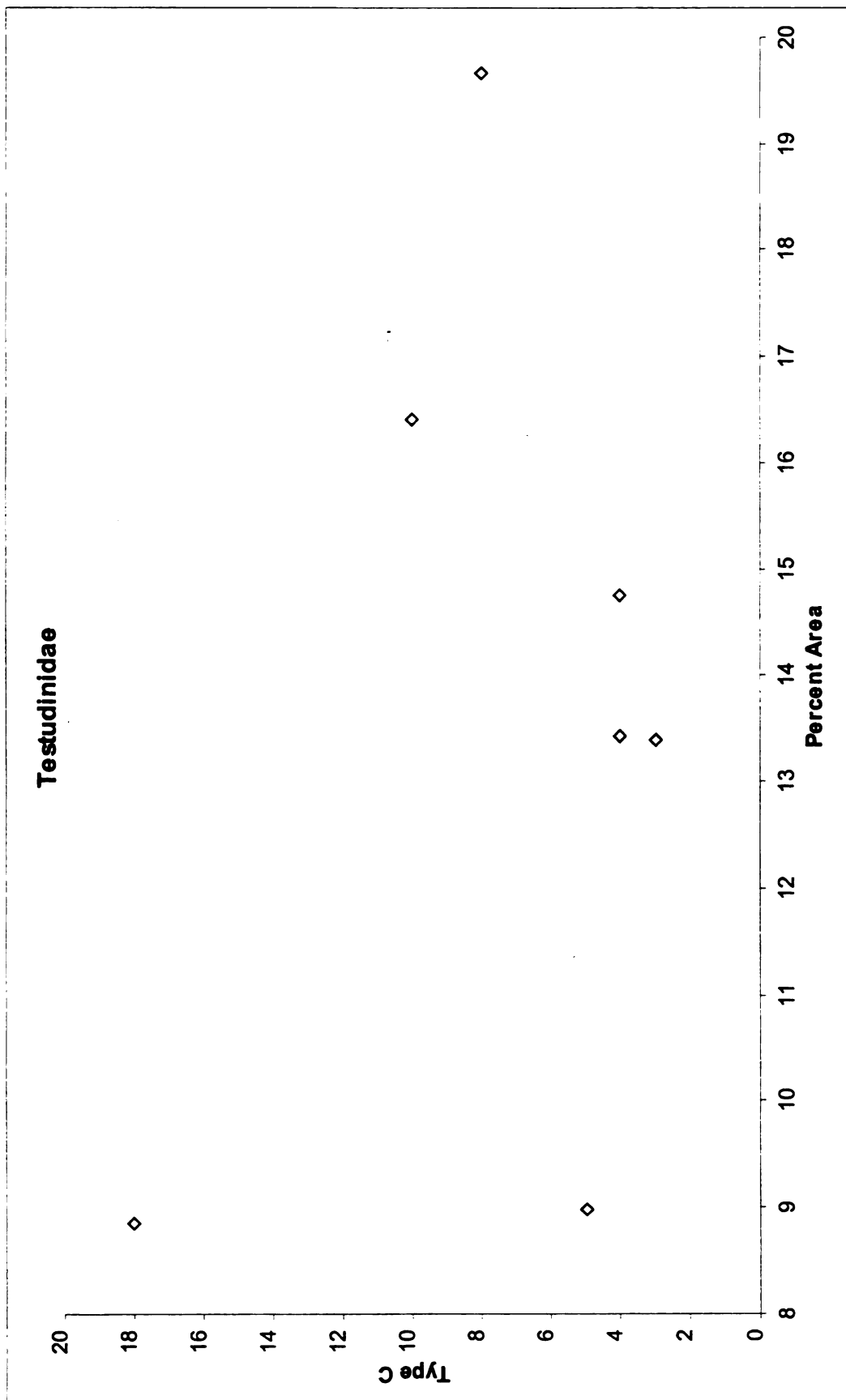


Figure 74. Percent area occupied by all canals versus number of Type C canals in the family Testudinidae.

be little need for large numbers of them in the shell.

The subscute blood layer is as small as one cell layer thick in some places which could enhance the ability of the outside environment to affect the blood, and could become the exact temperature of the scute in a short amount of time. Anatomical structures for the control of blood flow through the carapace (Avery, 1982) were not detected either in the SEM specimens or in the histology specimens. The extent of ability of the blood to fan out from the type A canal and thus gain or lose even more heat is unknown because the histological slides were sagittally sectioned at this level. My work shows that it flows across the shell (Fig. 75), but the ability of the blood to flow in more than two directions is unknown. Shallower transverse sections may have answered this question, but unfortunately, the transverse sections were made deeper in this study. The shape of the shell optimizes the amount of heat that can be obtained from the environment. The shape allows the sun to contact at least part of the carapace no matter what direction the light is coming from. This allows the subscute thin layer of blood to obtain heat from that area of the shell that is currently under direct sunlight. Bartholomew (1982) found that peripheral vasomotor activity was locally controlled independent of the core temperature and heart beat, although he did not discuss how this control



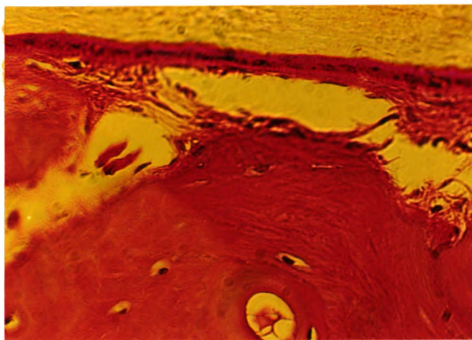


Figure 75. Photograph of a Hematoxylin and Eosin (H+E) prepared histological slide showing the subcutaneous blood flow.

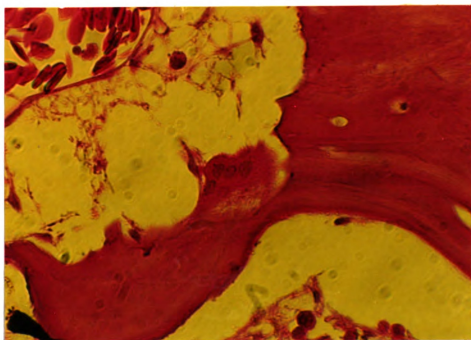


Figure 76. Photograph of a Hematoxylin and Eosin (H+E) prepared histological slide showing an osteoclast dissolving bone.

occurred. This mechanism would allow the organism to control where on the shell blood would flow and thereby where the subscute blood would be optimally heated by the radiant heat.

The hemispherical shape of the carapace gives chelonians a relatively small surface to volume ratio when compared with other reptiles of the same size (Bartholomew, 1982). Some chelonians are large enough that their mass endows them with an inertial homeothermy similar to crocodilians (Bartholomew, 1982). This small surface to volume ratio allows these very successful reptiles to retain more heat in their systems due to smaller amounts of heat lost through surface radiation. This retention of heat means that even small amounts of heat gain are kept for long periods of time. This would mean that a method of forcing or enhancing temperature control of the shell would be of great value to this animal's natural ability to retain heat.

#### **Actions of Temperature Control in the Plastron**

The large Type C canals on the plastral outer surface photograph (see Fig. 39) are exceptionally noteworthy. The proposed function of type C canals is to allow large quantities of blood over the thermodynamic surface in a relatively short amount of time. The arrangement of Type C canals next to the surface upon which this basking chelonian rests his weight, would allow the turtle to gain or lose

large amounts of heat rapidly. Obviously, the control of blood to this area would be of great importance. Though no mode of blood flow control was detected in this study, Hicks and Wang (1996) discuss the role cardiac shunting in reptiles. This ability to shunt most of the blood to either the pulmonary or systemic circulation is a perfect way to control large amounts of blood flow with relatively little physiological effort. Cardiac shunting in conjunction with the large numbers of Type C canals in the plastron would allow the chelonian to control temperature rapidly.

#### **Carapace as a Reservoir for Calcium and Phosphate**

The presence of osteoclasts in the spongy bone of carapace (Fig. 76) is solid evidence that the shell is a storage reservoir for calcium and phosphate. This reserve is in addition to any that the long bones provide. This leads to the supposition that osteoblasts are also present in the spongy bone of the carapace; leading to the constant remodeling of the shell as dictated by the needs of the organism. The process of remodeling of the shell is primarily a metabolic function and not a structural one, as the strength of the shell is determined primarily by the structure of the bridge that connects the carapace with the plastron (Currey, 1967).

Red eared sliders need a minimum of two percent dietary calcium during growth for the carapace to develop properly

(Kass, et al, 1982). This calcium can be taken directly from the aquatic medium and used in carapace structure (Jeffree, 1991). The ability to extract calcium from the environment and lay it down as Calcium Phosphate in the carapace facilitated by the presence of osteoclasts in the spongy bone of the carapace suggests a process of gaining calcium from the surrounding environment.

#### **Other Metabolic uses of the Shell**

The shell has been determined to be an agent for hematopoiesis in the spongy middle layer of the shell (Vasse and Beaupain, 1981). It has also been suggested that chelonians are capable of increasing bone marrow production in cases of certain diseases (Garner, et. al., 1996). These factors give additional evidence for the metabolic activities of the chelonian shell.

#### **Reduced Size of Long Bone Marrow Cavities for Support**

Currey and Alexander (1985) state that the median R/t for terrestrial mammals is 2.0. This value (even though it is for an endothermic animal) is of value for comparison with the testudine data. The terrestrial mammals have a R/t value that is optimal for impact strength but lower than the expected value for static strength and stiffness. The Average value for the family Testudinidae is 2.0784 for the smaller width and 2.1299 for the larger width, which is similar to the terrestrial mammals (Appendix 3). The

average R/t (2.0298 for the large and 2.0163 for the small) for the family Emydidae was also similar to terrestrial mammals even though they are primarily aquatic. It should be noted that they use their limbs extensively to climb out of the water frequently for basking purposes as well as excursions out of water for multiple purposes.

The marine turtle Eretmochelys imbricata had a R/t of 1.7826 for the smaller width and 1.6847 for the large width, which is much different than the R/t of 1.0 that Currey and Alexander (1985) found in the endothermic manatee (Trichechus manatus).

Excluding the sole marine turtle examined, important correlation occurs between chelonian shell size and the R/t of their long bones. The Emydidae and Testudinidae both have extensive shells and their R/t values are the lowest of the chelonians. The Kinosternidae have a somewhat reduced shell and their R/t value is larger. The Chelydridae have an even more reduced shell and their R/t value is higher yet. Finally, the Trionychidae have no external shell, only a much reduced internal shell, and their R/t value is the largest of all. This inverse correlation between the amount of shell that a chelonian has and its R/t value generally indicates the amount of metabolic activity that occurs in the shell. The higher the R/t value, the more marrow the long bone possesses. Therefore, the smaller the shell (and

consequently, the amount of bone in the shell), the larger the marrow cavity of the long bone.

The K value, which is considered to be at optimum strength at 0.67 (Currey and Alexander, 1985), is lower than the optimum strength value in almost every turtle examined (Appendix 3). Exceptions occur in two measurements of the smaller K value (one Kinosternid and one Trionychid) and three measurements of the larger K value (one Chelydrid, one Testudinid, and one Emydid). The ultimate strength value of K was calculated as 0.55 and a large number of the turtles examined have K numbers lower than this ultimate strength number. The terrestrial turtles (Terrapene and family Testudinidae) have K(large) values of 0.3146 to 0.6966 with an average of 0.5122. The Marine turtle *Eretmochelys* has a K (large) value of 0.4064. This very low value for the rear leg (which is not used in propelling the turtle through the water) is not surprising considering that this organism is marine and propels itself through the ocean with its anterior limbs. The rear limbs trail the body and may act as a rudder. Females also use them to dig the hole when nesting, but even when on land, the rear limbs are not used to propel the animal.

The linear regressions of the total length of the femora compared to the KR values (small and large) were the most informative of all the regressions performed on the

long bones (Tables 11, 12, and 13) (Figs. 77, 78, 79, 80, 81, and 82). The KR value is the radius of the marrow cavity in the femur. The fact that it can be used to determine the length of the bone is of great interest. This would suggest that the marrow cavity is affected by the length of the bone. This correlation should be examined more closely to determine if this is a true or a chance (stochastic) correlation.

The linear regressions of the K values (small and large) compared to the KR values (large and small) (Figs. 83 and 84), and compared to the R/t values (large and small) (Figs. 85 and 86) were primarily run as controls. The K value is the radius of the femur. The KR value is the radius of the marrow cavity. The R/t value is the ratio of the radius of the complete bone to the thickness of the bone wall. These are all derivatives of the same measurements and should therefore be highly correlated.

#### **Comments on Metabolic Uses of the Shell**

Without mention of the shell, Edgren (1960) stated that the long bones are used as a calcium reserve for the egg shell production in Sternotherus odoratus. Another well known use of calcium in animals is to bind to troponin, [activating the movement of tropomyosin and the exposure of active sites on the thin (actin) filaments] resulting in the contraction of muscles (Martini and Bartholomew, 2000).

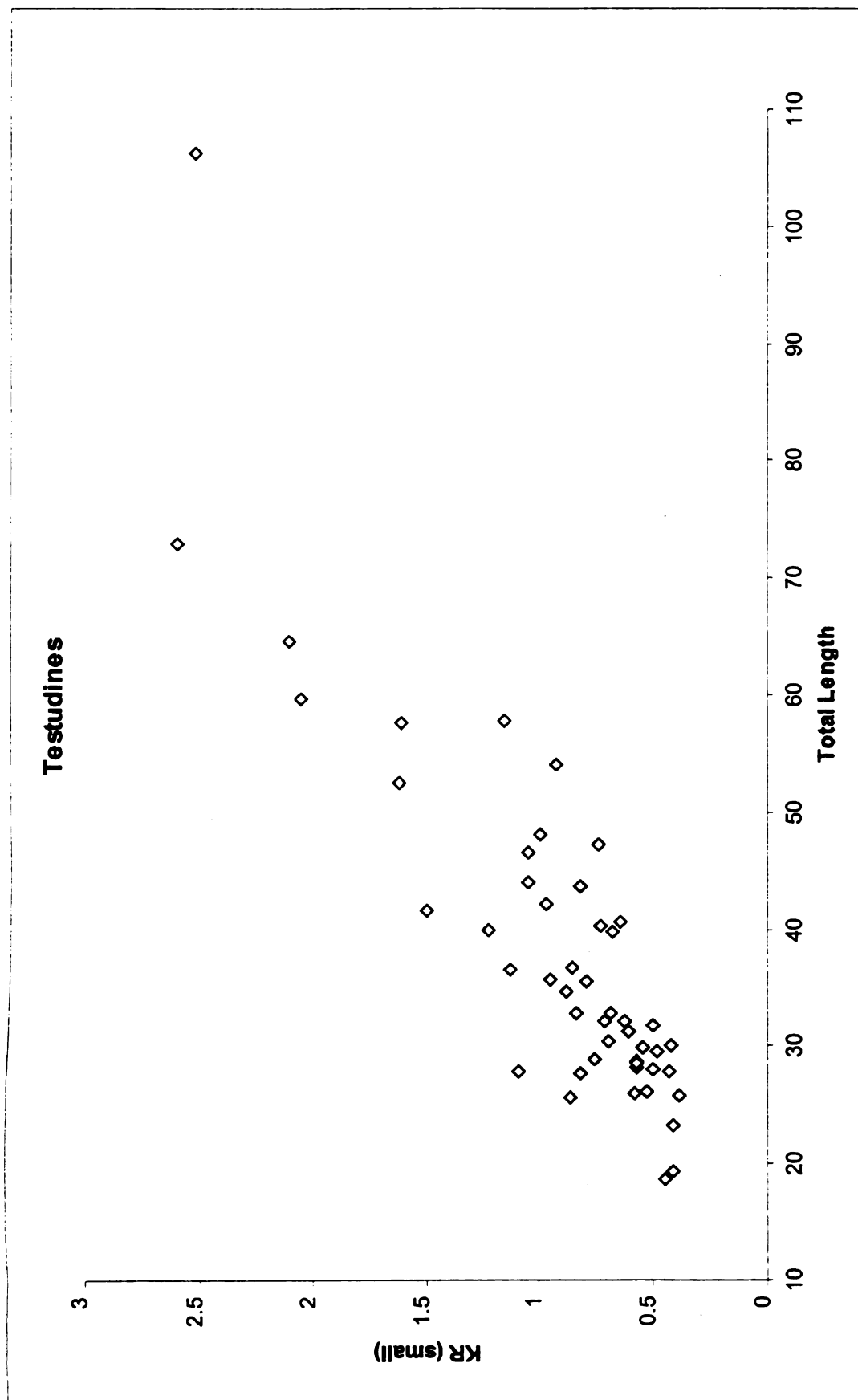


Figure 77. Total length of the femur versus the KR (small) value for all testudines examined.



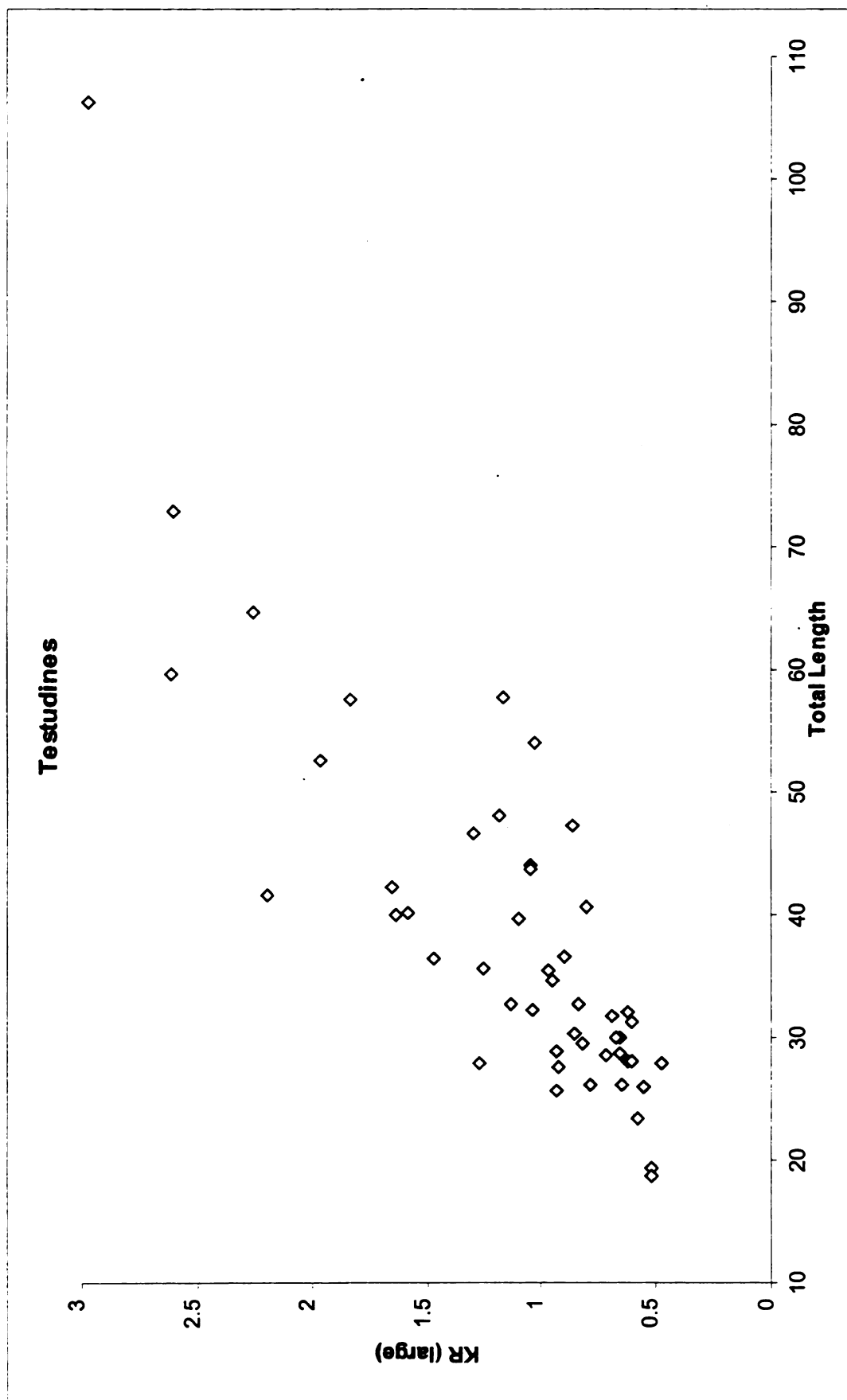


Figure 78. Total length of the femur versus the KR (large) value for all testudines examined.

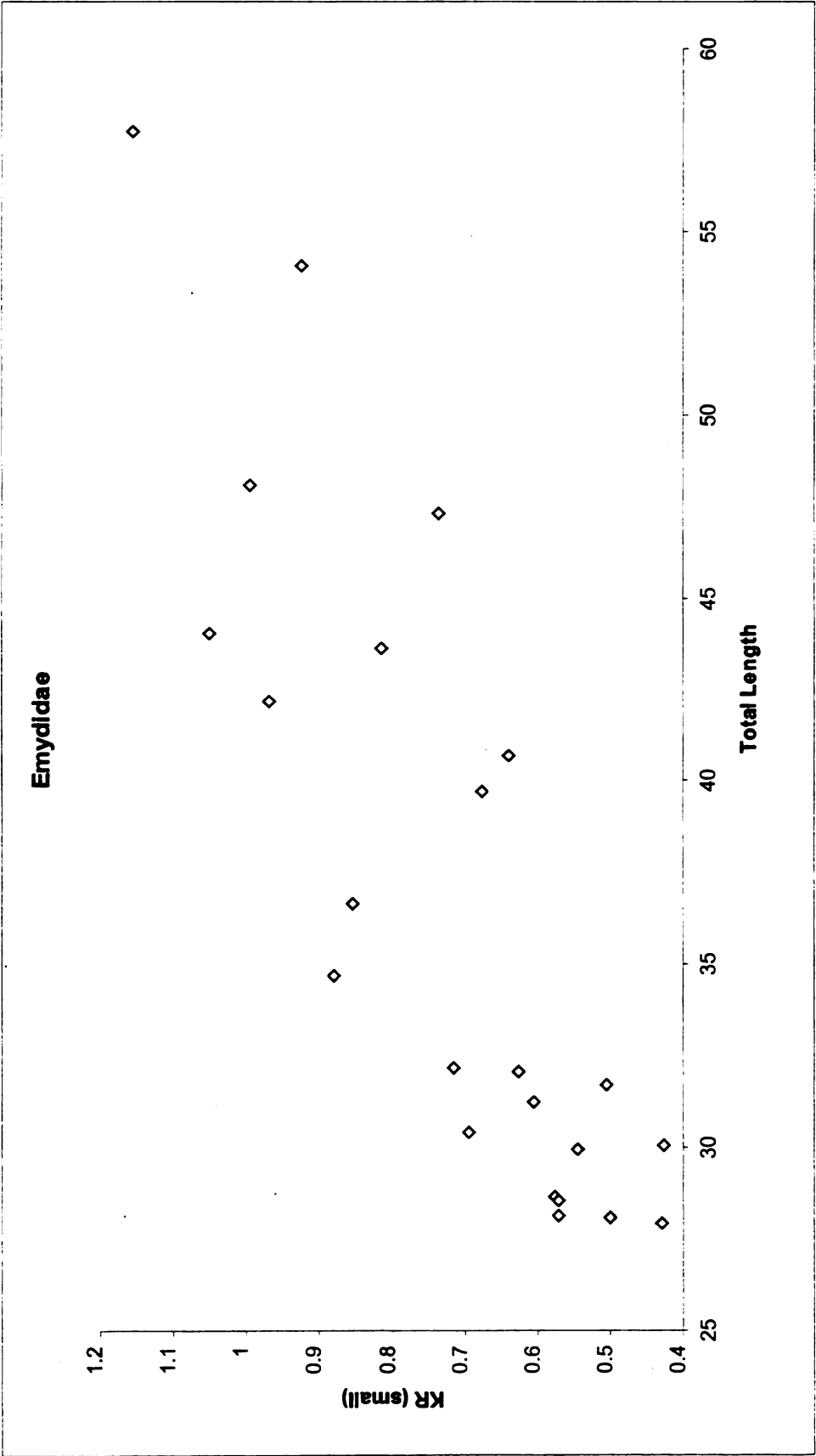


Figure 79. Total length of the femur versus the KR (small) value for the family Emydidae.

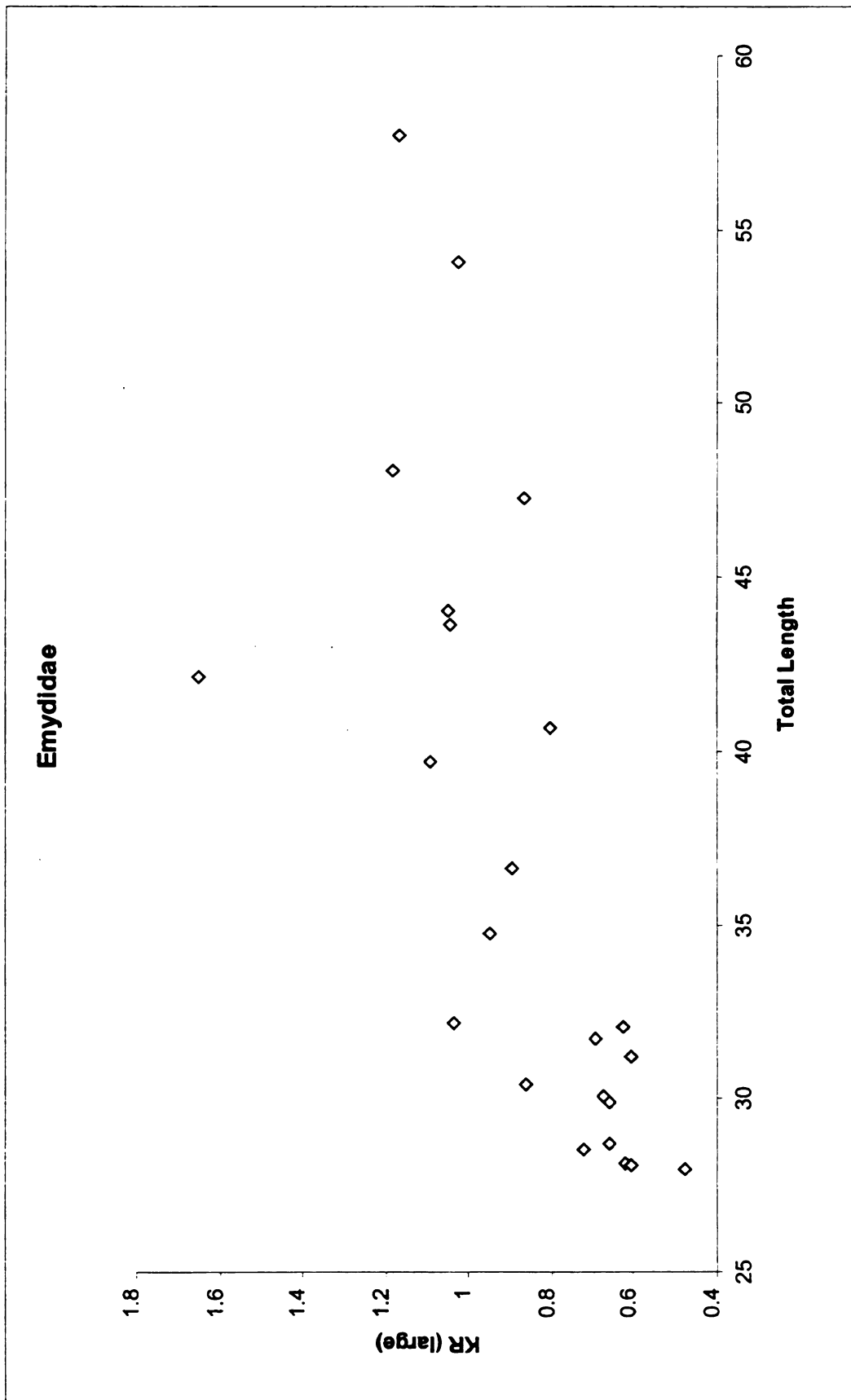


Figure 80. Total length of the femur versus the KR (large) value for the family Emydidae.

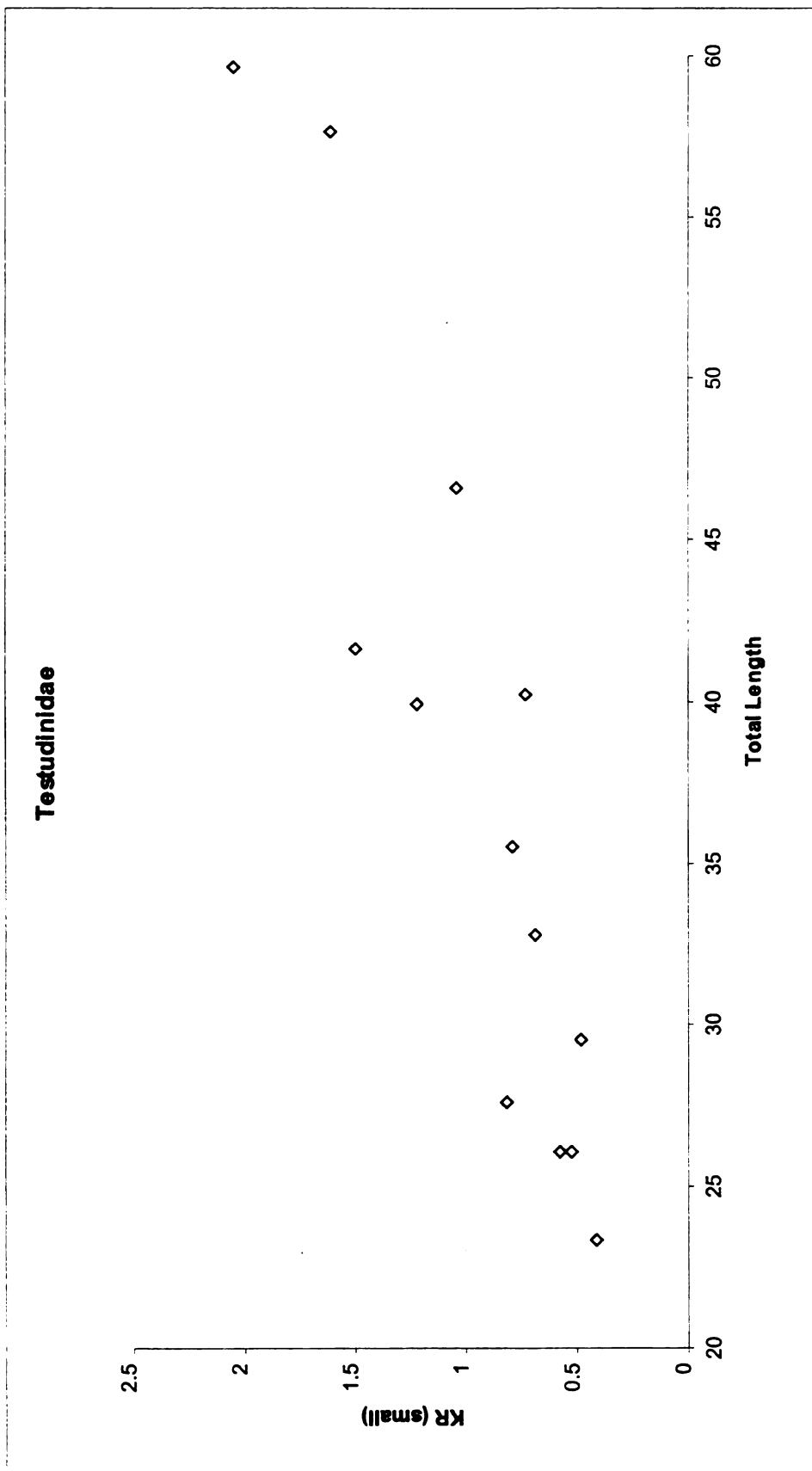


Figure 81. Total length of the femur versus the KR (small) value for the family Testudinidae.

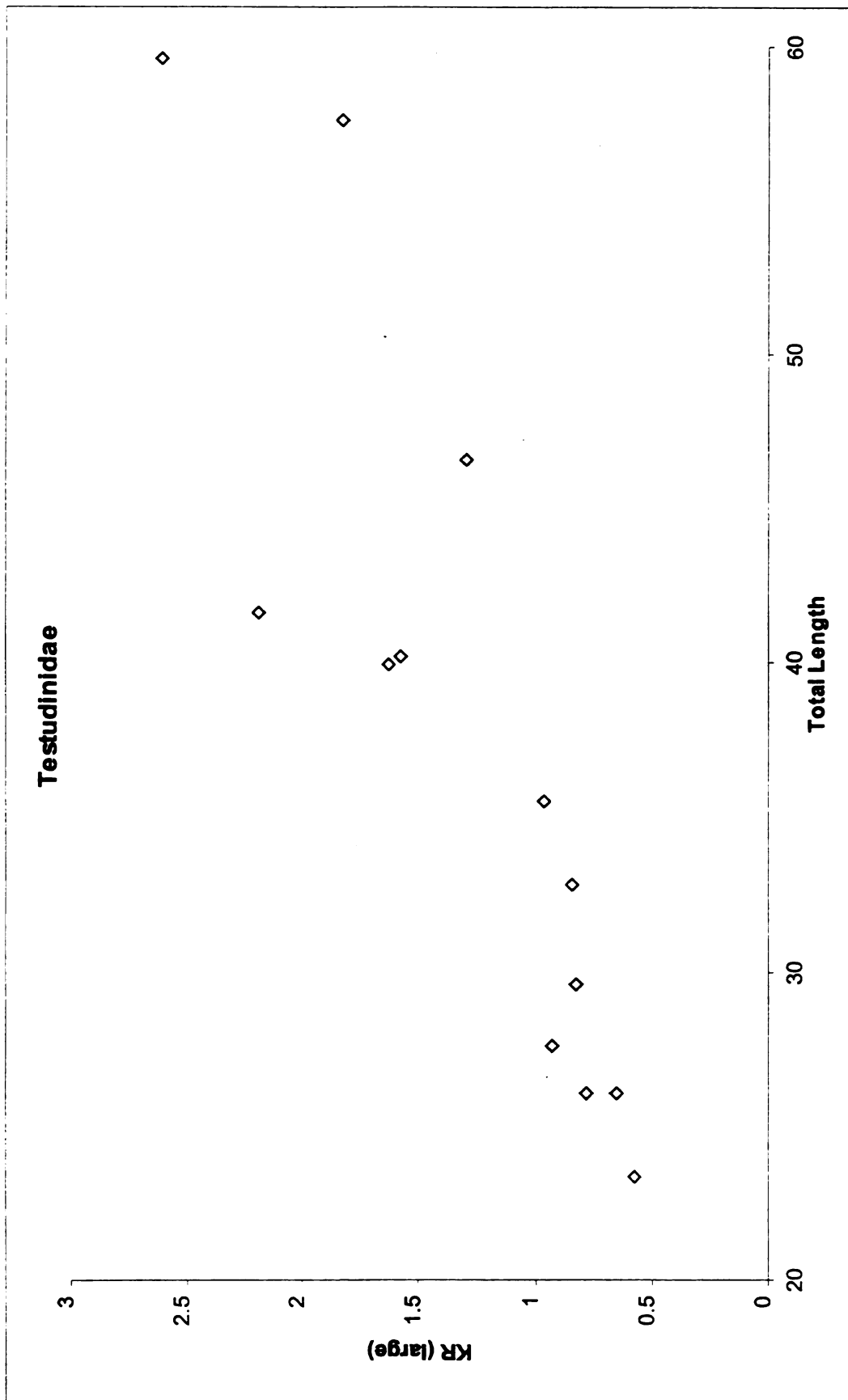


Figure 82. Total length of the femur versus the KR (large) value for the family Testudinidae.

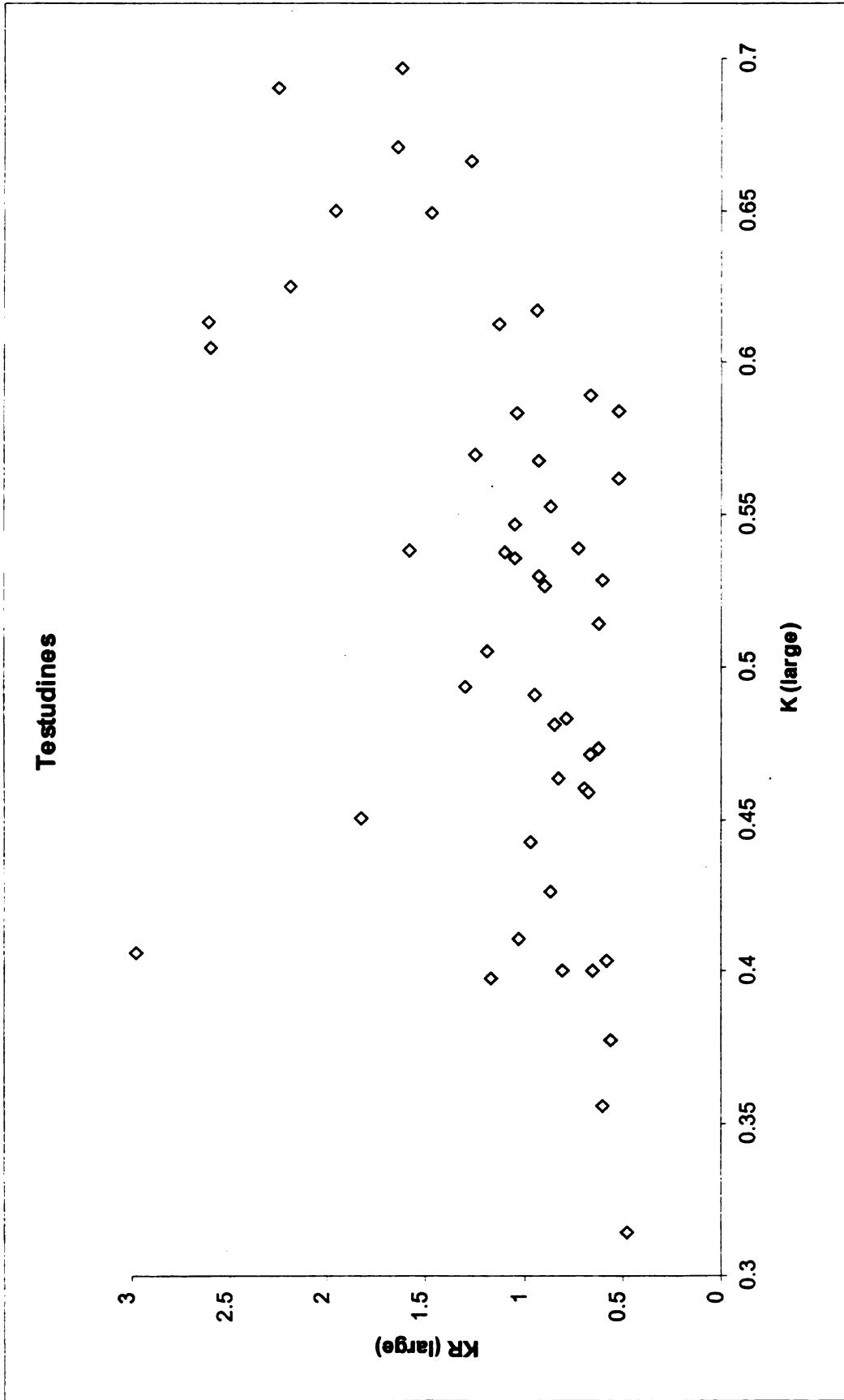


Figure 83.  $K (large)$  value versus the  $KR (large)$  value for all testudines examined.

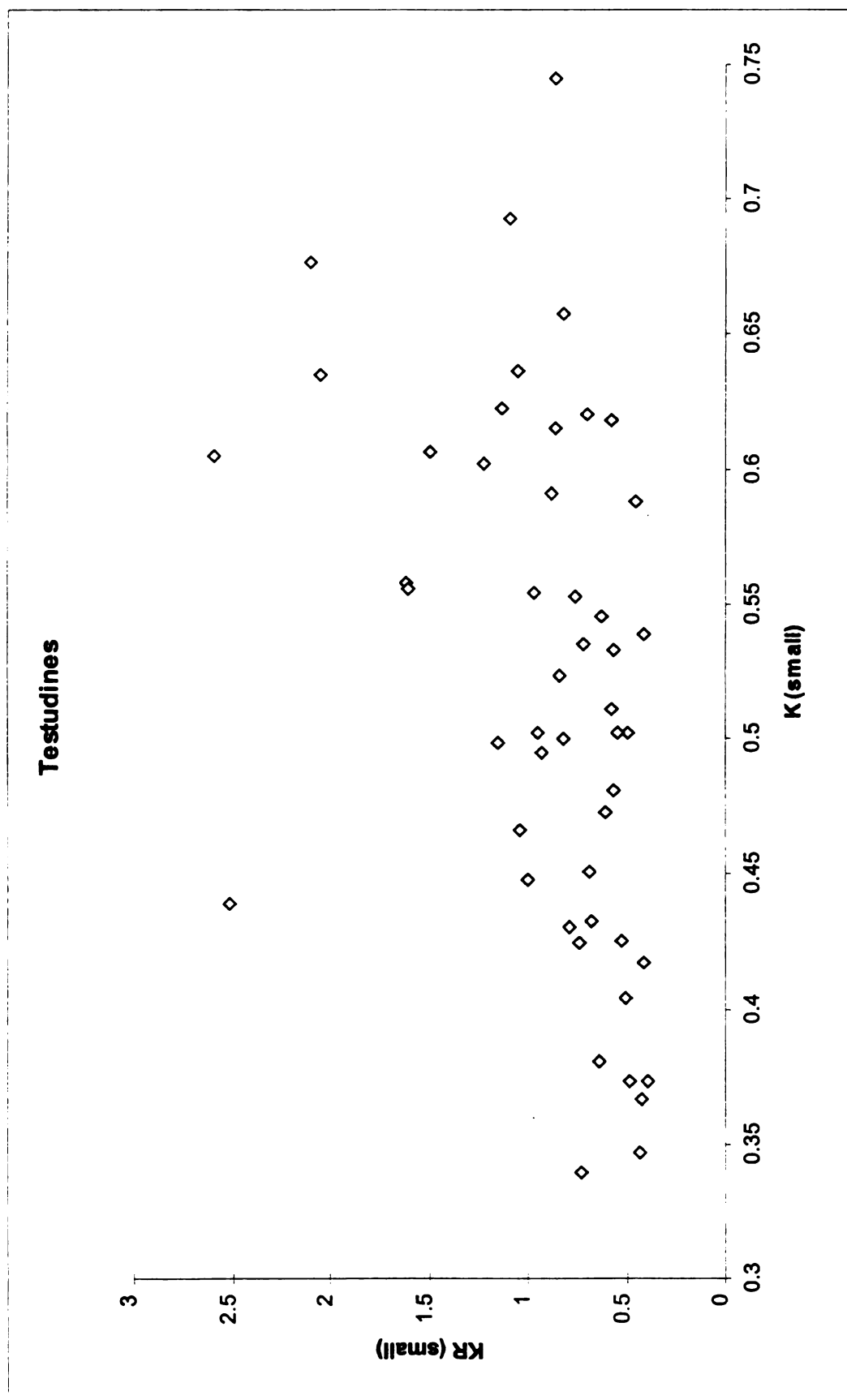


Figure 84. K (small) value versus the KR (small) value for all testudines examined.

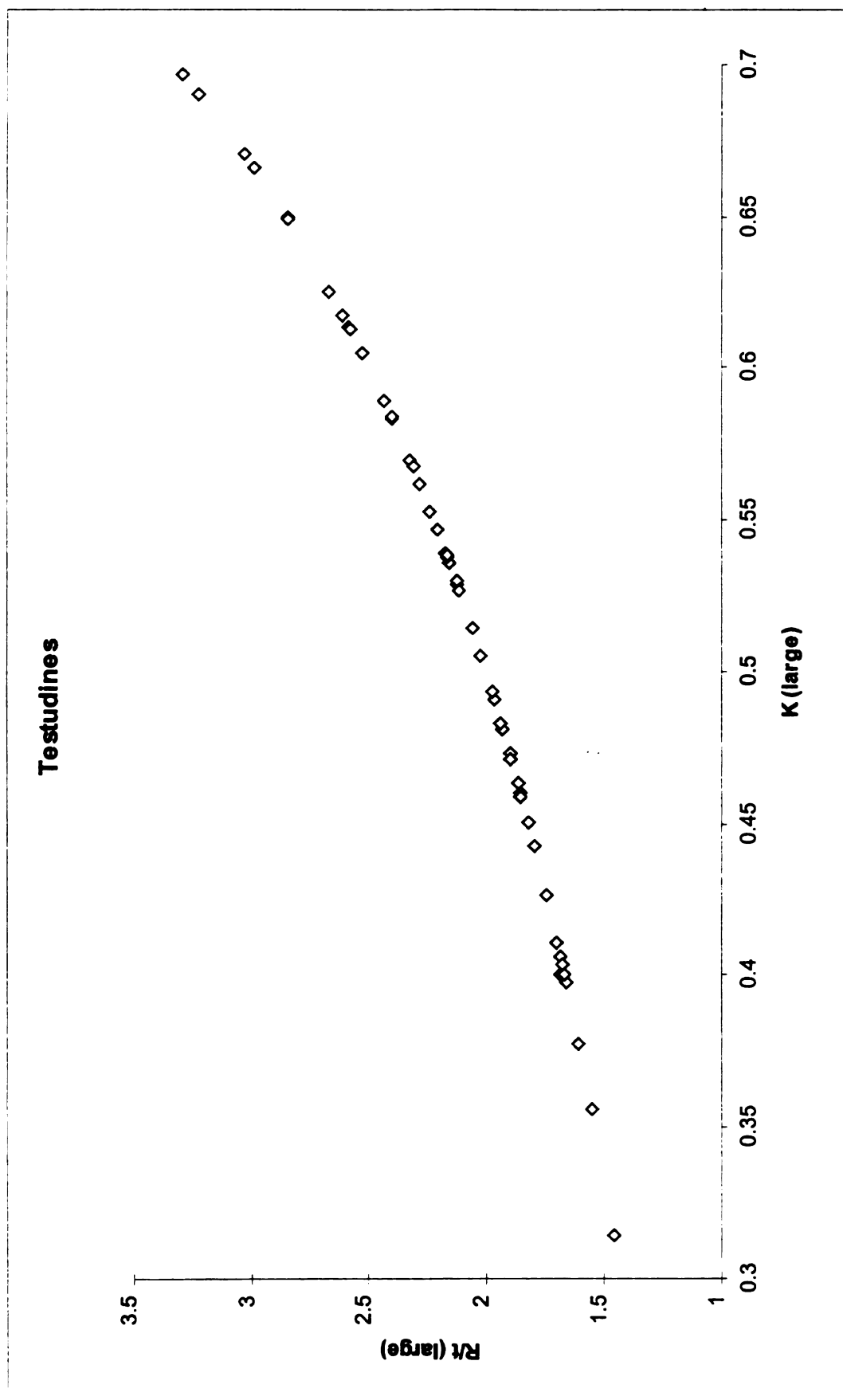


Figure 85.  $K$  (large) value versus the  $R/t$  (large) value for all testudines examined.



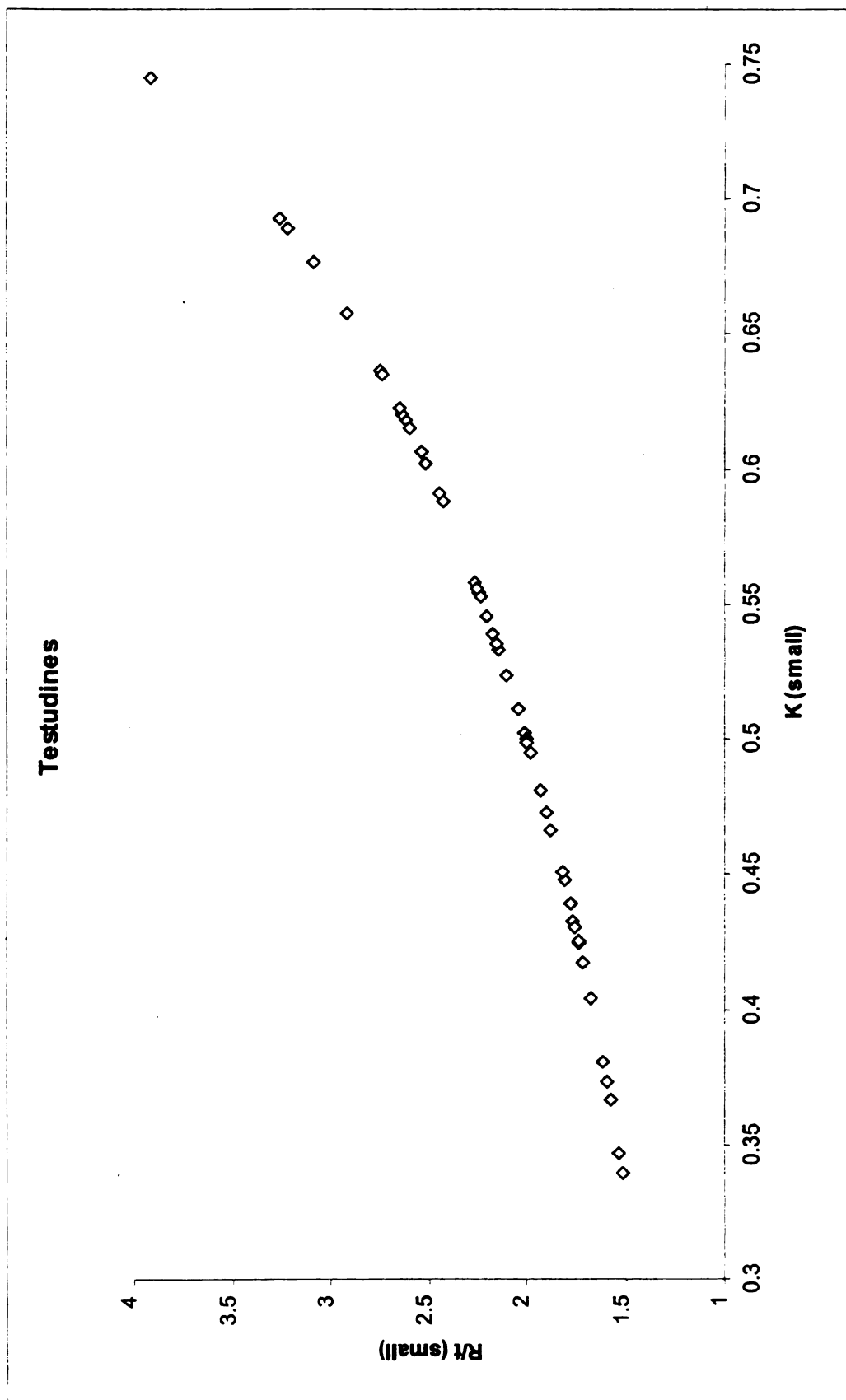


Figure 86. K (small) value versus the R/t (small) value for all testudines examined.

These are both areas of metabolic activity that require high amounts of calcium. If turtles did not use the shell as a source of calcium, the animals would not only be stressed by having to acquire enough calcium to maintain metabolic activities, but also by having to lay down the calcium of the shell's bone as well. Although the amount of marrow of most vertebrate long bones is quite large when compared to the total skeletal mass (Alexander, 1982), it is generally very small when compared to the overall skeletal size of testudines. The reason for the relatively small amount of turtle long bone marrow reflects the fact that their shells act as an additional large hemopoetic source. This extra hemopoetic source allows the animals to remodel their long bones for maximum stress resistance to carry the extra mass of the shell.

Some blood that flows throughout the carapace must feed the epithelial cells that produce the keratin the comprises the scutes. An alternative theory for the blood canals would be as a nutrient and gas source for these stem cells. The amount of blood that flows through the type C canals is much more than is needed to feed this single layer of cells under the scutes (Fig. 87).

### **Conclusions/Summation**

Citations and references of the shell as a metabolically inert structure has been continuously stated

in the chelonian literature as recently as December of 1999 (Stone and Iverson, 1999; Dunson, 1986).

My work found that the carapace was used as a calcium reserve as indicated by the presence of osteoclasts that reabsorb bone for metabolic purposes. Previous studies (Vasse and Beaupain, 1981) found that the chelonian shell is used in hematopoiesis. The presence of the vascular canals with their different types of interactions with the surface of the shell affect the thermodynamics of the organism. The subscute blood layer between the carapace and the plastron have rapid effects on the temperature of the blood that flows through those areas. All outer surfaces of the carapace were similar in appearance when these diverse areas were compared. Moreover, photographs of different outer surface areas of the same neural showed no significant differences between the numbers and types of canals present in them. This uniformity of the outer surface of the carapace and the significant numbers of Type A canals suggests that they are highly used in thermoregulation. The marrow cavity size of the long bones in chelonians is primarily restricted by the weight of the carapace and the mode of locomotion of the chelonian in question. The fact that the K value of most chelonians falls below the optimum strength values of Currey and Alexander (1985) means that the long bones of chelonians have much thicker walls than

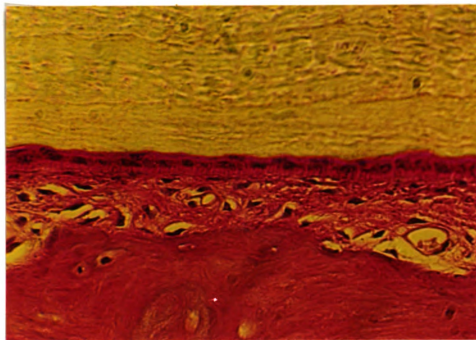


Figure 87. Hematoxylin and Eosin (H+E) photograph of a carapace showing the single cell layer that produces the scute of the shell.

other vertebrate animals. These thicker walls are needed to carry the weight of the heavy bony shell along with the soft tissues of the chelonian.

The much reduced marrow cavities of the long bones of chelonians requires that they must gain the calcium through their other bony structures, primarily the carapace and plastron. The calcium could not be lost from the long bones or risk reduced ability of the bones to support the animal. The carapace and plastron of chelonians has long been known as a source for thermoregulation although mechanisms for this thermal control were not known. The interaction of the ability of the chelonian for blood flow control to the shell and the surface arrangement of the vascular canals allows the chelonian to thermoregulate with little energy expenditure and fine control of the temperature change.

## LITERATURE CITED

- Alexander, R. McN. 1982. Optima for Animals. Edward Arnold (Publishers) Limited, London. 112 pp.
- Avery, R.A. 1982. Field studies of body temperatures and thermoregulation. 93-166. IN: Biology of the Reptilia vol. 12. C. Gans and F. H. Pough [Eds.] Academic Press, London. 536 pps.
- Bartholomew, G.A. 1982. Physiological control of body temperature. 167-211. IN: Biology of the Reptilia Vol. 12. C. Gans and F.H. Pough [Eds.] Academic Press, New York. 574 pps.
- Benedict, F.G. 1932. The physiology of large reptiles. Carnegie Inst. Washington Publ. 425 pps.
- Bennett, A.F., and W.R. Dawson. 1976. Metabolism. 127-223. IN: Biology of the Reptilia Vol. 5. C. Gans and W.R. Dawson [Eds.] Academic Press, London. 556 pps.
- Bloom, W., and D.W. Fawcett. 1962. A Textbook of Histology. Eighth Edition. W.B. Saunders Company. Philadelphia. 720 pp.
- Burke, A.C. 1989. Development of the turtle carapace: Implications for the evolution of a novel bauplan. J. Morph. 199:363-378.
- Cagle, F.R. 1950. The life history of the slider turtle Pseudemys scripta troostii (Holbrook). Ecological Monographs 20:31-54.
- Castanet, J., and M. Cheylan. 1979. Les marques de croissance des os et des ecailles comme indicateur de l'age chez Testudo hermanni et Testudo graeca (Reptilia, Chelonia, Testudinidae). Can. J. Zool. 57:1649-1665.
- Currey, J.D. 1967. The failure of exoskeletons and endoskeletons. J. Morph. 123:1-16.
- Currey, J.D. 1984. The mechanical adaptations of bones. Princeton, University Press.
- Currey, J.D., and R. McN. Alexander 1985. The thickness of the walls of tubular bones. J. Zool. Lond. A 206:453-468.

- Dunson, W.A. 1986. Estuarine populations of the snapping turtle (*Chelydra*) as a model for the evolution of marine adaptations in reptiles. *Copeia* 1986:741-756.
- Edgren, R.A. 1960. A seasonal change in bone density in female musk turtles, *Sternothaerus odoratus* (Latreille). *Comp. Biochem. Physiol.* 1:213-217.
- Enlow, D.H. 1969. The Bone of Reptiles. 45-80. IN: *Biology of the Reptilia*, Vol. 1, Morphology A. Carl Gans [Ed.] Academic Press, London. 373 pp.
- Enlow, D.H., and S.O. Brown. 1957. A comparative histological study of fossil and recent bone tissues. Part 2. *Texas Journal of Science* 9:186-214.
- Ernst, C.H., and R.W. Barbour. 1989. *Turtles of the World*. Smithsonian Institution Press, Washington, D.C. 313pp.
- Garner, M.M., B.L. Homer, E.R. Jacobson, R.E. Raskin, B.J. Hall, W.A. Weis, and K.H. Berry. 1996. Staining and morphologic features of bone marrow hematopoietic cells in desert tortoises (*Gopherus agassizii*). *AJVR* 57(11):1608-1615.
- Hall, F.G. 1924. The respiratory exchange in turtles. *J. Metab. Res.* 6:393-401.
- Hay, O.P. 1908. The fossil turtles of North America. *Carnegie Inst. Washington Publ.* 75:1-568.
- Hicks, J.W., and T. Wang. 1996. Functional role of cardiac shunts in reptiles. *J. Exp. Zool.* 275:204-216.
- Hughes, G.M., R. Gaymer, M. Moore, and A.J. Weakes. 1971. Respiratory exchange and body size in the Aldabra giant tortoise. *J. Exp. Biol.* 55:651-665.
- Hutton, K.E., D.R. Boyer, J.C. Williams, and P.M. Campbell. 1960. Effects of temperature and body size upon heart rate and oxygen consumption in turtles. *J. Cell. Comp. Physiol.* 55:87-93.
- Jayes, A.S., and R. McN. Alexander. 1980. The gaits of chelonians: walking techniques for very low speeds. *J. Zool. Lond.* 191:353-378.
- Jeffree, R.A. 1991. An experimental study of <sup>226</sup>Ra and <sup>45</sup>Ca accumulation from the aquatic medium by freshwater

- turtles (Fam. Chelidae) under varying Ca and Mg water concentrations. *Hydrobiologia* 218:205-231.
- Kass, R.E., D.E. Ullrey, and A.L. Trapp. 1982. A study of calcium requirements of the red-eared slider turtle (*Pseudemys scripta elegans*). *J. Zoo. An. Med.* 13:62-65.
- Kent, G.C. 1987. *Comparative Anatomy of the Vertebrates*. Times Mirror/Mosby College Publishing, St. Louis. 646pp.
- Martini, F.H., and E.F. Bartholomew. 2000. *Essentials of Anatomy and Physiology*. Prentice Hall, Upper Saddle River, New Jersey. 603 pp.
- Marvin, G.A., and W.I. Lutterschmidt. 1997. Locomotor performance in juvenile and adult box turtles (*Terrapene carolina*): A reanalysis for effects of body size and extrinsic load using a terrestrial species. *J. Herp.* 31(4):582-586.
- McDowell, S.B. 1964. Partition of the genus *Clemmys* and related problems in the taxonomy of the aquatic Testudinidae. *Proc. Zool. Soc. London* 143:239-279.
- Monteith, J.L. 1973. *Principles of Environmental Physics*. Arnold Publishing, London. 572 pp.
- Newman, H.H. 1906. The significance of scute and plate 'abnormalities' in chelonia. *Biol. Bull.* 10:86-114.
- Pritchard, P.C.H. 1979. *Encyclopedia of Turtles*. T.F.H. Publishing, Neptune, New Jersey. 895 pp.
- Procter, J.B. 1922. A study of the remarkable tortoise, *Testudo loveridgii* Blgr., and the morphogeny of the chelonian carapace. *Proc. Zool. Soc. London* 1922:483-526.
- Rhodin, A.G.J., J.A. Ogden, and G.J. Conlogue. 1981. Chondro-osseous morphology of *Dermochelys coriacea*, a marine reptile with mammalian skeletal features. *Nature* 290:244-246.
- Sheehan, and Hrapchak. 1980. *Theory and Practice of Histotechnology*, Second Edition. Battelle Press, Detroit, Michigan. 481 pp.
- Softstat Business Statistics Software. Version 2.0. 1996. Hagar, Inc. Tempe, AZ.



- Stone, P.A., and J.B. Iverson. 1999. Cutaneous surface area in freshwater turtles. *Chelonian Conserv. Biol.* 3(3):512-515.
- Suzuki, H.K. 1963. Studies on the osseous system of the slider turtle. *Annals New York Acad. Sci.* 109:351-410.
- Vasse, J., and D. Beaupain. 1981. Erythropoiesis and haemoglobin ontogeny in the turtle Emys orbicularis L. *J. Embryol. Exp. Morphol.* 62:129-138.
- Wallis, K. 1927. Zur Knochenhistologie und Kallusbildung beim Reptil (Clemmys leprosa Schweigg). *Z. Zellforsch. Mikroskop. Anat.* 6:1-26.
- Zangerl, R. 1939. The homology of the shell elements in turtles. *J. Morph.* 65(3):383-409.
- Zug, G.R. 1993. *Herpetology An Introductory Biology of Amphibians and Reptiles*. Academic Press, Inc., San Diego. 527 pp.

## APPENDIX A

### SPECIMENS EXAMINED

All Michigan State University Museum specimens have locality data on file in the museum data base.

Family Chelidae

Chelodina longicollis (MSU-H 12987).

Chelus fimbriatus (MSU-H 2613).

Family Cheloniidae

Eretmochelys imbricata (MSU-H 2117).

Family Chelydridae

Chelydra serpentina (MSU-H 3010); (MSU-H 3436); (MSU-H 3773).

Family Dermatemydidae

Dermatemys mawei (MSU-H 2330).

Family Emydidae, Subfamily Batagurinae

Siebenrockiella crassicollis (MSU-H 3054).

Family Emydidae, Subfamily Emydinae.

Chrysemys picta (MSU-14309); (MSU-H 14310); (MSU-H 14312);  
(MSU-H 14314); (MSU-H 14316); (MSU-H 14325); (MSU-H 14326);  
(MSU-H 14335); (MSU-H 14344); (MSU-H 14345); (MSU-H 14346);  
(MSU-H 14351); (MSU-H 13406); (MSU-H 1109); (MSU-H 2930);  
(MSU-H 3247); (MSU-H 967); (MSU-H 2025); (MSU-H 3306).

Clemmys insculpta (MSU-H 598); (MSU-H 3257); (MSU-H 4324);  
(MSU-H 4336).

Emydoidea blandingii (MSU-H 2231); (MSU-H 3955); (MSU-H  
13021).

Graptemys geographica (MSU-H 2911); (MSU-H 3303).

Graptemys pseudogeographica. USA. IL. Jackson County. (KDA 117).

Pseudemys floridana (MSU-H 522); (MSU-H 3183).

Pseudemys floridana peninsularis (MSU-H 3927).

Terrapene carolina bauri (MSU-H 629); (MSU-H 1306).

Terrapene carolina carolina (MSU-H 1696); (MSU-H 2379);  
(MSU-H 4053); (MSU-H 13019).

Terrapene carolina triunguis (MSU-H 4349); (MSU-H 12977).

Trachemys scripta (MSU-H 1730); (MSU-H 2929); (MSU-H 14307).

Trachemys scripta elegans (MSU-H 2716); (MSU-H 2721).

#### Family Kinosternidae

Kinosternon flavescens (MSU-H 2918); (MSU-H 2920); (MSU-H 2924).

Kinosternon leucostomum (MSU-H 1414).

Kinosternon subrubrum (MSU-H 2477); (MSU-H 2768); (MSU-H 4337).

#### Family Pelomedusidae

Pelusios derbianus (MSU-H 2100).

#### Family Testudinidae

Geochelone agassizi (MSU-H 1707).

Geochelone carbonaria (MSU-H3526).

Geochelone elegans (MSU-H 3238).

Geochelone elongata (MSU-H 3123).

Geochelone pardalis (MSU-H 2931); (MSU-H 3216).

Gopherus berlandieri (MSU-H 1400); (MSU-H 2220); (MSU-H 2221).

Gopherus polyphemus (MSU-H 497); (MSU-H 2102); (MSU-H 3221).

Kinixys belliana (MSU-H 4350).

Kinixys erosa (MSU-H 2077).

Malacochersus tornieri (MSU-H 4150).

Testudo graeca (MSU-H 4143); (MSU-H 4152); (MSU-H 4156);  
(MSU-H 4158).

Family Trionychidae

Apalone mutica (MSU-H 1442).

Apalone spinifera (MSU-H 1443); (MSU-H 2767).

Trionyx ferox (MSU-H 478); (MSU-H 2419).

Appendix 2. Percentage area of the scanning electron microscope (SEM) images occupied by canals at both a standard threshold and a variable threshold. Numbers of Type A, B, and C canals for each specimen photographed.

TAXON	MSU-H #	%AREA(100)	%AREA(VAR)	VAR.	TYPE A
<b>Family Chelidae</b>					
<u>Chelodina longicollis</u>	12987	35.27	6.57	30	37
<u>Chelus fimbriatus</u>	2613	50.83	25.17	50	17
F. Chelidae Ave.		43.05	15.87		27
<b>Family Chelydridae</b>					
<u>Chelydra serpentina</u>	3436	11.94	16.26	134	11
<b>Family Dermatemnydidae</b>					
<u>Dermatemys mawei</u>	2330	33.44	25.05	65	57
<b>Family Bataguridae</b>					
<u>Siebenrockiella crassicollis</u>	3054	35.82	14.12	60	79
<b>Family Emydidae</b>					
<u>Chrysemys picta</u>	967	9.11	9.87	105	36
<u>Chrysemys picta</u>	1109	9.86	8.16	80	63
<u>Chrysemys picta</u>	2025	9.71	10.09	110	45
<u>Chrysemys picta</u>	2930	6.80	7.89	73	27
<u>Chrysemys picta</u>	3247	10.29	9.01	80	72
<u>Chrysemys picta</u>	3306	10.27	10.00	90	57
<u>Chrysemys picta</u>	13046	9.31	12.39	137	59
<u>Chrysemys picta</u>	14309	10.17	10.28	111	73
<u>Chrysemys picta</u>	14310	8.74	10.03	120	51
<u>Chrysemys picta</u>	14312	8.22	8.54	76	52
<u>Chrysemys picta</u>	14314	9.88	9.61	102	38
<u>Chrysemys picta</u>	14316	8.70	7.60	83	35
<u>Chrysemys picta</u>	14325	10.28	7.12	53	48
<u>Chrysemys picta</u>	14326	9.77	8.36	66	58
<u>Chrysemys picta</u>	14335	9.55	8.63	80	39
<u>Chrysemys picta</u>	14344	8.89	11.32	145	48
<u>Chrysemys picta</u>	14345	14.28	9.10	60	41

Appendix 2. Continued.

TAXON	MSU-H #	%AREA(100)	%AREA (VAR)	VAR.	TYPE A
<b>Family Emydidae Continued</b>					
<u>Chrysemys picta</u>	14346	8.33	11.62	145	48
<u>Chrysemys picta</u>	14351	8.44	9.62	135	53
<u>C. picta</u> Ave.		9.51	9.43		49
<u>Clemmys insculpta</u>	4336	13.88	16.82	120	58
<u>Emydoidea blandingii</u>	2231	27.77	7.78	40	54
<u>Graptemys pseudogeographica</u>	(KDA117)	9.11	8.13	90	44
<u>Pseudemys floridana</u>	3927	35.42	9.70	55	55
<u>Terrapene carolina carolina</u>	2379	68.92	5.75	27	16
<u>Terrapene carolina carolina</u>	4053	11.72	13.88	110	64
<u>Trachemys scripta</u>	2716	13.46	8.30	57	71
<u>Trachemys scripta</u>	14307	12.16	14.94	108	66
Family Emydidae Ave.		13.32	9.80		50.3
<b>Family Kinosternidae</b>					
<u>Kinosternon flavescens</u>	2920	23.14	8.41	40	6
<u>Kinosternon leucostomum</u>	1414	55.54	16.65	46	33
<u>Kinosternon subrubrum</u>	2477	65.36	20.50	43	47
F. Kinosternidae Ave.		48.01	15.19		28.7
<b>Family Pelomedusidae</b>					
<u>Pelusios derbianus</u>	2100	31.23	9.75	50	26
<b>Family Platysternidae</b>					
<u>Platysternon megacephalum</u>	4103	22.99	8.31	52	69
<b>Family Testudinidae</b>					
<u>Geochelone agassizi</u>	1707	51.38	13.40	43	13
<u>Geochelone elegans</u>	3238	59.18	16.41	33	53
<u>Geochelone pardalis</u>	2931	11.80	8.99	73	41
<u>Kinixys belliana</u>	4250	29.88	14.75	50	50
<u>Kinixys erosa</u>	2077	51.99	13.42	45	18
<u>Malacochersus tornieri</u>	4150	63.90	19.67	37	13
<u>Testudo graeca</u>	4156	12.49	8.85	75	19

Appendix 2. Continued.

TAXON	MSU-H #	%AREA(100)	%AREA(VAR)	VAR.	TYPE A
F. Testudinidae Ave.		40.09	13.64	75	29.6
<b>Family Trionychidae</b>					
<u>Trionyx ferox</u>	478	9.99	9.88	45	33

## Appendix 2. Continued

TAXON	MSU-H #	TYPE B	TYPE C
<b>Family Chelidae</b>			
<i>Chelodina longicollis</i>	12987	3	2
<i>Chelus fimbriatus</i>	2613	5	10
F. Chelidae Ave.		4	6
<b>Family Chelydridae</b>			
<i>Chelydra serpentina</i>	3436	4	11
<b>Family Dermatemydidae</b>			
<i>Dermatemys mawei</i>	2330	8	8
<b>Family Bataguridae</b>			
<i>Siebenrockiella crassicollis</i>	3054	8	16
<b>Family Emydidae</b>			
<i>Chrysemys picta</i>	967	4	10
<i>Chrysemys picta</i>	1109	3	14
<i>Chrysemys picta</i>	2025	2	10
<i>Chrysemys picta</i>	2930	6	22
<i>Chrysemys picta</i>	3247	2	13
<i>Chrysemys picta</i>	3306	6	2
<i>Chrysemys picta</i>	13046	4	23
<i>Chrysemys picta</i>	14309	4	2
<i>Chrysemys picta</i>	14310	7	23
<i>Chrysemys picta</i>	14312	2	8
<i>Chrysemys picta</i>	14314	0	3
<i>Chrysemys picta</i>	14316	0	2
<i>Chrysemys picta</i>	14325	0	10
<i>Chrysemys picta</i>	14326	4	12
<i>Chrysemys picta</i>	14335	0	9
<i>Chrysemys picta</i>	14344	3	17
<i>Chrysemys picta</i>	14345	3	15
<i>Chrysemys picta</i>	14346	4	32
<i>Chrysemys picta</i>	14351	0	6



Appendix 2. Continued.

TAXON	MSU-H #	TYPE B	TYPE C
<u>C. picta</u> Ave.		2.8	12.3
<b>Family Emydidae Continued</b>			
<u>Clemmys insculpta</u>	4336	5	1
<u>Emydoidea blandingii</u>	2231	1	12
<u>Graptemys pseudogeographica</u>	(KDA117)	2	0
<u>Pseudemys floridana</u>	3927	6	5
<u>Terrapene carolina carolina</u>	2379	0	4
<u>Terrapene carolina carolina</u>	4053	8	2
<u>Trachemys scripta</u>	2716	1	11
<u>Trachemys scripta</u>	14307	5	4
Family Emydidae Ave.		3	10.1
<b>Family Kinosternidae</b>			
<u>Kinosternon flavescens</u>	2920	0	0
<u>Kinosternon leucostomum</u>	1414	3	40
<u>Kinosternon subrubrum</u>	2477	14	16
F. Kinosternidae Ave.		5.7	18.7
<b>Family Pelomedusidae</b>			
<u>Pelusios derbianus</u>	2100	7	4
<b>Family Platysternidae</b>			
<u>Platysternon megacephalum</u>	4103	2	5
<b>Family Testudinidae</b>			
<u>Geochelone agassizi</u>	1707	5	3
<u>Geochelone elegans</u>	3238	12	10
<u>Geochelone pardalis</u>	2931	4	5
<u>Kinixys belliana</u>	4250	4	4
<u>Kinixys erosa</u>	2077	1	4
<u>Malacochersus tornieri</u>	4150	2	8
<u>Testudo graeca</u>	4156	0	18
F. Testudinidae Ave.		4	7.4

Appendix 2. Continued.

TAXON	MSU-H #	TYPE B	TYPE C
<b>Family Trionychidae</b>			
<u>Trionyx ferox</u>	478	0	0

### Appendix 3. Measurements of femora and calculations derived from those measurements.

Measurements are total length of the femur, inside diameter of smaller and larger areas of the bisected femora, and outside diameter of the smaller and larger areas of the bisected femora. Calculations are ratio of the internal diameter to the outside diameter  $[K(sm) \text{ and } K(lg)]$ , radius of the outside measurements  $[R(sm) \text{ and } R(lg)]$ , radius of the marrow cavity  $[KR(sm) \text{ and } KR(lg)]$ , thickness of the bone wall  $[t(sm) \text{ and } t(lg)]$ , and ratio of the radius of the outside measurement to the thickness of the bone wall  $[R/t(sm) \text{ and } R/t(lg)]$ .

TAXON	MSU ID#	TOT.LENGTH	IN.D.(SM)	IN.D.(LG)	OUT.D.(SM)
<b>Family Chelonidae</b>					
<u>Eretmochelys imbricata</u>	2117	106.27mm	5.04mm	5.95mm	11.48mm
<b>Family Chelydridae</b>					
<u>Chelydra serpentina</u>	3010	52.53mm	3.23mm	3.93mm	5.79mm
<u>Chelydra serpentina</u>	3436	35.61mm	1.90mm	2.50mm	3.78mm
<u>Chelydra serpentina</u>	3773	64.65mm	4.21mm	4.52mm	6.22mm
<u>F. Chelydridae Ave.</u>		50.93mm	3.11mm	3.65mm	5.26mm
<b>Family Emydidae</b>					
<u>Chrysemys picta</u>	967	32.05mm	1.25mm	1.25mm	2.29mm
<u>Chrysemys picta</u>	2025	28.10mm	1.00mm	1.21mm	1.99mm
<u>Chrysemys picta</u>	3247	28.68mm	1.15mm	1.32mm	1.86mm
<u>Chrysemys picta</u>	3306	28.13mm	1.14mm	1.24mm	2.14mm
<u>Clemmys insculpta</u>	598	40.69mm	1.28mm	1.61mm	3.36mm
<u>Clemmys insculpta</u>	3257	44.06mm	2.10mm	2.10mm	3.30mm
<u>Clemmys insculpta</u>	4324	31.72mm	1.01mm	1.39mm	2.50mm
<u>Emydoidea blandingi</u>	3955	54.05mm	1.85mm	2.05mm	3.74mm
<u>Emydoidea blandingi</u>	13021	29.93mm	1.09mm	1.32mm	2.17mm
<u>Graptemys geographica</u>	2911	48.08mm	1.99mm	2.37mm	4.44mm
<u>Graptemys geographica</u>	3303	43.63mm	1.63mm	2.09mm	3.26mm
<u>Pseudemys floridana</u>	522	57.73mm	2.31mm	2.34mm	4.63mm
<u>Pseudemys floridana</u>	3183	42.18mm	1.94mm	3.30mm	3.50mm
<u>Terrapene carolina bauri</u>	629	27.94mm	0.86mm	0.95mm	2.48mm
<u>Terrapene carolina bauri</u>	1306	31.24mm	1.21mm	1.21mm	2.56mm

Appendix 3. Continued.

TAXON	MSU ID#	TOT. LENGTH	IN.D. (SM)	IN.D. (LG)	OUT.D. (SM)
<b>Family Emydidae (Continued)</b>					
<u>Terrapene carolina carolina</u>	1696	39.71mm	1.35mm	2.19mm	3.12mm
<u>Terrapene carolina carolina</u>	13019	34.72mm	1.76mm	1.90mm	2.98mm
<u>Terrapene carolina triunguis</u>	4349	30.40mm	1.39mm	1.72mm	2.24mm
<u>Terrapene carolina triunguis</u>	12977	32.18mm	1.43mm	2.07mm	2.67mm
<u>Trachemys scripta</u>	1730	47.30mm	1.47mm	1.73mm	3.46mm
<u>Trachemys scripta</u>	2716	28.54mm	1.14mm	1.44mm	2.37mm
<u>Trachemys scripta</u>	2721	30.07mm	0.85mm	1.35mm	2.32mm
<u>Trachemys scripta</u>	2929	36.65mm	1.71mm	1.79mm	2.78mm
<u>F. Emydidae Ave.</u>		36.86mm	1.43mm	1.74mm	2.88mm
<b>Family Kinosternidae</b>					
<u>Kinosternon flavescens</u>	2918	25.89mm	0.78mm	1.11mm	2.09mm
<u>Kinosternon flavescens</u>	2924	25.65mm	1.72mm	1.87mm	2.31mm
<u>Kinosternon subrubrum</u>	2768	18.69mm	0.90mm	1.04mm	1.53mm
<u>Kinosternon subrubrum</u>	4337	19.38mm	0.83mm	1.04mm	1.54mm
<u>F. Kinosternidae Ave.</u>		22.40mm	1.06mm	1.27mm	1.87mm
<b>Family Testudinidae</b>					
<u>Geochelone carbonaria</u>	3526	39.95mm	2.45mm	3.26mm	4.07mm
<u>Geochelone elongata</u>	3123	46.62mm	2.09mm	2.60mm	4.48mm
<u>Geochelone pardalis</u>	3216	23.35mm	0.83mm	1.15mm	1.99mm
<u>Gopherus agassizi</u>	1707	40.23mm	1.46mm	3.17mm	4.30mm
<u>Gopherus berlandieri</u>	1400	35.50mm	1.58mm	1.93mm	3.67mm
<u>Gopherus berlandieri</u>	2220	29.57mm	0.97mm	1.65mm	2.60mm
<u>Gopherus berlandieri</u>	2221	32.79mm	1.38mm	1.68mm	3.06mm
<u>Gopherus polyphemus</u>	497	41.65mm	3.00mm	4.39mm	4.95mm
<u>Gopherus polyphemus</u>	2102	59.63mm	4.10mm	5.23mm	6.46mm
<u>Gopherus polyphemus</u>	3221	57.63mm	3.22mm	3.67mm	5.79mm
<u>Testudo graeca</u>	4143	26.08mm	1.05mm	1.57mm	2.47mm
<u>Testudo graeca</u>	4152	26.07mm	1.16mm	1.30mm	2.27mm
<u>Testudo graeca</u>	4158	27.63mm	1.63mm	1.85mm	2.48mm
<u>F. Testudinidae Ave.</u>		37.44mm	1.92mm	2.57mm	3.74mm

Appendix 3. Continued.

TAXON	MSU ID#	TOT. LENGTH	IN. D. (SM)	IN. D. (LG)	OUT. D. (SM)
<b>Family Trionychidae</b>					
<u>Apalone mutica</u>	1442	28.93mm	1.52mm	1.86mm	2.75mm
<u>Apalone spinifera</u>	1443	36.48mm	2.26mm	2.94mm	3.63mm
<u>Apalone spinifera</u>	2767	72.92mm	5.19mm	5.21mm	7.53mm
<u>Trionyx ferox</u>	478	32.77mm	1.68mm	2.26mm	3.21mm
<u>Trionyx ferox</u>	2419	27.90mm	2.19mm	2.55mm	3.16mm
F. Trionychidae Ave.		39.80mm	2.57mm	2.96mm	4.06mm

Appendix 3. Continued.

TAXON	OUT. D. (LG)	K (SM)	K (LG)	R (SM)	R (LG)
<b>Family Chelonidae</b>					
<u>Eretmochelys imbricata</u>	14.64mm	0.44	0.41	5.74	7.32
<b>Family Chelydridae</b>					
<u>Chelydra serpentina</u>	6.05mm	0.56	0.65	2.90	3.03
<u>Chelydra serpentina</u>	4.39mm	0.50	0.57	1.89	2.20
<u>Chelydra serpentina</u>	6.55mm	0.68	0.69	3.11	3.28
<u>F. Chelydridae Ave.</u>	5.66mm	0.58	0.64	2.63	2.83
<b>Family Emydidae</b>					
<u>Chrysemys picta</u>	2.64mm	0.55	0.47	1.15	1.32
<u>Chrysemys picta</u>	2.29mm	0.50	0.53	1.00	1.15
<u>Chrysemys picta</u>	2.24mm	0.62	0.59	0.93	1.12
<u>Chrysemys picta</u>	2.41mm	0.53	0.51	1.07	1.21
<u>Clemmys insculpta</u>	3.96mm	0.38	0.40	1.68	1.98
<u>Clemmys insculpta</u>	3.92mm	0.64	0.54	1.65	1.96
<u>Clemmys insculpta</u>	3.02mm	0.40	0.46	1.25	1.51
<u>Emydoidea blandingi</u>	4.99mm	0.49	0.41	1.87	2.50
<u>Emydoidea blandingi</u>	2.80mm	0.50	0.47	1.09	1.40
<u>Graptemys geographica</u>	4.69mm	0.45	0.51	2.22	2.35
<u>Graptemys geographica</u>	3.82mm	0.50	0.55	1.63	1.91
<u>Pseudemys floridana</u>	5.88mm	0.50	0.40	2.32	2.94
<u>Pseudemys floridana</u>	4.92mm	0.55	0.67	1.75	2.46
<u>Terrapene carolina bauri</u>	3.02mm	0.35	0.31	1.24	1.51
<u>Terrapene carolina bauri</u>	3.40mm	0.47	0.36	1.28	1.70
<u>Terrapene carolina carolina</u>	4.07mm	0.43	0.54	1.56	2.04
<u>Terrapene carolina carolina</u>	3.87mm	0.59	0.49	1.49	1.94
<u>Terrapene carolina triunguis</u>	3.11mm	0.62	0.55	1.12	1.56
<u>Terrapene carolina triunguis</u>	3.55mm	0.54	0.58	1.34	1.78
<u>Trachemys scripta</u>	4.06mm	0.42	0.43	1.73	2.03
<u>Trachemys scripta</u>	2.67mm	0.48	0.54	1.19	1.34
<u>Trachemys scripta</u>	2.94mm	0.37	0.46	1.16	1.47
<u>Trachemys scripta</u>	3.40mm	0.62	0.53	1.39	1.70

Appendix 3. Continued.

TAXON	OUT.D. (LG)	K (SM)	K (LG)	R (SM)	R (LG)
<b>Family Emydidae</b> (continued)					
F. Emydidae Ave.	3.55mm	0.50	0.49	1.44	1.78
<b>Family Kinosternidae</b>					
Kinosternon <u>flavescens</u>	2.94mm	0.37	0.38	1.05	1.47
Kinosternon <u>flavescens</u>	3.03mm	0.74	0.62	1.16	1.52
Kinosternon <u>subrubrum</u>	1.85mm	0.59	0.56	0.77	0.93
Kinosternon <u>subrubrum</u>	1.78mm	0.54	0.58	0.77	0.89
Kinosternon <u>subrubrum</u>	2.40mm	0.56	0.54	0.93	1.20
F. Kinosternidae Ave.					
<b>Family Testudinidae</b>					
Geochelone <u>carbonaria</u>	4.68mm	0.60	0.70	2.04	2.34
Geochelone <u>elongata</u>	5.27mm	0.47	0.49	2.24	2.64
Geochelone <u>pardalis</u>	2.85mm	0.42	0.40	1.00	1.43
Gopherus <u>agassizi</u>	5.89mm	0.34	0.54	2.15	2.95
Gopherus <u>berlandieri</u>	4.36mm	0.43	0.44	1.84	2.18
Gopherus <u>berlandieri</u>	3.56mm	0.37	0.46	1.30	1.78
Gopherus <u>berlandieri</u>	3.49mm	0.45	0.48	1.53	1.75
Gopherus <u>polyphemus</u>	7.02mm	0.61	0.63	2.48	3.51
Gopherus <u>polyphemus</u>	8.52mm	0.63	0.61	3.23	4.26
Gopherus <u>polyphemus</u>	8.15mm	0.56	0.45	2.90	4.08
Gopherus <u>polyphemus</u>	3.25mm	0.43	0.48	1.24	1.63
Testudo <u>graeca</u>	3.25mm	0.51	0.40	1.14	1.63
Testudo <u>graeca</u>	3.26mm	0.66	0.57	1.24	1.63
Testudo <u>graeca</u>	4.89mm	0.50	0.51	1.87	2.44
F. Testudinidae Ave.					
<b>Family Trionychidae</b>					
Apalone <u>mutica</u>	3.51mm	0.55	0.53	1.38	1.76
Apalone <u>spinifera</u>	4.53mm	0.62	0.65	1.82	2.27
Apalone <u>spinifera</u>	8.61mm	0.69	0.61	3.77	4.31
Trionyx <u>ferox</u>	3.69mm	0.52	0.61	1.61	1.85
Trionyx <u>ferox</u>	3.83mm	0.69	0.67	1.58	1.92
F. Trionychidae Ave.	4.83mm	0.60	0.61	2.03	2.42

Appendix 3. Continued.

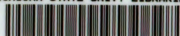
TAXON	KR (SM)	KR (LG)	t (SM)	t (LG)	R/t (SM)	R/t (LG)
<b>Family Chelonidae</b>						
<u>Eretmochelys imbricata</u>	2.52	2.98	3.22	4.35	1.78	1.68
<b>Family Chelydridae</b>						
<u>Chelydra serpentina</u>	1.62	1.97	1.28	1.06	2.26	2.85
<u>Chelydra serpentina</u>	0.95	1.25	0.94	0.95	2.01	2.32
<u>Chelydra serpentina</u>	2.11	2.26	1.01	1.02	3.09	3.23
<u>F. Chelydridae Ave.</u>	1.56	1.83	1.08	1.01	2.46	2.80
<b>Family Emydidae</b>						
<u>Chrysemys picta</u>	0.63	0.63	0.52	0.70	2.20	1.90
<u>Chrysemys picta</u>	0.50	0.61	0.50	0.54	2.01	2.12
<u>Chrysemys picta</u>	0.58	0.66	0.36	0.46	2.62	2.43
<u>Chrysemys picta</u>	0.57	0.62	0.50	0.59	2.14	2.06
<u>Clemmys insculpta</u>	0.64	0.81	1.04	1.18	1.62	1.69
<u>Clemmys insculpta</u>	1.05	1.05	0.60	0.91	2.75	2.15
<u>Clemmys insculpta</u>	0.51	0.70	0.75	0.82	1.68	1.85
<u>Emydoidea blandingi</u>	0.93	1.03	0.95	1.47	1.98	1.70
<u>Emydoidea blandingi</u>	0.55	0.66	0.54	0.74	2.01	1.89
<u>Graptemys geographica</u>	1.00	1.19	1.23	1.16	1.81	2.02
<u>Graptemys geographica</u>	0.82	1.05	0.82	0.87	2.00	2.21
<u>Pseudemys floridana</u>	1.16	1.17	1.16	1.77	2.00	1.66
<u>Pseudemys floridana</u>	0.97	1.65	0.78	0.81	2.24	3.04
<u>Terrapene carolina bauri</u>	0.43	0.48	0.81	1.04	1.53	1.46
<u>Terrapene carolina bauri</u>	0.61	0.61	0.68	1.10	1.90	1.55
<u>Terrapene carolina carolina</u>	0.68	1.10	0.89	0.94	1.76	2.16
<u>Terrapene carolina carolina</u>	0.88	0.95	0.61	0.99	2.44	1.96
<u>Terrapene carolina triunguis</u>	0.70	0.86	0.43	0.70	2.64	2.24
<u>Terrapene carolina triunguis</u>	0.72	1.04	0.62	0.74	2.15	2.40
<u>Trachemys scripta</u>	0.74	0.87	1.00	1.17	1.74	1.74
<u>Trachemys scripta</u>	0.57	0.72	0.62	0.62	1.93	2.17
<u>Trachemys scripta</u>	0.43	0.68	0.74	0.80	1.58	1.85
<u>Trachemys scripta</u>	0.86	0.90	0.54	0.81	2.60	2.11



Appendix 3. Continued.

TAXON	KR (SM)	KR (LG)	t (SM)	t (LG)	R/t (SM)	R/t (LG)
<b>Family Emydidae</b> (continued)						
<i>F. Emydidae</i> Ave.	0.72	0.87	0.72	0.91	2.03	2.02
<b>Family Kinosternidae</b>						
<i>Kinosternon flavescens</i>	0.39	0.56	0.66	0.92	1.60	1.61
<i>Kinosternon flavescens</i>	0.86	0.94	0.30	0.58	3.92	2.61
<i>Kinosternon subrubrum</i>	0.45	0.52	0.32	0.41	2.43	2.28
<i>Kinosternon subrubrum</i>	0.42	0.52	0.36	0.37	2.17	2.41
<i>F. Kinosternidae</i> Ave.	0.53	0.63	0.41	0.57	2.53	2.23
<b>Family Testudinidae</b>						
<i>Geochelone carbonaria</i>	1.23	1.63	0.81	0.71	2.51	3.30
<i>Geochelone elongata</i>	1.05	1.30	1.20	1.34	1.87	1.97
<i>Geochelone pardalis</i>	0.42	0.58	0.58	0.85	1.72	1.68
<i>Gopherus agassizi</i>	0.73	1.59	1.42	1.36	1.51	2.17
<i>Gopherus berlandieri</i>	0.79	0.97	1.05	1.22	1.76	1.79
<i>Gopherus berlandieri</i>	0.49	0.83	0.82	0.96	1.60	1.86
<i>Gopherus berlandieri</i>	0.69	0.84	0.84	0.91	1.82	1.93
<i>Gopherus polyphemus</i>	1.50	2.20	0.98	1.32	2.54	2.67
<i>Gopherus polyphemus</i>	2.05	2.62	1.18	1.65	2.74	2.59
<i>Gopherus polyphemus</i>	1.61	1.84	1.29	2.24	2.25	1.82
<i>Testudo graeca</i>	0.53	0.79	0.71	0.84	1.74	1.93
<i>Testudo graeca</i>	0.58	0.65	0.56	0.98	2.05	1.67
<i>Testudo graeca</i>	0.82	0.93	0.43	0.71	2.92	2.31
<i>F. Testudinidae</i> Ave.	0.96	1.29	0.91	1.16	2.08	2.13
<b>Family Trionychidae</b>						
<i>Apalone mutica</i>	0.76	0.93	0.62	0.83	2.24	2.13
<i>Apalone spinifera</i>	1.13	1.47	0.69	0.80	2.65	2.85
<i>Apalone spinifera</i>	2.60	2.61	1.17	1.70	3.22	2.53
<i>Trionyx ferox</i>	0.84	1.13	0.77	0.72	2.10	2.58
<i>Trionyx ferox</i>	1.10	1.28	0.49	0.64	3.26	2.99
<i>F. Trionychidae</i> Ave.	1.28	1.48	0.74	0.94	2.69	2.62

MICHIGAN STATE UNIV. LIBRARIES



31293020486324